An Overview of Steam Injection Projects in Fractured Carbonate Reservoirs in the Middle East

Zuhair Al Yousef[1], Hussain AlDaif[2], and Mohammed Al Otaibi[3]

[1-3]Harold Vance Department of Petroleum Engineering, Texas A&M University, Texas

[1]zuhair.alyousef@pe.tamu.edu; [2]hussain.aldaif@pe.tamu.edu; [3]m.alotaibi@pe.tamu.edu

Abstract

Steam injection is one of the most common and widely spread thermal recovery methods. It is mainly used in heavy oil reservoirs. In this paper, the use of steam injection in heavy and light oil fractured carbonate reservoirs in the Middle East region will be discussed. Heavy oil contained in fractured reservoirs represents a large portion of the total oil in place in the Middle East. Beside the status and the results of the commercial and pilot steam injection projects that have been conducted in the Middle East, this paper will review the results of some simulation studies that were conducted on heavy and light oil fractured carbonate reservoirs in that region. The paper will also include some descriptions and discussions of the mechanism of steam injection, steamflooding screening guide, steamflooding design and steamflooding operational problems. Although the paper will focus on the Middle East steam injection projects, it still can serve as a guide for other regions that have similar reservoir and oil properties.

Keywords

Steam Injection; Fractured Carbonate Reservoirs; Middle East

Introduction

The recent increase in oil prices as well as the continuous growth in the global oil consumption has made the investment in heavy oil resources more attractive to oil companies. In fact, bitumen and tar sand, extra heavy oil, and heavy oil account for 30%, 25%, and 15%, respectively of the world oil in place while conventional oil accounts for 30% only (Alikhlalov and Dindoruk 2011). In heavy oil reservoirs, 60% or more of oil in place will not be producible due to the high oil viscosity (Dietz 1975). In addition, according to Alshmakhy and Maini in 2012, cold heavy oil production with sand (CHOPS), a

recovery method used in heavy oil reservoirs, usually yield in very low recovery factors (5-10%). Therefore, thermal recovery methods can be applied in order to enhance the heavy oil recovery. Steam flooding is proven to be successful in light, heavy, and extra heavy oil reservoirs.

Since 1930's, interest in the injection of hot fluid including hot water and steam in order to recover more oil has appeared. Laboratory and field trials of steam injection were described by Stovall in 1934 (Henry and Ramey 1967). As a pilot, steam injection was first implemented in California in 1952 in Yorba Linda field (Blevins 1990). Over time, different types of steam injection were introduced.

There are three main types of steam injection techniques. The first one is Cyclic Steam Stimulation (CSS) which was first implemented in eastern Venezuela in 1959 (Trebolle et al. 1993). In this method steam is injected for some period of time followed by a soaking period and finally a production period. The second method is the circulation of steam above a packer (KEPLINGER 1965). In this method, steam is injected above the packer and perforations are opened below the packer to produce the well. A modified version of this method is Steam Assisted Gravity Drainage (SAGD). In SAGD, a horizontal steam injector is drilled above a horizontal oil producer to take advantage of gravity in moving the oil downward to the producer. The third method is the continuous steam injection which is also known as steamflooding. In this type of steam injection, steam is injected in some wells and oil is produced from different wells. So, this method is similar to water flooding with steam

replacing water.

This paper will focus on the steam injection projects in the fractured carbonate reservoirs in the Middle East (ME) region which has around 48% of the world total proved reserves (BP Statistical Review of World Energy, June 2012), **Fig. 1**.
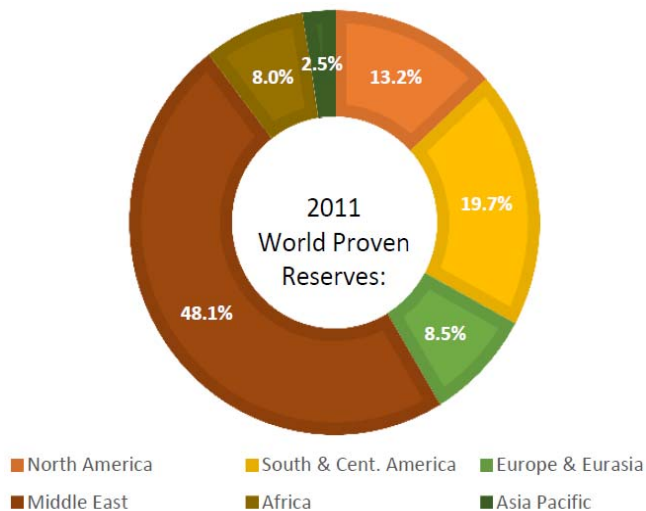

FIG. 1 PROVEN RESERVES BY REGION
(BP Statistical Review of World Energy, June 2012)

Overview of Steam Injection Projects in the Middle East

Although heavy oil in fractured carbonate reservoirs represents 25-30% of the total oil in place in the Middle East (Saidi 1988), there are very few steam injection projects and most of which are implemented recently. The projects mentioned here are all the projects conducted regardless of the formation rock type. More details about fields with fractured carbonate reservoirs will be provided in a later section. **Fig. 2** shows the current enhanced oil recovery project in the Middle East (Al-Mutairi and Kokal 2011).

There are three main steam injection projects in Oman (Al-Mutairi and Kokal 2011). The first one is in Qarn Alam Field (Steam Assisted Oil Gas Gravity Drainage) where the pilot was initiated in 1996 with a plan to reach full rate steam injection by late in 2009 (Macaulay et al. 1995; Penney et al. 2007). The second one is in Mukhaizna Field where the steam injection (modified SAGD) started in 2007 (Malik et al. 2011). The third project is in "A" Field where pilots of steam injection (both continues injection and CSS) started in 2007 (Thum et al. 2010).

There is one main project in Kuwait and there is another one in the partitioned neutral zone between

Kuwait and Saudi Arabia. There were two pilots steam injection (CSS) in Ratqa Lower Fars Field in Kuwait, one in 1982 and the other in 1986, where the results of the pilots showed that the field was suitable for thermal recovery methods (Milhem and Ahmed 1987). The other steam injection (steamflooding) is on Wafra Field which started on 2006 (Barge et al. 2009).

There is only one steam injection project in Issaran which had its first trial on one well in 2004 (Samir 2010).

As mentioned previously, more details about fields with fractured carbonate reservoirs will be provided in a later section. The paper will discuss both the current steam injection projects in the ME as well as selected simulation studies of steam injection that have not yet been implemented on the field.
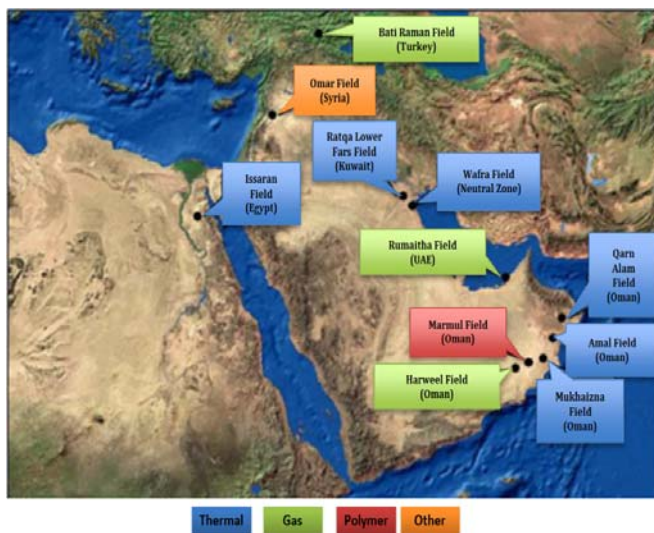

FIG. 2 EOR PROJECTS IN THE MIDDLE EAST
(Al-Mutairi and Kokal 2011)

Steamflooding Mechanism

There are several mechanisms that govern the recovery of oil via steamflooding. Some of the main mechanisms are thermal expansion, viscosity reduction, wettability alteration, steam distillation and gas generation (Reis 1990), **Fig. 3**. For naturally fractured reservoirs, it is important to understand how different mechanisms affect both the matrix and the natural fracture network. **Table 1** and **Table 2** (Holladay 1966, Reis 1990, Cathles et al. 1987, Al-Hadhrami and Blunt 2000, Al-Yousef et al. 1995, Baviere 1991, Willhite and Green 1998, Mollaei, and Maini 2010, Shahin et al. 2006) provide a brief summary on the steamflooding mechanisms in naturally fractured reservoirs.
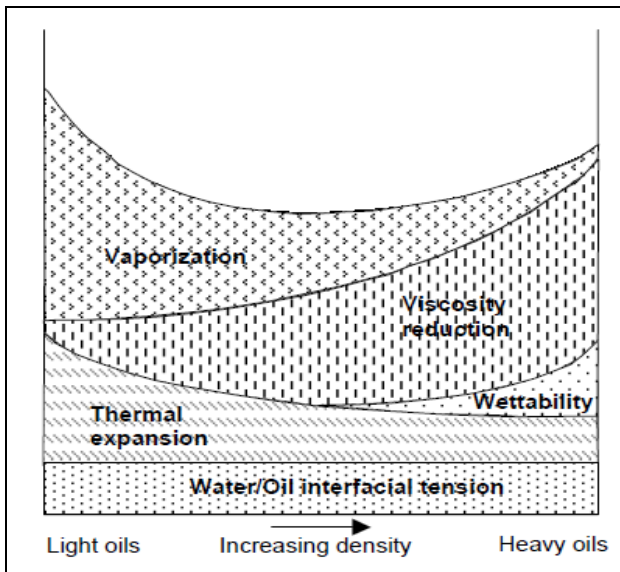
FIG. 3 STEAMFLOODING RECOVERY MECHANISM
CONTRIBUTION VS. OIL DENSITY (Burger et al. 1985)

TABLE 1 STEAMFLOOD EFFECTS ON RESERVOIR MATRIX

Mechanism	Effect	Significant
Viscosity Reduction	high temperature can increase the mobility ratio	Very important in high viscosity reservoirs
Thermal Expansion	Expand in matrix will result in reduction in porosity and oil will be expel from matrix	Important. Increasing the matrix temperature to 400 ^{0}F can lead to about 20% volume expansion of the heavy oil core PV.
Gas Generation	Chemical reactions may occur at higher temperatures. CO2 and lighter HC may be produced.	Important. It could be similar effect as the solution-gas drive and can increase the recovery by up to 25%.
Steam Distillation	Lighter components will evaporate and be produced	Not significant in matrix because steam will flow mainly in fractures
Wettability Alteration	Increase in temperature will make the rock more water-wet which will increase the recovery of oil	Its significant depends on the matrix properties (oil-wet or water-wet). Carbonate reservoirs in Saudi Arabia are usually neutral to slightly oil-wet. So, altering the wettability can improve recovery.

TABLE 2 MECHANISMS OF OIL DISPLACEMENT FROM FRACTURES TO THE
PRODUCTION WELL

Mechanism	Effects	Significant
Reduction of Viscosity Ratio (μo/μw)	As reservoir temperature increase, oil viscosity decreases faster than water viscosity, increasing the oil mobility. Fractured reservoirs have higher transmissibility, this means oil transports faster.	Considers being the strongest recovery mechanism in fractured system.

Evolution of Absolute and Relative Permeability	Studies showed that (kro) either increases or does not change (depends on oil properties) as temperature increases. (krw) has small changes as temperature increases.	Oil relative permeability changes found to be stronger if the fracture networks exist. Both Reduction of (μo/μw) and evolution of (kro) can improve the oil mobility
Distillation (Oil Vaporization)	As temperature gets higher due to steam injection, light components of oil in the fractures will vaporize leaving the heavy ones as residual oil saturation (Sor).	The advantage is that (Sor) will decrease, however the residual heavy components may result in asphaltenes precipitation which may change the reservoir and fluid properties.

TABLE 3 STEAMFLOOD GENERAL SCREENING GUIDE (CHU 1985)

Ref. No.	φSo	φ	So	°API	h, ft
1	0.15-0.22	0.3	-	12-15	≥30
2	>0.10	-	-	>10	>20
3	>0.065	-	>0.5	>10	>20
4	>0.065	>0.3	>0.5	10-20	30-400
5	>0.08	>0.2	>0.4	<36	>10
Ref. No.	D, ft		k, md	μ, cp	kh/μ, md-ft/cp
1	<3000		~1000	<1000	-
2	<4000		-	-	>20
3	<5000		-	-	>100
4	2500-5000		>1000	200-1000	>50
5	>400		-	-	-

TABLE 4 SCREENING GUIDE FOR STEAM INJECTION
(BOURDAROT AND GHEDAN, 2011)

Property	Units	Recommended
Oil Gravity	API	8 to 25
Viscosity	cp	< 100,000
Oil Saturation	% PV	>40
Formation	-	Sand or sandstone but can be used in carbonates
Fracture	-	Not fractured reservoirs
Gas Cap	-	No extensive gas cap
Net Thickness	ft	>20
Permeability	md	>200
Transmitivity	md-ft/cp	>50
Depth	ft	<4,500
Pressure	psi	<3,200
Temperature	°F	Not critical

Steamflooding Screening Guide

Based on the experience obtained from field projects, reservoir and oil criteria of successful steam injection project were proposed by many authors. All the criteria proposed have common findings, steamflooding works well with relatively thick

shallow reservoir and high oil saturation, as it is shown in **Table 3** (Chu 1985). At depth higher than 5000 ft, steam will condense to hot water, thus the heating value of injected fluid will decrease the efficiency of steamflood. Furthermore, heat losses from thin reservoirs are significant resulting in very low heating efficiency, thus it is recommended to perform steam injection in reservoirs with 30 ft thicknesses or more (Donaldson et al., 1989). A more recent screening criterion was proposed by Bourdarot and Ghedan, **Table 4**. **Table 4** shows that it is recommended to use steamflooding in non-fractured reservoirs. However, several field examples have shown that steamflooding can be successful in heavy oil fractured reservoirs. Examples of such fields in the Middle East are Qarn Alam field in Oman, Issaran field in Egypt and the Wafra field between Kuwait and Saudi Arabia.

Steamflooding Design

The design parameters of steam injection are vital to produce economical project, the following parameters will be examined; steam to oil ratio (SOR), steam injection rate and steam quality. According to (Chu 1985), the steam oil ratio (SOR) is a crucial element defining the success or failure of a steamflood project and should be less than 10 and ideally around 4. This number is based on old study where oil prices were much lower than the current price; economic project can be achieved even with higher SOR. Steam injection rate can greatly affect the performance and the efficiency of steamflood project. Although, high injection rate will lead to high initial oil production rate and high oil recovery, it will also lead to high SOR and early steam breakthrough resulting in a decline oil rate at later stages (Ali 1974). Therefore, it is important to optimize the steam injection rate via experimental and simulation methods to achieve high recovery and low SOR.

Another important design parameter in steam injection project is steam quality. One simulation study indicated that high steam quality would improve both the cumulative production and production rate for heavy oil reservoirs. The same study showed that steam quality to some degree was not significant for light oil reservoirs and similar steam.

Field Pilots and Simulation Studies

The performance of steam injection projects in three heavy oil carbonate fractured Middle Eastern fields will be reviewed in this section. In addition, the results of two simulation studies of one light oil fractured carbonate field and another heavy oil fractured carbonate field will be discussed.

Issaran Field, Egypt (Waheed et al. 2001) (Samir 2010)

Issaran oil field, with an area of 20,000 acres located in 290KM southeast of Cairo and 3KM inland from the western shore of the Gulf of Suez, was discovered on 1981. From nine wells, the cumulative oil produced up to 1998 was 0.7 MMbbls. The total oil produced made the overall recovery factor less than 1%. The small volume of oil produced reflects the difficulties and big challenges to produce this field. This field as shown in **Fig. 4** consists of five formations: Zeit sand formation, upper dolomite formation, lower dolomite formation, Gahrandal formation, and Nukhul formation. Zeit Formation considered as a massive sandy formation, Upper and Lower dolomite could not be produced naturally due to the low pressure, Gahrandal formation consists of three limestone and the last formation is Nukhul formation which can be produced naturally due to the existence of naturally fractures. One of the biggest challenges with this field is that it consists of several zones and each zone has its own unique properties and characteristics. This means that new technologies must be applied to solve the potential problems and optimize the production and reserve.
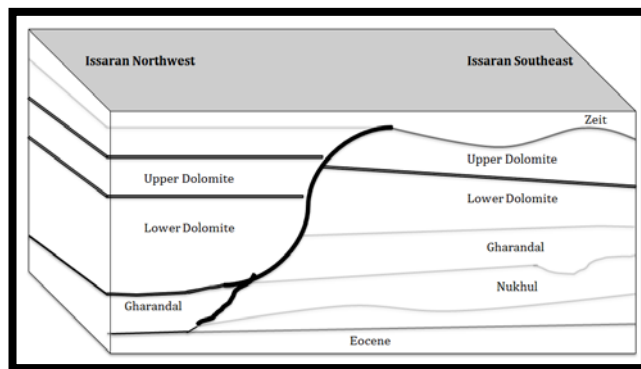

FIG. 4 ISSRAN FIELD FORMATION (Samir 2010)

The general properties that these zones share are; oil type, oil contents and pressure. The average gravity of oil exists in all zones is between 10 to 12 API with a viscosity up to 4000 cp at standard conditions. The oil also consists of 10% H_2S, 10% CO_2, and asphalting content around 15%. Moreover, the pressure of all zones is very low and considered being below the normal gradient. All these characterizations make it difficult to produce the field naturally.

According to Samir in 2010, out of five formations, three formations have been produced by applying

cyclic steam injection. First formation is Zeit sand formation which has a 12 ft as a pay zone. Second is the upper dolomite which is characterized by a depleted fractured dolomite reservoir and has an average thickness of 400 ft, with the top of the formation located at 1,000 ft and has an average pressure of 250 psia. The third formation is the lower dolomite formation located at 1,500 ft and has almost same characteristics and an average thickness as the upper dolomite formation. Both the upper and lower dolomite formations have been produced by applying cyclic steam injection technology. The Issaran Field cumulative production has increased after applying the new technologies and the right reservoir management practices from 1.5 MMSTB (oil produced since the field was discovered and before applying the new techniques) to more than 10 MMSTB during the last 10 years. Moreover, for the upper and lower dolomite formations, the steam injection project is considered the first successful cyclic steam project in the Middle East.

Qarn Alam Field, Oman (Macaulay et al. 1995) (Penney et al. 2007) (Penney et al. 2005)

Qarn Alam Field was discovered in 1972. It was located in central Oman south of the western Hajar Mountains. This large accumulation of 16 API oil with a viscosity of 220 cp was trapped in shallow Cretaceous limestone units at a depth of around 656-1312 ftss with an initial pressure of around 6527 psi at around 1,100 ftss. The field was put on primary production in 1975. The reservoir rock properties of this field were showing a limestone formation with 29% porosity and low permeability in range of 5-14 md. The historical primary production of this field, which was from1975 to 1995, showed a large peak in oil during the first year. Then, the field showed a reduction in the oil rate to a very low sustainable rate. The large amount of oil produced in the first year was caused by the fracture network as a major contributor and the fluid expansion caused by the pressure reduction as a minor contributor. Some of the field characteristics such as low matrix permeability and high oil viscosity made the primary recovery of Qarn Alam Field to be very small. It was expected to be only 3-5 % of the original oil in place. Due to the intensely fractures observed in the field, recoveries using matrix floods of water, polymers or steam were discounted as development options. To overcome the low productivity of the field, number of attempts has been tried. A trial of hot water injection to reduce the oil

viscosity and therefore increase the oil mobility in 1980s failed to provide any improvement in production. As another option to resolve the problem was to initiate a Crestal Steam Pilot, Thermally – Assisted Gas Oil Gravity Drainage (TA-GOGD), in 1996.

TA-GOGD process can be described as follow:

- As the steam is injected into the formation, the oil at the top of the matrix block is heated up by conduction of heat from the fractures into the matrix.

- Then, steam injected heats up oil gradually deeper in the matrix block.

- As a result of heat transfer into the matrix, two oil zones exist: hot (less viscous) oil zone and cold (high viscous) oil zone. The hot oil starts draining down the matrix at an accelerated rate until it faces the cold oil zone.

- Because the cold oil (high viscous) acts as a flow barrier in a similar way to a vertical permeability barrier, hot oil (less viscous) will flow out of the matrix into the gas filled fracture system.

- After the oil enters the fracture system, the gravity will force the oil to flow downward into the oil rim. **Fig. 5** shows a schematic of all steps during TA-GOGD process.
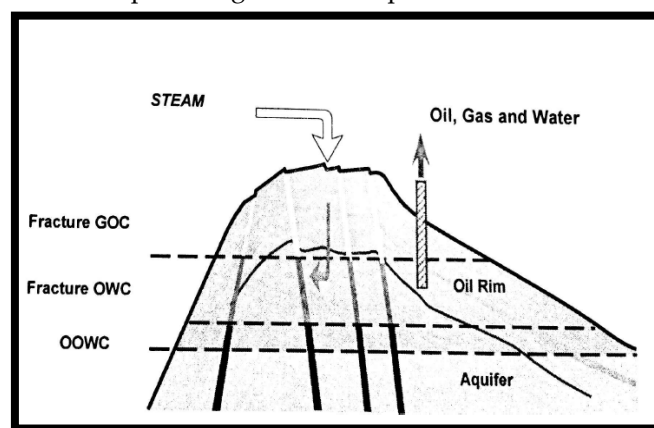

FIG 5 TA- GOGD PROCESS SCHEMATIC (Penney et al. 2005)

In a fractured low permeability carbonate reservoir, TA-GOGD of the Qarn Alam was considered to be the world's first full field development thermal project. A study had been conducted to evaluate the performance of TA-GOGD and compare it with GOGD mechanisms. It showed that the recovery factor under steam injection of 18000 tonnes per day would be in the range of 20-35% of the original oil in place. The oil to steam ratio would be in the range of 0.16-0.3 m^3

oil/tone of steam. One of the most advantages of this project was minimizing the number of wells needed to produce the field and hence minimize the development costs. Based on the great results that had been achieved during the pilot test, the project has proved to be viable. Beside the subsurface uncertainties lesson learned during the pilot test, the pilot trial provided significant insight into the engineering design and operational issues.

The Wafra Field, (Kuwait & Saudi Arabia)
(Meddaugh et al. 2012) (Meddaugh et al. 2007) (Hale, 2002) (Brown et al. 2011)

The Wafra Field consists of several reservoirs with different characteristics. The formation of our interest is the First Eocene reservoir, which was discovered in 1953. The First Eocene reservoir is one of the five significant producing reservoirs in the Wafra Field in the Partitioned Zone (PZ), Saudi Arabia and Kuwait; it was put on production in 1954. Among the five important reservoirs producing from Wafra Field, the First Eocene reservoir is the shallowest one, it is located at a depth of about 1,000-1,400 ftss with an average thickness of 750 ft. This dolomite reservoir can be classified as heavy oil reservoir with oil gravity between 13° to 20° API and the oil viscosity in the range of 100-500 cp with a maximum viscosity around 1000-1200 cp. This reservoir has a porosity of 37% and a permeability of 250 md. The original oil in place is 10 billion bbl.

Due to the low productivity and recovery performance of the First Eocene reservoir, a great IOR/EOR opportunity has been suggested to resolve the problem and produce the reservoir. A study conducted to evaluate the possibility of applying continues steam flooding to produce the reservoir. The study was conducted based on a dynamic modeling and economic analysis. The results of the study helped to make the decision to conduct a pilot test to assess the ability and performance of the steamflood to produce the reservoir economically. The pilot test was conducted in two locations in the field: the initial pilot Small Scale Steamflood Test (SST) and the Large Scale Steamflood pilot (LSP). The SST started in 2005 and consisted of a single 1.25-acre 5 spot with a central injector and one temperature observation well. As part of the preparation for the larger pilot test, injectivity tests and water treatment technology were conducted in SSP to assess the performance. The larger pilot test (LSP), which was planned in the very high original oil in place (OOIP), was conducted in 16, 2.5-acre inverted

5 spot patterns. The construction of the LSP project began in 2007 and steam injection started in June 2009 in the lower C Zone (Steam Zone 3). In November 2011, the project was extended to have the steam injection in the middle B Zone (Steam Zone 2). One of the main goals of the (LSP) was to reduce uncertainties in several parameters and features; these uncertainties include:

- Reservoir response to steamflooding
- Steamflood recovery
- Reservoir variability by pattern and by steam zone
- Organizational capability and scale mitigation (e.g. chemical, dosage, delivery system)

Based on the LSP result, a very good response to steam injection has been obtained from both zones, middle B and lower C.

As part of this study to make a proper plan and improve the injection performance for the next steam injection for the entire field, a two-dimensional reactive transport model (2D-RTM) was built to evaluate the interaction between fluid and rock during the injection of high temperature and high pH steams. The results of this model showed that the injection of high quality steam (steam quality >95% and neutral pH) would not negatively impact the injectivity near the wellbore. However, the injection of low quality steam and high pH may result in mineral precipitations, but their capacity to affect injectivity was uncertain.

Reservoir A, Iran (Haghighi and Shabaninejad, 2010)

This part is highlighting the results of a simulation study to assess the performance of steamflooding process in an Iranian highly fractured light oil carbonate reservoir. The reservoir under analysis was named (Reservoir A) with some reservoir properties described in **Table 5**. This reservoir was put on production for about 40 years ago. The reservoir was considered as a good candidate for EOR due to the decline in the oil production rate. To evaluate the performance of different EOR methods as it is shown in **Table 6**, sensitivity analyses were conducted to measure the feasibility of each method to produce the field and enhance the oil recovery. The study was conducted and several parameters were tested and evaluated. These parameters included:

- Producing the reservoir by water flooding or steamflooding.

- Location of new injection wells.
- Appropriate injection time.
- Steam injection rate
- Steam quality
- Injection well perforation.

A study was conducted in a small sector of the field. The main results of this study can be summarized as follow:

- Steam injection process is likely to be economical for producing this reservoir. The results showed that the water flooding can lead to a recovery factor of 10.24% and the steamflooding gives higher recovery factor, 14.17%. **Table 6** gives a comparison among three methods to produce this reservoir.

- Among three injection strategies: the edge water, five spot patterns and nine spot patterns, the injection with five spot patterns results in the highest ultimate oil recovery.

- There is a relation between the oil rate and the injection rate, the cumulative oil production rate increases as steam injection rate increases.

- The result of this study shows that the steam quality has no significant effect on the overall performance of producing the light oil reservoir.

- One of the main operational parameters is well completion. Three strategies were tested to evaluate this parameter: completing the well with perforating four bottom layers, perforating four top layers and perforating all layers. The best completion strategy was found to be completing the well with perforating four top layers.

TABLE 5 SOME PROPERTIES OF RESERVOIR "A"
(HAGHIGHI AND SHABANINEJAD, 2010)

Property (unit)	Value
Area of the reservoir (acre)	3036
Original oil in place (barrel)	1x109
Solution gas density (lbm/m3)	16.49
Dead oil density (lbm/m3)	2.21x10-6
Initial pressure at 7546 ft (psi)	4350
Initial temperature (oF)	172.2

TABLE 6 COMPARISON OF WATER INJECTION WITH STEAMFLOODING
(HAGHIGHI AND SHABANINEJAD, 2010)

Process	Cumulative Oil Production (bbl)	Incremental Oil Production (bbl)	Recovery factor (%)
Natural Depletion	5.4395x108	1.1845x108	9.13
Water Injection	5.5384x108	1.2834x108	10.24
Steam Flooding	5.8661x108	1.7004x108	14.17

Reservoir K- Iran (Bahonar et al. 2007)

This part is summarizing the results of a simulation study to evaluate the performance of steam injection process in an Iranian highly fractured heavy oil carbonate reservoir. The field is located in southwest of Iran at the coast of Persian Gulf. The field which was discovered in 1959 is producing from two main formations: Jahrum and Sarvak. The formation under investigation was Sarvak with initial oil in place estimated to be 2.7 billion barrels. The oil, which is considered as extra heavy oil, has a gravity of 7.24 API with a viscosity of about 2700 cp. The top depth of Sarvak formation is around 3,652 ft with an average thickness of 985 ft, initial pressure of 927 psi and reservoir temperature of 139.3 ^{o}F. Based on a correlation from a core sample of the wells, the porosity ranges between 11-27% and the permeability ranges between 0.2-850 md. The reservoir is considered as a good candidate for EOR due to the low oil API and high viscosity. Sensitivity analysis was conducted to measure the feasibility of each method to produce the field and enhance the oil recovery. The study was conducted and several parameters were tested and evaluated. These parameters included:

- Well spacing, well type pattern type and size
- Capillary pressure.
- Steam injection and oil production rate
- Steam quality
- Injection well perforation.

A study was conducted as mentioned previously in Sarvak formation. The main results of this study can be summarized as follow:

- Steam injection process is likely to be good method for producing this reservoir. The results showed that steam injection could result in higher oil recovery. It was shown that the recovery could be improved from zero up to nearly12%.

- There is a relation between the steam quality and the cumulative oil rate. As steam quality increases, more oil can be produced consequently.

  One of the main operational parameters is well completion. Four strategies were tested to evaluate this parameter. The best completion strategy was found to be producing from the top 3 layers and injecting into the top 3 layers.

- Oil- water capillary pressure must be determined carefully due to its significant effect on the final cumulative oil and water produced.

- Due to the intensive fractures existing in the reservoir, the result of this study stated that the best way to achieve high recovery was to keep a balance between the steam injection rate and the oil produced and to keep the rates as low as possible.

Conclusion

The performance of steam injection projects in three heavy oil carbonate fractured Middle Eastern fields was reviewed in this paper. In addition, the results of two simulation studies of one light oil fractured carbonate field and another heavy oil fractured carbonate field were discussed in the paper. Both the projects and the simulation studies showed promising results. The results of these projects and studies are summarized in **Table 7**.

TABLE 7 STEAM INJECTION PROJECTS IN THE MIDDLE EAST

Field Name	Formation	Method Applied	Result
Issaran Field Egypt	Upper dolomite formation,	Cyclic steam injection	The first successful cyclic steam project in the Middle East. The cumulative production increased from 1.5MMSTB to 10MMSTB.
	Lower dolomite formation	Cyclic steam injection	
Qarn Alam Field Oman	Carbonate formation	TA-GOGD	The recovery factor under steam injection of 18,000 tonnes per day will be in the range of 20-35% of the original oil in place
The Wafra Field (Kuwait & Saudi Arabia)	First Eocene reservoir (Dolomite formation)	Continues steamflooding	Based on the LSP result, a very good response to steam injection has been obtained from both zones, middle B and lower C
Reservoir A Iran	Oil-wet carbonate reservoir	Continues steamflooding (Simulation)	The results showed that the water flooding can lead to a recovery factor of 10.24% and the steamflooding gives higher recovery factor, 14.17%.
Reservoir K Iran	Sarvak Formation carbonate reservoir	Continues steamflooding (Simulation)	The results showed that steam injection could improve oil recovery from zero up to nearly12%

REFERENCES

Al-Hadhrami, H.S. and Blunt, M.J. "Thermally Induced Wettability Alteration to Improve Oil Recovery in Fractured Reservoirs." Paper presented at the SPE/DOE Improved Oil Recovery Symposium, Tulsa, Oklahoma, April 3-5, 2000.

Al-Mutairi, S.M. and Kokal, S.L.. "EOR Potential in the Middle East: Current and Future Trends." Paper presented at the SPE EUROPEC/EAGE Annual Conference and Exhibition, Vienna, Austria, May 23-26, 2011.

Al-Yousef, H. Y., Lichaa, P. M., Al-Kaabi, A. U., & Alpustun, H. "Wettability Evaluation of a Carbonate Reservoir Rock from Core to Pore Level". Paper presented at the SPE Middle East Oil Show, Bahrain, March 11-14, 1995.

Ali, S.M.F. "Current Status of Steam Injection as a Heavy Oil Recovery Method." Journal of Canadian Petroleum Technology 13 (1) (1974): 54-68. Accessed March 3, 2013. doi: 10.2118/74-01-06.

Alikhlalov, K. and Dindoruk, B. "Conversion of Cyclic Steam Injection to Continous Steam Injection." Paper presented at the SPE Annual Technical Conference and Exhibition, Denver, Colorado, USA, Oct. 30-Nov. 2, 2011.

Alshmakhy, A. and B. B. Maini. "A Follow-Up Recovery Method After Cold Heavy Oil Production Cyclic CO2 Injection." Paper presented at SPE Heavy Oil Conference Canada. Calgary, Alberta, Canada, June 12-14, 2012.

Bahonar, M., Ataei, A., Masoudi, R. Mousavi Mirkalaei, S.M. "Evaluation of Steam Injection in a Fractured Heavy-Oil Carbonate Reservoir in Iran." Paper presented at the SPE Middle East Oil and Gas Show and Conference, Kingdom of Bahrain, March 11-14, 2007.

Barge, D.L., Carreras, P.E., Uphold, D.D. et al. "Steamflood Piloting the Wafra Field Eocene Reservoir in the Partitioned Neutral Zone, Between Saudi Arabia and Kuwait." Paper presented at the SPE Middle East Oil and Gas Show and Conference, Bahrain, March 15-18, 2009.

Baviere, M. "Basic Concepts in Enhanced Oil Recovery Processes." Vol. 33, London: Critical Reports on Applied Chemistry, SCI/ Elsevier publishing, London, 1991.

Bennion, D.B., Thomas, F.B., and Sheppard, D.A. "Formation Damage Due to Mineral Alteration and Wettability Changes During Hot Water and Steam Injection in Clay-Bearing Sandstone Reservoirs." Paper presented at the SPE Formation Damage Control Symposium, Lafayette, Louisiana, February 26-27, 1992.

Blevins, T. R. "Steamflooding in the U.S.: A Status Repor." SPE Journal of Petroleum Technology 42(5) (1990): 548-554. Accessed February 17, 2013. doi:10.2118/20401-PA.

Bourdarot, G., and Ghedan, S. G. "Modified EOR Screening Criteria as Applied to a Group of Offshore Carbonate Oil Reservoirs." Paper presented at SPE Reservoir Characterisation and Simulation Conference and Exhibition, Abu Dhabi, UAE, October 9-11, 2011.

BP, "BP Statistical Review of World Energy." June 2012. Accessed November 10, 2012. http://www.bp.com/sectiongenericarticle800.do?categoryId=9037128&contentId=7068555.

Brown, J., Hoadley, S.F., Lekia, S.D.L. et al. "Early Results from a Carbonate Steamflood Pilot in 1st Eocene Reservoir, Wafra Field, PZ." Paper presented at the SPE Heavy Oil Conference and Exhibition, Kuwait City, Kuwait, December 12-14, 2011.

Burger, J., Sourieau, P., Combarnous, M. "Thermal Methods of Oil Recovery." Edition Technip, Paris, France 89, 1985.

Cathles, L. M., Schoell, M., & Simon, R. "A Kinetic Model of CO2 Generation and Mineral and Isotopic Alteration During Steamflooding." Paper presented at the SPE International Symposium n Oilfield Chemistry, San Antonio, Texas, February 4-6, 1987.

Chu, C. "State-of-the-Art Review of Steamflood Field Projects." SPE Journal of Petroleum Technology 37 (10) (1985): 1887-1902. DOI: 10.2118/11733-PA

Dietz, D.N. "Review of Thermal Recovery Methods". Paper presented at the Fall Meeting of the Society of Petroleum Engineers of AIME, Dallas, Texas, Sept. 28- Oct. 1, 1975.

Donaldson, E.C., Chilingarian, G.V., Yen, T.F., Sharma, M.K. "Enhanced Oil Recovery, II Processes and Operation." New York, NY, U.S.A. Elsevier Science Publishing Company INC. Original publication. ISBN 0-444-42933-6, 1989.

Haghighi, M.B., Ayatollahi, S., and Shabaninejad, M. "Comparing the Performance and Recovery Mechanisms for Steam Flooding in Heavy and Light Oil Reservoirs." Paper presented at the SPE Heavy Oil Conference Canada, Calgary, Alberta, Canada, June 12-14, 2012.

Haghighi, M. and Shabaninejad, M. "Feasibility Analysis of the Steam Flooding Process in an Iranian Fractured Light Oil Reservoir." Brazilian Journal of Petroleum and Gas, v.4, p. 147-153 (2010), Accessed June 6, 2013. doi:10.5419/bjpg 2010-0016.

Hale, J.L. "Steamflood Potential for Heavy Oil Carbonate Reservoir in the Partitioned Neutral Zone of Kuwait and Saudi Arabia." Paper presented at Kuwait International Petroleum Conference and Exhibition, Kuwait, 2-5 February, 2002.

Henry, J. Ramey, Jr. "A Current Review of Oil Recovery by Steam Injection." World Petroleum Congress WPC, 1967.

Holladay, C. H. "The Basic Effects of Steam on a Reservoir." Paper presented at the Third Annual Eastern Regional Meeting of the Society of Petroleum Engineers of AIME, Columbus, Ohio, November 11-12, 1966.

Keplinger, C.H. "Economic Considerations Affecting Steam Flood Prospects." Paper presented at the Symposium on Petroleum Economics and Evaluation, Dallas, Texas, February 8-9, 1965.

Macaulay, R.C., Krafft, J.M., Hartemink, M. Escovedo, B. "Design of a Steam Pilot in a Fractured Carbonate Reservoir - Qarn Alam Field, Oman." Paper presented at the SPE International Heavy Oil Symposium, Calgary, Alberta, Canada, June 19-21, 1995.

Malik, S., Zhang, E., Asimi, M.A. Gould, Thomas. "Steamflood with Vertical Injectors and Horizontal

Producers in Multiple Zones." SPE Reservoir Evaluation & Engineering 14 (2) (2011): pp. 161-170. Accessed August 23, 2013. doi: 10.2118/129248-pa

Meddaugh, W.S., Dull, D., Garber, R., Griest, S., Barge D. "The Wafra First Eocene Reservoir, Partitioned Neutral Zone (PNZ), Saudi Arabia and Kuwait: Geology, Stratigraphy, and Static Reservoir Modeling." Paper presented at the SPE Middle East Oil and Gas Show and Conference, Kingdom of Bahrain, March 11-14, 2007.

Meddaugh, W.S., Osterloh, W.T., Gupta, I. et al. "The Wafra Field First Eocene Carbonate Reservoir Steamflood Pilots: Geology, Heterogeneity, Steam/Rock Interaction, and Reservoir Response." Paper presented at the SPE Annual Technical Conference and Exhibition, San Antonio, Texas, USA, October 8-10, 2012.

Milhem, M.M. and Ahmed, K.N. "Performance of a Pilot Cyclic Steam Stimulation Project in Kuwait." Paper presented at the Middle East Oil Show, Bahrain, March 7-10, 1987.

Mollaei, A. and Maini, B. "Steam Flooding of Naturally Fractured Reservoirs: Basic Concepts and Recovery Mechanisms." Journal of Canadian Petroleum Technology 49 (1) (2010): 65-70. doi: 10.2118/132485-pa

Penney, R.K., Lawati, S.B.A., Hinai, R. et al. 2007. "First Full Field Steam Injection in a Fractured Carbonate at Qarn Alam, Oman." Paper presented at the SPE Middle East Oil and Gas Show and Conference, Kingdom of Bahrain, March 11-14, 2007.

Penney, R.K., Moosa, R., Shahin, G.T. et al. 2005. "Steam Injection in Fractured Carbonate Reservoirs: Starting a New Trend in EOR." Paper presented at the International Petroleum Technology Conference, Doha, Qatar, November 21-23, 2005.

Perez-Perez, A., Gamboa, M., Ovalles, C., Manrique, E. "Benchmarking of Steamflood Field Projects in Light/Medium Crude Oils." Paper presented at the SPE Asia Pacific Improved Oil Recovery Conference, Kuala Lumpur, Malaysia, October 8-9, 2001.

Reis, J. C. "Oil Recovery Mechanisms in Fractured Reservoirs During Steam Injection." Paper presented at the

SPE/DOE Seventh Symposium on Enhanced Oil Recovery, Tulsa, Oklahoma, April 22-25, 1990.

Saidi, A. M. "Reservoir Engineering of Fractured Reservoirs: Fundamental and Practical Aspects" edited by Saidi. Total Edition Pressa, Paris, 1988.

Samir, M.A. "Rejuvenation Issaran Field - Success Story." Paper presented at the North Africa Technical Conference and Exhibition, Cairo, Egypt, February 14-17, 2010.

Samir, M. A. "Role of Steam Injection Pressure to Achieve Successful Cyclic Steam Project Issaran Field - Egypt." Paper presented at the North Africa Technical Conference and Exhibition, Cairo, Egypt, February 14-17, 2010.

Shahin, G.T., Moosa, R., Kharusi, B., Chilek, G. "The physics of Steam Injection in Fractured Carbonate Reservoir: Engineering Development Options That Minimize Risk." Paper Presented at SPE Annual Technical Conference and Exhibition, San Antonio, Texas, September 24-27, 2006.

Thum, M., Leith, E.S., Wunnik, J.N.M.V., Mandhari, M.S., Clark, H.P. "Thermal Developments in Petroleum Development Oman's Southern Fields - an Update." Paper presented at the SPE EOR Conference at Oil & Gas West Asia, Muscat, Oman, April, 11-13, 2010.

Trebolle, R.L., Chalot, J.P., and Colmenares, R. "The Orinoco Heavy-Oil Belt Pilot Projects and Development Strategy." Paper presented at the SPE International Thermal Operations Symposium, Bakersfield, California, February 8-10, 1993.

Waheed, A., El-Assal, H., Negm, E. et al. "Practical Methods to Optimizing Production in a Heavy-Oil Carbonate Reservoir: Case Study from Issaran Field, Eastern Desert, Egypt." Paper presented at the SPE International Thermal Operations and Heavy Oil Symposium, Porlamar, Margarita Island, Venezuela, March, 12-14, 2001.

Willhite, G.P. and Green, D.W. Enhanced Oil Recovery, first edition, SPE text book series, Richardson, Texas, 1998.

Utilization of Voronoi Gridding for Simulation of Heterogeneous Discrete Fracture Networks Using Outcrop and X-ray CT

Zuher Syihab[*1], Jianlei Sun[1], Weirong Li[2], David Schechter[2]

[1]Institue Technology Bandung, Indonesia, [2,3]Texas A&M University, Department of Petroleum Engineering, USA

[1]zuher.syihab@tm.itb.ac.id; [2]jianlei.sun@pe.tamu.edu; [3]david.schechter@pe.tamu.edu

Abstract

In this paper, we propose a workflow to simulate fluid flow in discrete fracture networks. This includes fracture characterization using fractal theory and distribution of fracture aperture as determined by X-ray CT scanning of rough fracture surfaces. Voronoi grids or Perpendicular Bisector, PEBI, are then generated using a newly developed algorithm that conforms to fracture patterns as observed on fractured outcrop. Once the fractures and matrix have been gridded, the simulator is benchmarked against conventional commercial simulators. Voronoi grids are generated in a way to align Voronoi edges along fractures. Special treatment has to be taken to populate Voronoi nodes in order to avoid the distortion of Voronoi grids around fracture tips and fracture intersection points. A connection list including geologic information of Voronoi grids can then be generated as an input mesh file to simulate fluid flow using a finite volume discretization based reservoir simulator. Simple gas injection simulation examples show that discrete fractures with variable aperture in individual fractures and non-uniform orientation of the fracture system might be a barrier to fluid flow or enhance conductivity depending on aperture distribution and orientation of the fracture system relative to injector-producer pairs.

Introduction

Dual porosity/permeability models have been extensively used in the petroleum industry to simulate fluid flow through fractured porous media. In the dual porosity model, the matrix is assumed to be the main storage media with no direct flow into the wellbore, and only fractures contribute to the fluid flow. The dual permeability model assumes that fluid flow occurs from both matrix and fractures. However, the assumption behind those idealized models is that the porous media has uniform distributed and well-connected orthogonal fractures, and thus dual porosity/permeability models are not applicable for disconnected fractured media especially when a few large-scale fractures dominate the flow behaviour of the whole reservoir. Therefore, a discrete fracture network model (DFN) is needed to represent the large-scale fractures, where each fracture is modelled explicitly and contributes to the fluid flow.

Since the fracture geometry of DFN is too complex to be modelled and simulated accurately with Cartesian and corer-point grid system, unstructured grids are considered as more suitable discretization schemes. Unstructured grid system such as Voronoi grids (PEBI) was introduced to the petroleum industry by Heinemann (1991). He discussed about the basic grid construction method, and the finite-volume discretization scheme. Verma and Aziz (1997) investigated many aspects regarding reservoir simulation using unstructured grids. It showed how to generate 2D and 3D unstructured grids for simple reservoir geometry. And most importantly, he showed us the well-known $2\frac{1}{2}$ D Voronoi grids, and introduced the concept of grid generation along wells and streamlines. Karimi-Fard, Durlofsky (2003) solved the problem regarding how to discretize fracture networks, and compute transmisibilities. He also introduced the

concept of volume correction to convert grids from the geometrical domain to the computational domain. Prévost and Lepage (2005) introduced the concept of flow-based unstructured grid generation. He mentioned in this paper: "grids are generated to conform not only to geological features but are also used to introduce higher resolution in regions of high flow." More recently, Branets and Ghai (2008) solved the problem of how to treat fracture intersections. In his paper, he proposed to describe 2D features as Planar Straight Line Graphs (PSLG) and to define protection areas around them by placing Voronoi seeds in mirror images. Recently, Romain (2011) introduced the concept of optimization-method based unstructured grid generation to generate quad-dominant grids in 2D and hex-dominant grids in 3D. He simply converted the unstructured grid generation process to an optimization problem, where he implemented an algorithm to find the optimized Voronoi centers. The most important feature of this method is that it can easily incorporate both static information and dynamic information into the meshing process though an anisotropy tensor. Simply speaking, the algorithm uses L_P norm to control cell shape, an anisotropy tensor to control cell density and cell facet orientations.

In the area of Voronoi grid simulation for discrete fracture networks, although some attempts have been pursued, the utilization of Voronoi grid systems, particularly to represent realistic fracture networks from outcrop data and aperture distribution provided by laboratory experiments (X-ray CT Scan) has not been investigated yet.

In this paper, we will first discuss about how to extract fracture aperture distribution using X-ray CT scanning and how to use fractal theory (Voss 1988; Davy 1990) to represent fracture networks, which is followed by detailed techniques for gridding a single fracture, fracture intersections and fracture tips, as well as incorporation of fracture aperture distribution. Finally, we will demonstrate these techniques with three examples, each for a single fracture, isolated fractures, and connected fractures.

Characterization of DFN

Fracture networks can be obtained by a variety of approaches such as fractal theory and outcrop analysis. In this study, discrete fracture networks were generated by running 2D fractal codes developed by Kim (2007). The discrete fracture network consists of

line segments. Each line is represented by two pairs of (X, Y) coordinates. Then log-normal or fractal fracture aperture distribution can be applied for each individual fracture.

Fracture aperture distribution can be obtained from X-ray CT-scanning experiments or assumed as a random distribution. Based on our previous research (Muralidharan 2004), we could build a relationship between the fracture aperture distribution and integration of the CT signals along the fracture from X-ray CT-scanning experiments as follows:

First of all, an artificially fractured rock was CT-scanned with different sizes of feeler gauges to create a known fracture aperture. Then a graph of CT number vs. sizes of feeler gauges (i.e., aperture in the direction perpendicular to the fracture) was constructed as seen in Figure 1a. Then we need to establish a calibration curve, which is simply a linear relationship between the fracture aperture and the integration of the CT signals in Figure 1A along the fracture. Figure 1B is the computed calibration curve, in which if a CT signal is given, the authors can read its corresponding fracture aperture value in the ordinate.
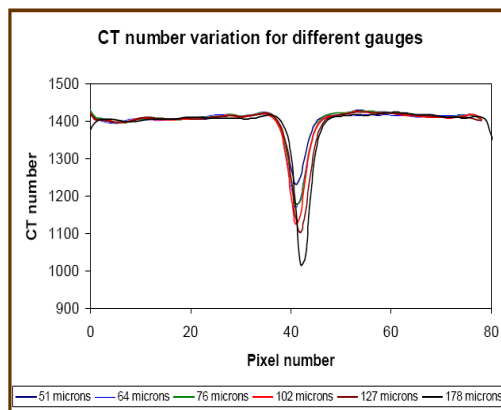

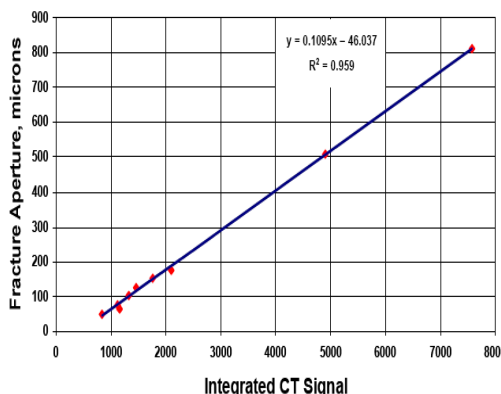
FIG. 1A CT NUMBER VS. DIFFERENT FILLER GAUGES

FIG. 1B FRACTURE APERTURE VS. INTEGRATED CT SIGNAL

(Muralidharan and Chakravarthy 2004)

Voronoi Grid Generation

Given a set of points in a plane, the initial step to generate Voronoi grids is essentially to build a Delaunay Tessellation, since the Voronoi grids are also considered to be the dual structure of the Delaunay triangles (DTs). The Delaunay triangulation is a collection of edges satisfying an "empty circle" property. For example, Figure 2 shows an example of the incorrect DTs, where a unique circle passing through three vertices of a triangle is containing one point in the system.
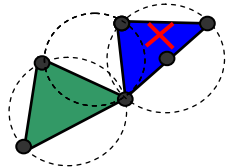
FIG. 2 INVALID DELAUNAY TRIANGLE CONTAINS AN EXTRA POINT WITHIN A CIRCLE

Once the Delaunay triangulation process has been finished, Voronoi grids can be finally generated by the perpendicular-bisectors of the edges of the DTs. Due to this property, the Voronoi grid is also called perpendicular-bisector (PEBI) grid.

In our workflow to generate Voronoi grids for discrete fracture networks, we firstly populate cell centers for the fractures and their intersections as well as the matrix blocks. Those cell locations can be generated either manually or by calling pre-defined functions such as random (), rectangular (), hexagonal (), radial () or hybrid (). Finally, we can execute the Voronoi algorithm with all the cell locations of fractures and matrix blocks as input information. Additional nodes representing the cell centers of fracture blocks are added and volume correction should be carried out.

Placement of Voronoi Nodes for a Single Fracture

A single fracture is represented as a straight line. In order to conform to the fracture geometry, we need to place Voronoi nodes and align Voronoi edges along the fracture in a specific manner. First ,we divide a fracture into several segments (e.g. eight as seen in Figure 3). Then, several pairs of nodes are evenly distributed perpendicular and equidistant (emphasized by the circles) with the fracture. The location of each pair of nodes is determined by the following two steps. First, we draw a virtual small circle with the middle point of each segment as the circle center. Then, we draw lines perpendicular to the fracture and passing through the center of each segment. From the equation of each circle and its corresponding perpendicular line equation, we can solve for the coordinates of each pair of nodes.

Treatment of Fracture Intersections

For discrete fracture networks formed by multiple intersecting fracture sets, each single fracture is still treated as a straight line segment. Away from intersection points of fracture line segments, nodes can be still distributed similar to a single fracture as discussed in the previous section.
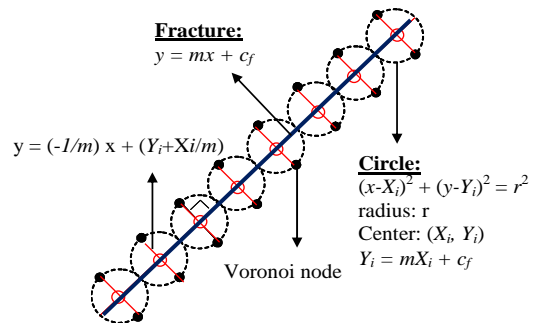
FIG. 3 PLACEMENT OF PAIR OF VORONOI NODES FOR A SINGLE FRACTURE IN THE GEOMETRICAL DOMAIN

For intersection points, different methods need to be carried out to avoid distortion of Voronoi edges along each single fracture. For example, in Figure 4, two fractures (labelled as fracture 1 and fracture 2) intersect at a single point. Points 1 to points 8 are nodes of control volumes, with point 1 and point 2 being a mirror image with respect to Fracture 2, similarly for point 5 and point 6; with point 3 and point 4 being a mirror image with respect to Fracture 1, similarly for point 7 and point 8. F (1, 2) and F (2, 1) are virtual lines which divide fracture sets into the same angles. In order to avoid the distortion of Voronoi edges, the points sited on the region between two fractures, for example, point 1 and 8, 4 and 5 have to be pairs of mirror images with respect to F(1,2) , and point 2 and 3, 6 and 7 have to be pairs of mirror images with respect to F(2,1).
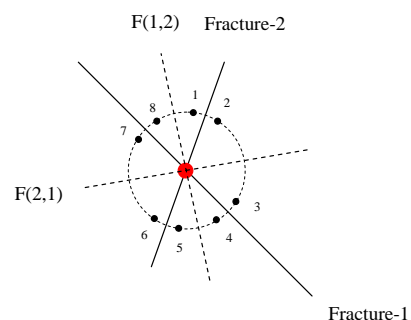
FIG. 4 PLACEMENT OF PAIRS OF VORONOI NODES AROUND A FRACTURE INTERSECTION POINT

Treatment of Fracture Tips

Figure 5 shows a single fracture with and without fracture tip treatment. Without treating fracture tips, the fracture length generated by the Voronoi algorithm may not be accurate, which results in the extension of Voronoi edges and inaccurate volume of fractures. Therefore, an additional node for each fracture tip is required in order to terminate the Voronoi edges at the correct location. Each additional node is located on the extension of the fracture, and should be passing through a virtual circle (blue circle in Figure 5) centered at the fracture tip.
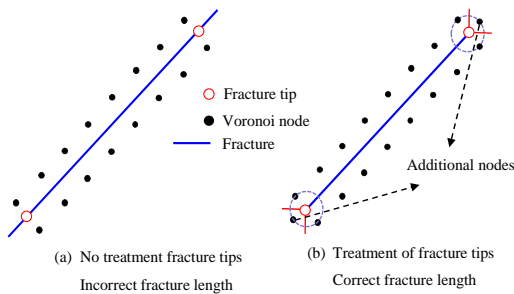
FIG. 5 TREATMENT OF FRACTURE TIPS TO TERMINATE VORONOI EDGES AT BOTH ENDS OF FRACTURES

Incorporation of Fracture Aperture Variations

The method described in the previous sections is merely to generate Voronoi grids for the geometrical domain, where fractures are simplified as line segments without aperture distribution. In order to incorporate known distribution of fracture aperture (e.g. log-normal distribution), thickness and fracture roughness, we need to add additional fracture grid blocks for each fracture line to convert the Voronoi grids from the geometrical domain to the computational domain. For example, in Figure 6, we have three fracture line segments connected with six matrix grid blocks in the geometrical domain. The bulk volume of the fracture grid blocks in the computational domain can be computed based on given fracture aperture distribution. Simply speaking, the bulk volume of matrix blocks directly connected to fracture segments should be decreased by half the bulk volume of the fracture grid blocks.

For the geometry illustrated in Figure 6, d1 and d2 are the distances from the block A and D in the geometrical domain. After the volume correction, due to the aperture of the fracture (d_f), the distances become $d_{1'}$ and $d_{2'}$ in the computational domain. We can express the relationship between the original volume, V and the corrected volume, V' of a particular matrix gridlock by the following equation

Discrete Fracture Network (DFN) Simulator

In order to run simulations for unstructured Voronoi grids, a finite volume discretization scheme based DFN simulator was developed.
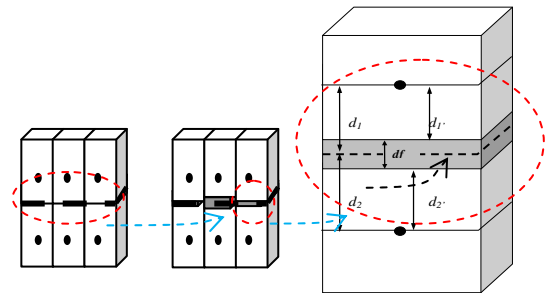

FIG. 6 ADD FRACTURE GRID BLOCKS AND MODIFY MATRIX BLOCK VOLUME TO HONER AN APERTURE DISTRIBUTION

$$V' = \left(1 - \frac{1}{2}\frac{d_f}{d}\right)V \qquad \text{........ Equation 1}$$

The implementation structure of the DFN simulator (fully implicit, 3D, 3 phase, and black oil simulator) developed in this study is illustrated in Figure 7. First of all, we have to create control volume (CV) objects. Each CV object contains a connection list, a connection type, a PVT ID, and a rock ID, among which connection list is the most important since it contains the geometric information of the Voronoi cells. For a given time step, flow coefficients can be calculated from the CV objects and used to construct residual equations and a Jacobian matrix. Once the Jacobian matrix is solved by any iterative solver, solutions will be checked against a given convergence criteria. If convergence is satisfied, the simulator will move onto the next time step until it reaches the total simulation time, otherwise the flow coefficients as well as the Jacobian matrix will be recomputed with updated fluid and rock properties and repeat the matrix solver process.
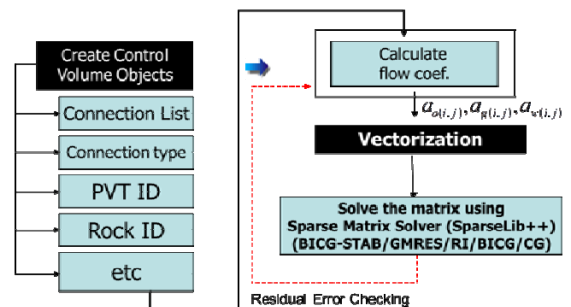

FIG. 7 IMPLEMENTATION STRUCTURE OF THE SIMULATOR FOR THE DISCRETE FRACTURE NETWORK

The DFN simulator has already been validated against analytical solutions of pressure transient analysis and commercial simulators for homogeneous and heterogeneous cases (Syihab 2009).

Simulation Results and Discussions

Example 1: Gridding a Single Fracture from CT Scan Measurements

In this example, we will demonstrate how to apply the previously discussed techniques to generate Voronoi grids for a fractured core sample from a CT scan experiment (Muralidharan 2004). A fractured core sample is shown in Figure 8, where the dark color represents an artificial fracture created in the lab. After CT scanning, a log-normally distributed fracture aperture is determined, and used as input information to convert Voronoi grids from the geological domain to the computational domain.

A connection list would be generated from the Voronoi grids, and used as an input mesh file to simulate water injection into this single fracture system as Muralidharan et al. did in their paper. Instead of running a simulation for the simple water injection case, in this paper, we will extend this approach to simulate gas injection into an isolated fractured system, and a connected fractured system in the following two examples.
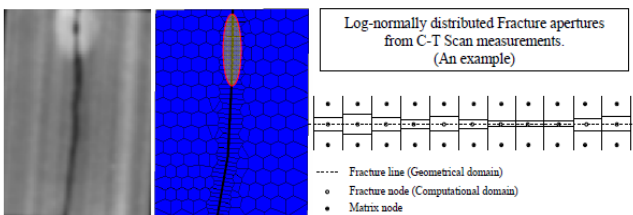
FIG. 8 A GRIDDED REAL CORE SAMPLE IN THE GEOMETRICAL DOMAIN AND COMPUTATIONAL DOMAIN

Example 2: DFN Simulation of Isolated Discrete Fractures

A relatively small 2D model with the dimension of 100 ft x 100 ft x 20 ft was built with six vertical fractures. Each fracture has a different length and orientation and they are not intersecting each other (isolated fractures). Fracture apertures are log-normally distributed with the mean of 0.01 ft and $\sigma^2 = 1.0$.

Initially, only the fractures are gridded as seen in the left part of Figure 9. After matrix refinement, we have a model of 580 grid blocks (control volumes). Since the number of control volumes to represent the fracture grid blocks in the computational domain is 40, the total number of control volumes is 580 + 40 = 620.

The matrix permeability is 100 md, and log-normally distributed permeabilities (ranging from 0.25 md to 1500 md) applied for six isolated fractures. Rock and

fluid properties are from SPE-1 comparison case. A producer is located in the bottom-left corner, while a gas injector in the top-right corner. The simulation is run for 2 years with a constant oil production rate of 2 STB/D and a constant gas injection rate of 3000 SCF/D. For comparison, a model with no fracture was also simulated to demonstrate the differences of pressures and saturation profiles due to the presence of isolated fractures.
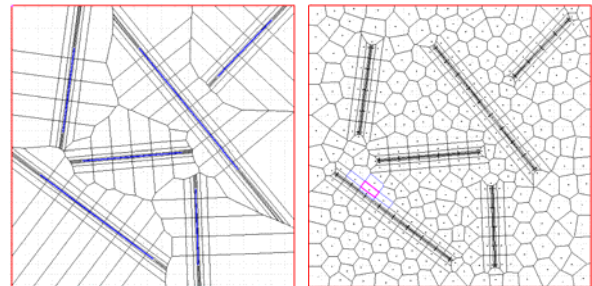

FIG. 9 ISOLATED FRACTURES WITH ONLY FRACTURES GRIDDED AND WITH BOTH THE FRACTURES AND MATRIX GRIDDED

From the simulation results (Figure 10 to Figure 13), it is clearly seen that the fractures act as both conduits and barriers for fluid flow since fracture aperture is small and fracture orientation random in this case. At early time (time = 1 day), pressure plots in Figure 10 shows a higher pressure region in the top right corner due to the gas injection than that of when no fracture exists. A similar conclusion can be reached from the saturation plot in Figure 11. This observation is more obvious from the simulation results at 2 years. In Figure 12, injected gas in fact bypasses the reservoir area behind the fractures, displacing more oil as seen in Figure 13 close to the top and bottom boundary into the lower left oil producer. Figure 14 and Figure 15 are the plots of GOR, block pressures, oil and water saturation at the end of simulation (time = 730 days). Due to the presence of isolated fractures as barriers, GOR and water saturation increases slightly slower than the case when no fracture exists. On the contrary, block pressure and oil saturation for isolated fractures are still higher at the end of the simulation.
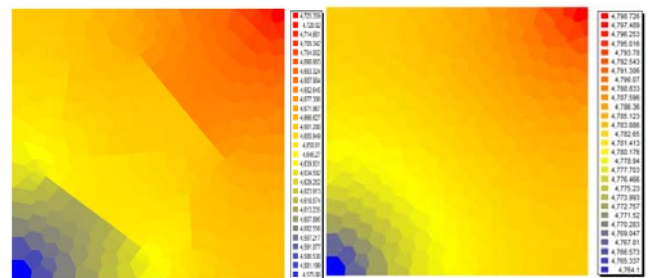

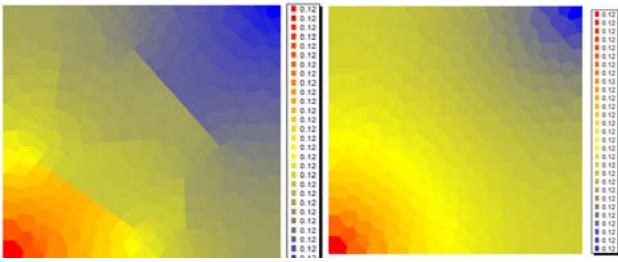FIG. 10 PRESSURE FIELD AT T = 1 DAY (ISOLATED FRACTURES AND NO FRACTURE)

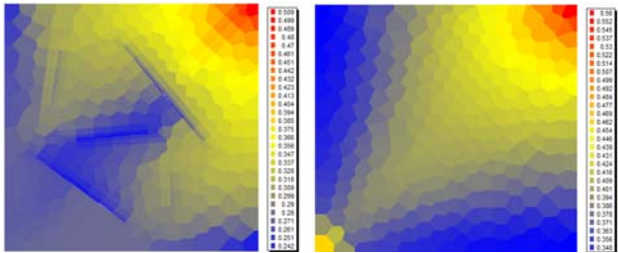FIG. 11 WATER SATURATION AT TIME = 1 DAY (ISOLATED FRACTURES AND NO FRACTURE)

FIG. 12 GAS SATURATION AT TIME = 730 DAYS (ISOLATED FRACTURES AND NO FRACTURE)
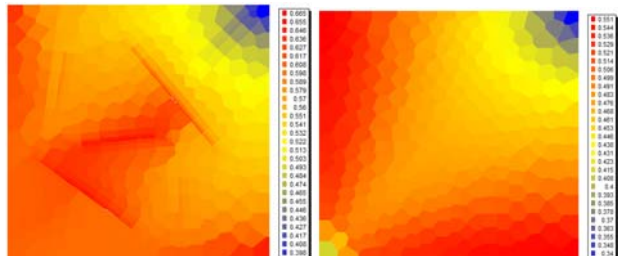

FIG. 13 OIL SATURATION AT TIME = 730 DAYS (ISOLATED FRACTURES AND NO FRACTURE)
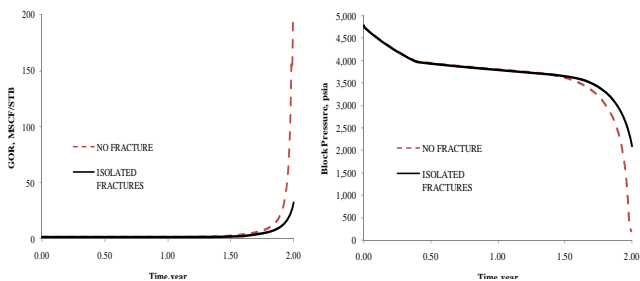

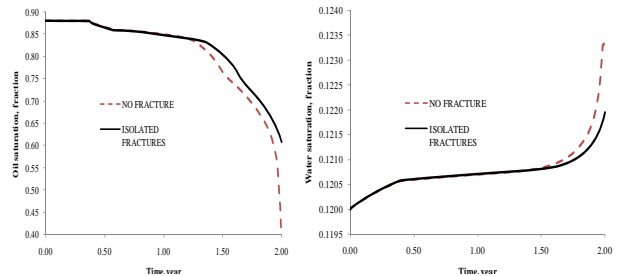FIG. 14 GOR AND BLOCK PRESSURES AT PRODUCER (ISOLATED FRACTURES AND NO FRACTURE)

FIG. 15 OIL SATURATION AND WATER SATURATION AT PRODUCER (ISOLATED FRACTURES AND NO FRACTURE)

Example 3: DFN Simulation of Connected Discrete Fractures

This fracture network is based on fracture patterns as measured in an outcrop with regional extension

fractures. By applying the same method as for isolated fractures and the special approach to populate points surrounding fracture intersections, we grid the DFN in Figure 16A and Figure 16B.

The initial number of control volumes in Figure 16B is 784. After matrix refinement and adding additional grid blocks to fracture segments for conversion from the geometric domain to the computational domain, the total number of control volumes increases to 1593 (1403 for the geometric domain, and 190 for the fracture grid blocks). Figure 17 shows the final simulation grids in the computational domain, and the log-normal fracture aperture distribution incorporated in each fracture segment.
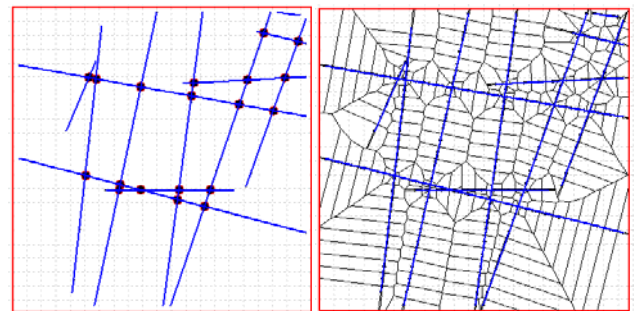

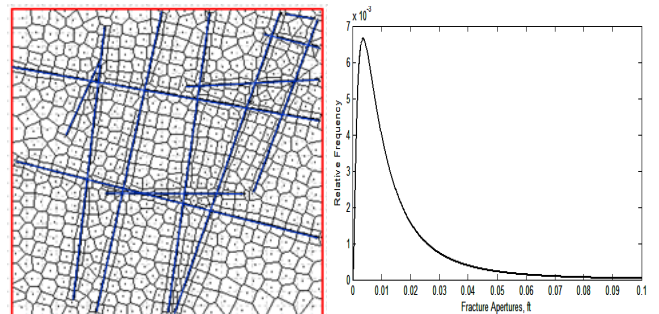FIG. 16 (A) FRACTURE INTERSECTIONS FROM THE DFN (B) GRIDDED FRACTURE NETWORKS

FIG. 17 FINAL SIMULATION GRIDS IN THE COMPUTATIONAL DOMAIN AND THE LOG-NORMAL FRACTURE APERTURE DISTRIBUTION

The fracture permeabilities are computed using the cubic law (Iwai 1976), ranging from 0.1 md to 3000 md. The rock and fluid properties as well as well constraints are exactly the same as the previous case of isolated fractures. Figure 18 to Figure 21 are the plots for pressure, water saturation at 1 day, and gas and oil saturation at the end of the simulation (time = 730 days). Results without fractures which have been used for comparison with isolated fractures in Example 2 are also summarized in the following.

As seen from Figure 18 to Figure 21, due to the variation of conductivities along the connected fractures, the injected gas is more sporadic and stream lines are more distorted compared with the isolated

and no fracture cases. Moreover, we observe that more injected gas displaces the oil at the top of the reservoir to the producer at the left bottom corner, in other words, large-scale fractures dominate the reservoir flow behaviour, and alter sweep efficiency significantly.
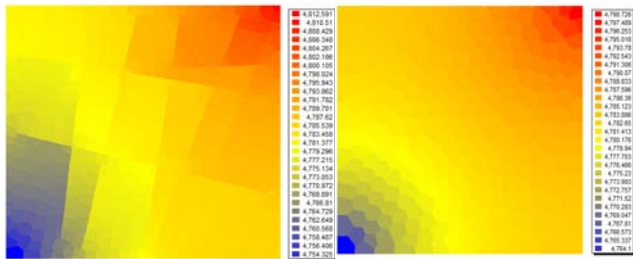

FIG. 18 PRESSURE PROFILE AT TIME = 1 DAY (CONNECTED FRACTURES AND NO FRACTURE)
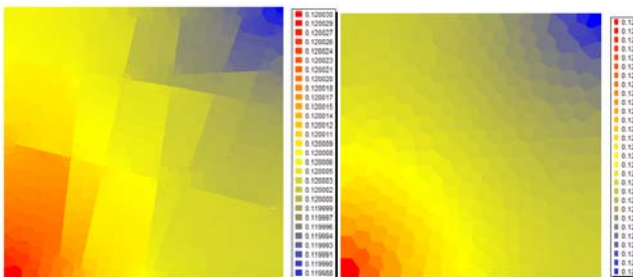

FIG. 19 WATER SATURATION AT TIME = 1 DAY (CONNECTED FRACTURES AND NO FRACTURE)
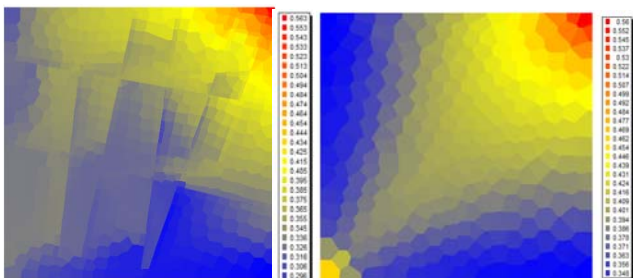

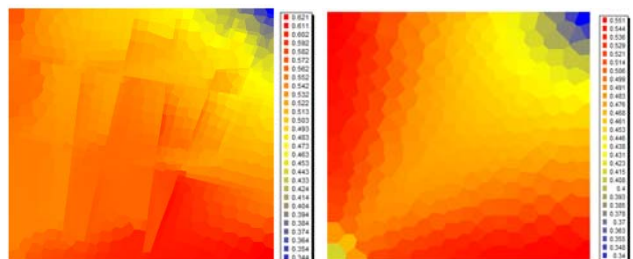FIG. 20 GAS SATURATION AT TIME = 730 DAYS (CONNECTED FRACTURES AND NO FRACTURE)

FIG. 21 OIL SATURATION AT TIME = 730 DAYS (CONNECTED FRACTURES AND NO FRACTURE)

Figure 22 and Figure 23 are the plots of the GOR, block pressure, oil, and gas saturations at the producer. Even though no significant difference is found between isolated and connected fractures, we should be able to see more significant changes if we continued the simulation based on the observation of the pressure and saturation plots of Figure 18 to Figure 21.
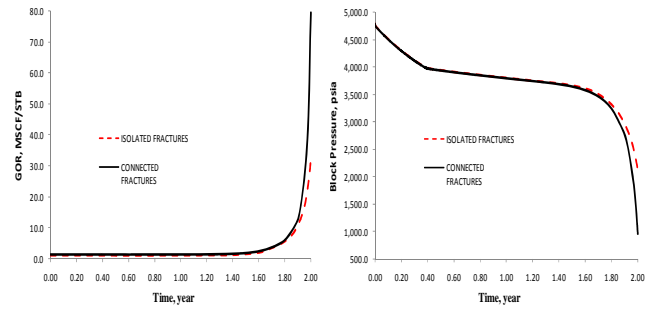

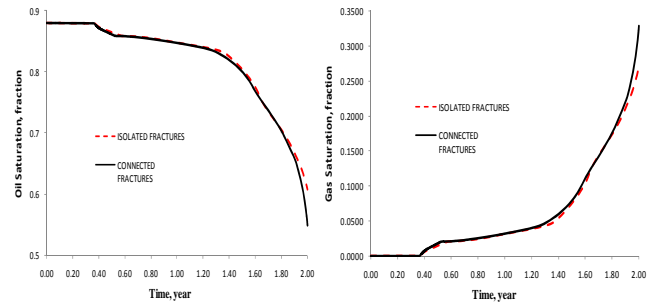FIG. 22 GOR AND BLOCK PRESSURES AT THE PRODUCER (CONNECTED AND ISOLATED FRACTURES)

FIG. 23 OIL AND GAS SATURATIONS AT THE PRODUCER (CONNECTED AND ISOLATED FRACTURES)

Conclusions

A new method for simulating naturally fractured reservoirs has been proposed that incorporates laboratory, geological and petrophysical data to model natural fractures explicitly.

Fracture aperture distribution could be obtained by a calibration curve, which describes the relationship between the fracture aperture distribution and integrated CT signal.

Voronoi grid generation techniques are developed for discrete fracture networks, which mainly comprise of three steps: gridding a single fracture, gridding fracture intersection and fracture tips. This technique incorporates the fracture aperture variation.

Two simulation cases of both isolated and connected fractures show us the significance of large-scale fractures on the reservoir flow behavior. Discrete fractures might be considered as either flow barrier or a conductor depending on fracture orientation and aperture distribution.

REFERENCES

Branets, L.V., Ghai, S.S., Lyon, S.L., and Wu, X.H. 2008. Challenges and Technologies in Reservoir Modelling. Communications in Computational Physics 6: 23.

Davy, P., Sornette, A., and Sornette, D. 1990. Some Consequences of a Proposed Fractal Nature of Continental Faulting. Nature 348 (6296): 56-58.

Heinemann, Z.E., Brand, C.W., Munka, M., and Chen, Y.M. 1991. Modeling Reservoir Geometry with Irregular Grids. SPE Reservoir Engineering (05).

Iwai, K. 1976. Fundamental Studies of Fluid Flow through a Single Fracture: University of California at Berkeley. Original edition. ISBN.

Karimi-Fard, M., Durlofsky, L.J., and Aziz, K. 2003. An Efficient Discrete Fracture Model Applicable for General Purpose Reservoir Simulators. Paper presented at the SPE Reservoir Simulation Symposium, Houston, Texas. Copyright 2003, Society of Petroleum Engineers Inc. 79699.

Kim, T.H. and Schechter, D.S. "Estimation of Fracture Porosity of Naturally Fractured Reservoirs With No Matrix Porosity Using Fractal Discrete Fracture Networks," SPE Reservoir Evaluation & Engineering," April 2009, 232 – 241.

Muralidharan, V., D. Chakravarthy, Putra, E., Schechter, D.S. (2004). Investigating Fracture Aperture Distributions Under Various Stress Conditions Using X-ray CT Scanner. Canadian International Petroleum Conference. Calgary, Alberta, Petroleum Society of Canada.

Prévost, M., Lepage, F., Durlofsky, L.J., and Mallet, J.-L. 2005. Unstructured 3d Gridding and Upscaling for Coarse Modelling of Geometrically Complex Reservoirs. Petroleum Geoscience 11 (4): 339-345.

Romain Merland, B. L., Guillaume CAUMON (2011). "Building PEBI Grids Conforming To 3D Geological Features Using Centroidal Voronoi Tessellations.".

Syihab, Z. (2009). Simulation on Discrete Fracture Network Using Flexible Voronoi Grid System. Petroleum Engineering, Texas A&M University. PHD.

Verma, S. and K. Aziz (1997). A Control Volume Scheme for Flexible Grids in Reservoir Simulation. SPE Reservoir Simulation Symposium. Dallas, Texas, 1997 Copyright 1997, Society of Petroleum Engineers, Inc.

Voss, R.F. 1988. Fractals in Nature: From Characterization to Simulation. In The Science of Fractal Images: Springer-Verlag New York, Inc.

Gas-Oil-Water Production and Water-Gas Injection Forecasts in Williston Basin

Kegang Ling[*1], Jun He[2], Peng Pei[3]

[1,2]Petroleum Engineering Department, University of North Dakota
Grand Forks, ND, USA, 58202

[3]Institute of Energy Studies, University of North Dakota
Grand Forks, ND, USA, 58202

[1]kegang.ling@engr.und.edu; [2]jun.he@my.und.edu; [3]peng.pei@engr.und.edu

Abstract

Production and injection forecasts are of significance in terms of constructing infrastructure to accommodate the booming of unconventional oil and gas development and production in Williston Basin in North American (United States part). Underestimate or overestimate of future production will lead to an inappropriate plan of infrastructure development in this geographic area. Insufficient infrastructure will slow down the growth of hydrocarbon development and affect the revenue from fossil energy and the United States' (U.S.) energy security. Oversized infrastructure will result in waste of investment and leaving large footprint that impacts the environment significantly. Conventionally, production forecast is conducted at well or field level. A thoroughly literature review indicates that no study is available to predict the production of unconventional resource at basin level. To fill this gap, we propose a procedure to forecast the total production of a basin. Our study provides a guideline for forecasting production in a basin with similar geological settings.

Keywords

Bakken Oil; Production Forecast; Unconventional Oil and Gas

Introduction

Recent oil and gas-related growth in Williston Basin, North America (United States part), is affecting the ability to plan for future infrastructure development in North Dakota, Montana and South Dakota. Production and injection forecasts are important in terms of constructing infrastructure to accommodate the boom of unconventional oil and gas development and production. Underestimate or overestimate of future production will lead to inappropriate plan of infrastructure development in this geographic area.

Insufficient infrastructure will slow down the growth of hydrocarbon development and affect the revenue from fossil energy and U.S. energy security. Oversized infrastructure will result in waste of investment and leaving large footprint that impacts the environment significantly.

Conventionally, production forecast is conducted at well or field level. Many studies have been focused on the production forecast. Arps (1945) proposed four types of declines: exponential, hyperbolic, harmonic, and ratio decline. Arps (1956) also estimated the primary oil reserves using decline curves and reservoir drive mechanism. Lefkovits et al. (1958) derived the exponential decline form for gravity drainage reservoirs by neglecting capillary pressure. Fetkovich (1971 and 1980) constructed type curves combining the transient rate and the pseudo-steady-state decline curves, and derived single-phase flow from material balance and Darcy law. Da Prat et al. (1981) derived single-phase oil flow for two-porosity reservoir in closed boundary systems. Doublet et al. (1994) developed the theoretical basis for combining transient and boundary dominated production behavior for the pressure transient solution to the diffusivity equation. Ling et al. (2012) proposed an economical model to optimize horizontal well producing a box-shape oil reservoir with close-boundary. His study showed exponential decline for oil flow at constant bottomhole pressure.   Other investigator conducted research on production forecast. Ehilg-Economides and Ramey (1981), Chen and Poston (1989), Duong (1989), Palacio and Blasingame (1993), Rodriguez and Cinco-Ley (1993), Callard (1995), Agarwal et al. (1999) had published

papers on methods to forecast production. Ling and He (2012) indicated that Arp's empirical production declines had theoretical base. Ling et al. (2013) presented tactics and pointed out pitfalls in production forecast. A thoroughly literature review indicates that no study is available to predict the production of unconventional resource at basin level. To fill this gap, we propose a procedure to forecast the total production of a basin with similar geological setting.

Geological Setting and Production History of Williston Basin

The Williston Basin is a roughly oval-shaped, sub-surface sedimentary basin with the deepest point near Williston, ND. The Williston Basin, an intracratonic basin, is a major structural feature of central North America that covers surface areas between 120,000 and 240,000 square miles (Landes, 1970). The basin reaches approximately 475 miles north-south from southern Saskatchewan to northern South Dakota and 300 miles east-west to western North Dakota and eastern Montana. It underlies most of North Dakota, western Montana, northwestern South Dakota, southeastern Saskatchewan and a small section of southwestern Manitoba (Fig. 1). The Williston Basin began to subside during the Ordovician Period, around 495 million years ago and underwent episodic subsidence throughout the rest of the Phanerozoic Eon. The Phanerozoic Eon extended from approximately 600 million years ago to the present. Although the Williston Basin was subsiding, marine sediments were not deposited in it continuously. The basin contains a complete rock record compared with many basins (Heck et al., 2002). All sedimentary systems from Cambrian through Quaternary are presented in the basin (Fig. 2), with a rock column more than 15,000 ft thick in the deepest section. This nearly continuous deposition of sediments shown in the geologic record makes the Williston Basin one of only a handful of basins worldwide with that distinction.

Several companies explored for oil starting in 1917, and although several wells hit shallow gas, it was not until 1951 that Amerada's Clarence Iverson No. 1 well struck commercial quantities of oil south of Tioga, ND at a depth greater than 11,000 feet below the surface. This discovery led to a boom in leasing and drilling activities in the Williston Basin, especially along the prolific Nesson Anticline. The discovery well was completed in the Silurian Interlake Formation but subsequent development on the anticline focused on

the Mississippian Madison Group. The basin became a major oil province in the 1950s. From 1953 to 1987, vertical wells were drilled to recover the crude oil from Bakken Formation. Successful wells were those that encountered natural fractures which displayed high production at the beginning and soon dropped rapidly to a steady, low level production rate. It has been experiencing a steady and substantial increase in oil production since 2004, when the application of horizontal drilling technologies and stage fracing facilitated the ability to extract oil from previously unviable deposits, the Bakken shales.
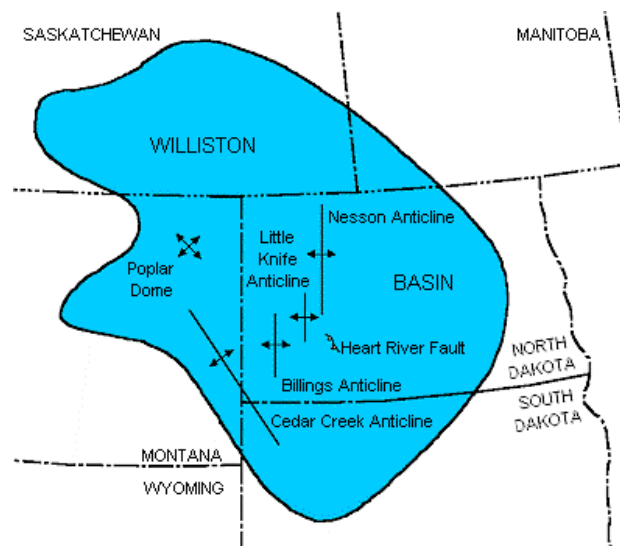

FIG. 1. WILLISTON BASIN AND ITS MAJOR STRUCTURES (HECK ET AL, 2002).

FIG. 2. GENERALIZED STRATIGRAPHIC COLUMN FOR WILLISTON BASIN (HECK ET AL., 2002).

Methodology

Recovery of hydrocarbons from an oil reservoir commonly occurs in three recovery stages, which are primary recovery, secondary recovery, and tertiary recovery or enhanced oil recovery (EOR). Primary recovery occurs in the first stage of a reservoir producing life. At this stage, pressure from the reservoir forces the hydrocarbons from the pores to the formation, moves them to the well, and up to the surface using the natural energy of the reservoir as a drive. The three principal primary recovery drive mechanisms are water drive, gas drives, and gravity drainage. In Williston Basin, all three drive mechanisms and their combinations are of importance. Secondary recovery is the second stage of hydrocarbon production during which an external fluid such as water or gas is injected into the reservoir that has fluid communication with production wells. The injection maintains reservoir pressure and displaces hydrocarbons toward the wellbore. The secondary recovery stage reaches its limit when the injected fluid is produced in considerable amounts from the production wells and the production is no longer economical. The successive use of primary recovery and secondary recovery in an oil reservoir produces about 15% to 40% of the original oil in place. Waterflooding and high-pressure air injection have been implemented in Williston Basin. The primary recovery and secondary recovery account for about 80% of total oil production in Williston Basin. The third stage is tertiary recovery or enhanced oil recovery. It covers gas injection, chemical injection, microbial injection, and thermal recovery. In Williston Basin, CO_2-EOR projects have been successful in recovering huge volume of oil. Tertiary recovery accounts for about 20% of total oil production in the Basin. Oil production from a single well can be the combined result of the two or three recovery methods.

Construction of Typical Well Production Profiles

To forecast the total production of a basin, it is necessary to construct typical well production profile. Economically, a well's life ends when revenue from production cannot cover cost. A well's life can end due to mechanical problems, low reservoir potential, wellbore collapse, producer converted to injector, excessive water production, excessive gas production, or simply an expiration of the lease. In the study of well life, we reviewed geological and petroleum engineering data in the Williston Basin, and identified the reservoir model by integrating geological and engineering interpretations. It was determined that well lifecycles in North Dakota, Montana, and South Dakota were different. Wells in North Dakota and Montana have longer well lifecycle, 25-years, than that of wells in South Dakota, which has a 15-year lifecycle.

The estimated ultimate recovery is critical for a well. A well lifecycle alone is not enough to define the total production of a well, the annual production rate accounts for the remainder. The production rate is controlled by reservoir pressure, size of reservoir, drive mechanism, rock and fluid properties, heterogeneity of reservoir, well spacing, well geometry, recovery method and reservoir energy measurement. Oil and gas production rates decline as a function of time. Loss of reservoir pressure or the changing relative volume of produced fluids is usually the cause. For shale oil and gas, production decline has the characteristics of fast decline rate in the early stages and low decline rate in the late stages.

History matching is the fundamental of production forecast. Statistical analysis and fitting a curve through performance history and assuming this same line trends similarly into the future forms the basis for the decline curve analysis concept. Historical production and injection data was analyzed to identify effects and construct three different typical well production profiles through their expected life for the three regions with a non-linear regression method. Fig. 3 shows the production profiles of typical wells in North Dakota, Montana, and South Dakota. All three declines in production follow hyperbolic decline indicating the typical reservoir performance of shale oil.

Determinations of Drilling Rig Efficiency

Advancements in technology and management optimization will increase rig efficiency, or reduce rig time for each well drilled assuming same well-geometry and reservoir properties. Total rig time, from drilling to completion, includes rig mobilization, rig-up, drilling, completion, demobilization, maintenance, and nonproductive time due to downhole problems. Well stimulation, such as fracking, is performed by a fracking rig and is not counted toward rig time. This study assumes that the average number of wells to be drilled in a single pad in the previous five years will increase as drilling multi-well pads increases. Operators have implemented a batch drilling campaign reducing moving and rig-up times in Williston Basin, however; no significant improvement in moving rigs between
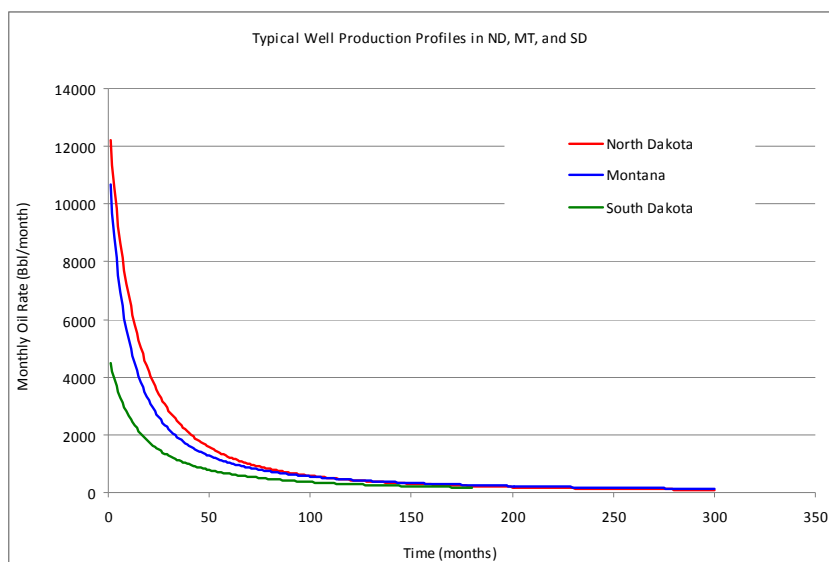
FIG. 3. THE PRODUCTION PROFILES OF TYPICAL WELLS IN NORTH DAKOTA, MONTANA, AND SOUTH DAKOTA

wellheads in the same pad and to different pads is expected. Due to limitations such as winter weather, road weight or clearance restriction, and moving vehicle capacity, the rig-up and demobilization times cannot be substantially reduced; therefore, the percentage reduction in moving and rig-up times is expected to be less than 10 percent over the next 20 years.

Substantial technological advancements and increases in management optimization are necessary for escalating the rate of penetration, or a reduction of the completion time or non-productive time per well and are expected to follow recent historical trends. Assuming similar well geometry and reservoir properties exist throughout the region, without advancements in technology and management optimization, productive time will not substantially increase. The unconventional nature of the Bakken Formation creates a longer learning curve than a conventional reservoir, and the high uncertainty in the reservoir's properties is an obstacle to increase drilling times.

The lateral lengths of existing horizontal wells are shown in Fig. 4 below. Lateral lengths are expected to continue to increase to retain an oil rate that economically justifies the initial costs, and some of the existing rigs in the Williston Basin will eventually need upgrading before drilling the longer lateral length wells. The rig efficiencies from 1998 to 2011 are shown in Fig. 5. The decline in wells drilled per rig, per year during 2005 to 2011 in comparison with the data from 1998 to 2004 is the result of an increase in the overall percentage of horizontal wells. The average

rig efficiency during the 2005 to 2011 period was 8.8 wells drilled per rig, per year. An analysis of the aforementioned factors and information gained from stakeholder interviews resulted in a reasonable forecast of an increase from 10 wells per rig per year in 2012 to 12 wells per rig per year in 2032.

Forecast of Drilling Activity

Annual production volume relies on the number of existing producer and the well to be drilled. Projections of future drilling activity primarily depend upon review of historical drilling activities and assessments of current and near-term drilling climate. Typical drilling plans are controlled by several factors such as the size of reservoir, utility of wellbore, well pattern, well spacing, reservoir flow capacity, recovery method, well life, production plan, drill site preparation, well numbers per drill site, well construction time, drilling rigs availability, labor, and service, drilling and completion cost and oil price. Since most wells in the Williston Base require stimulation, the availability of fracturing equipment and fracturing materials will constrain the drilling plan. Historical drilling activity helps to clarify how the aforementioned factors can affect the drilling activity.

Historical drilling activities are the best indicators of how the above factors affect analysis of drilling plans. In a typical wellbore scenario, well spacing and the well pattern of most reservoirs in the Williston Basin follow development of unconventional shale oilfields in other geographic regions. Reservoir flow capacity after stimulation, drive mechanism, well life, drilling
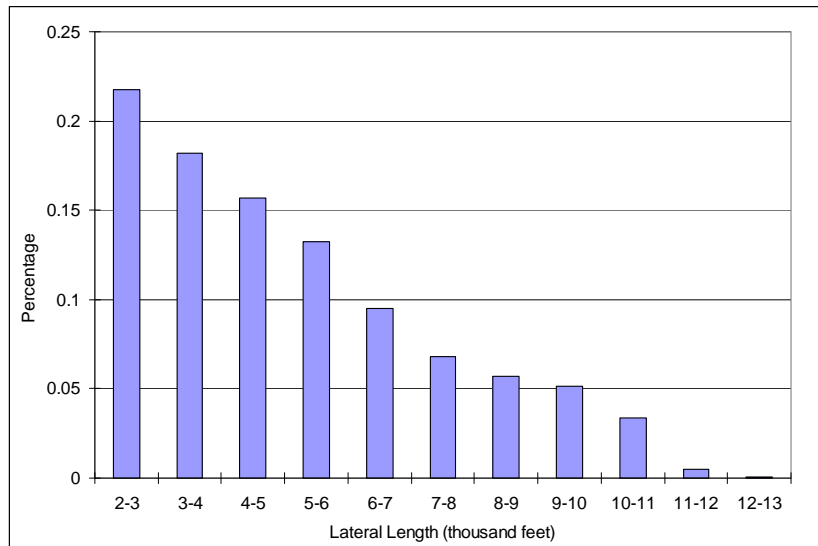
FIG. 4. PERCENT DISTRIBUTION OF DIFFERENT LATERAL LENGTHS OF EXISTING HORIZONTAL WELLS
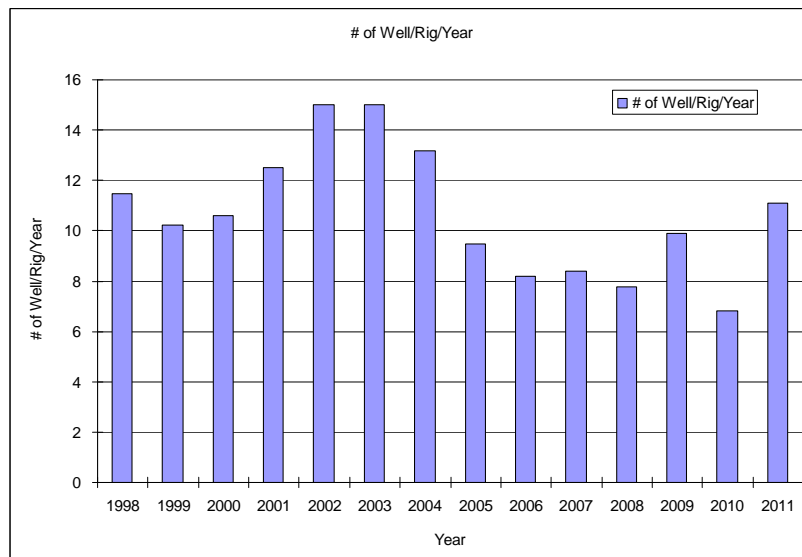

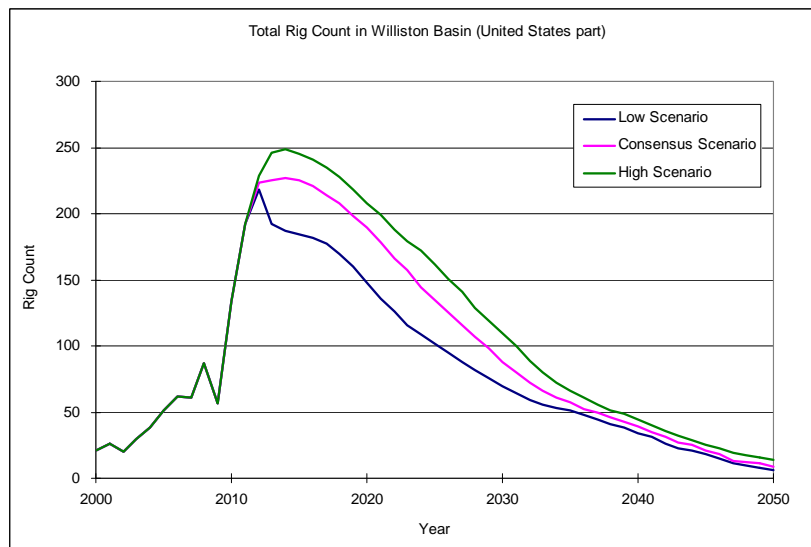FIG. 5. DRILLING RIG EFFICIENCIES DURING 1998-2011

FIG. 6. TOTAL RIG COUNT IN WILLISTON BASIN (UNITED STATES PART)

and completion cost and environmental relief cost are also key factors in the design of drilling plans. The total number of wells to be drilled was phased out according to production plan, the preparation of drill site, well number per drill site, well construction time, and the availability of rigs, labor and service. Effects of a reduction in well construction cost and well complexity on drilling activity were examined. It was found that the reduction of cost was a tradeoff of any increase in well complexity to maintain an economical oil rate. The majority of wells in the Williston Basin require stimulation, therefore the availability of fracturing equipment, fracturing materials and fracking crews acts as a constraint to developers drilling plans.

However, we should notice that the high uncertainty in future drilling activity in Williston Basin is due to two facts: volatile oil prices and the geological nature of the Bakken Formation. A higher than average oil price is a main driver to produce Bakken oil. The high heterogeneity of Bakken shale leads to two-year drilling plans instead of five-year plans, as is common in conventional oil and gas reservoirs. Operator plans for drilling activities beyond one to two years are highly uncertain and rely on the results of new wells in the next two years. Oil prices lower than the economic threshold will reduce or scale back many drilling plans in the Williston Basin, therefore, it is necessary to forecast low, consensus and high scenarios for drilling activity to account for oil price uncertainty and heterogeneity of Bakken shale. Drilling forecasts were estimated for the Williston Basin after studying historical drilling activity, evaluating drilling efficiency, examining the availability of rigs, and reviewing the drilling plans as shown in Fig. 6.

Existing and Undrilled Well Production Forecast

Given the uncertain future of petroleum development in Williston Basin, production forecast scenarios corresponding to three drilling activity scenarios are developed. These probable futures will be largely based on the rate and extent of development of the Bakken/Three Forks shale formation. They will model a robust expansion of the current Bakken/Three Forks shale play, an expected or consensus viewpoint of oilfield development and less than expected expansion of each scenario over a 20-year period.

With the typical well production profiles and future drilling activity, we forecast three production scenarios that are corresponding to the three drilling activity scenarios. Following assumptions are applied in the production forecast:

1) In case of no drilling plans provided by operator, well number/rig/year in the future will be the same as the averaged well number/rig/year in last five years.

2) There is no enough time and manpower to interview all operators in the Basin. The drilling plan from the interview of operators who contracted 80% of rig in the Basin will be extrapolated to get the total drilling activity plan.

3) The time to prepare well site, drill and complete a typical well or wells in a well site will be the same as that of last five years if no such data is available from the operator.

4) The energy required for drilling and completion for each wellsite will be the same as that of last five years.

5) The successful rates of the oil and gas producer are the same as that of last five years.

6) There are enough fracing crews to simulate the new wells if no detail plans are provided by operator.

7) New EOR projects are forecasted only if operators have solid plans.

8) Production profiles of typical well are valid for existing and new wells.

9) Gas-oil ratio, water-oil ratio, and well-life of new well are the same as those of existing wells.

10) Performances of new injectors are the same as those of the existing wells.

11) Water injection follows the historical trend if no data is available from operators.

12) Gas injection trends become flat if no data is available from operators.

13) The energy required producing unit oil, water, or gas keeps constant.

14) The energy required injecting unit water and gas keeps constant.

The forecasts of oil, gas, and water from existing wells follow the steps below:

1) Identify reservoir fluids (gas, oil, gas with oil leg, or oil with gas cap), reservoir properties (low, moderate, or high porosity and permeability), drive mechanism in each region

2) List different regions that are corresponding to

different production profiles in Williston Basin.

3) Existing wells consist of dry holes, producers, water resource wells, gas or water injectors, water disposal wells, monitor/observation wells, and stratigraphic test wells. The percentage of producer is used as the successful rate for future wells production forecast. The study indicates that successful rates are different in three regions

4) Existing active wells are forecasted using typical well production profile.

5) Gas-oil and water-oil ratio trends in three regions: North Dakota, Montana, and South Dakota, are predicted. The gas and water rates are back-calculated using oil rate and gas-oil and water-oil ratios

6) For the same location with different formations, a synthesized single rate will be used since wells producing single layer can be recompleted to produce multilayer thus all wells can produce layers they penetrated

7) The typical well production profiles are applied to both primary and EOR wells.

8) We extrapolate the forecast to the three regions: North Dakota, Montana, and South Dakota, basing on typical production profile, existing well history, and total number of active wells.

9) Gas and water injection profiles follow the historical trend

10) Sum of North Dakota, Montana, and South Dakota productions gives the total production of existing wells in Williston Basin

The forecasts of oil, gas, and water from undrilled wells follow similar steps as existing wells. Typical well production profiles are applied to undrilled wells:

1) Classify undrilled wells basing on locations

2) Start-ups of the undrilled wells are two months after the completion. Initial oil rate and production decline rate follow the typical well production profile derived from existing wells in the same region, historical succeed rates are multiplied to total new well number to get real producer number

3) The production start-up date is not available in the plan, the typical time to prepare well site, drill and complete a well or wells in a well site in Williston basin will be used to estimate the start-up date.

4) Existing wells' gas-oil and water oil ratio trends

are applied to undrilled wells

5) The undrilled well production forecasts in different regions: North Dakota, Montana, and South Dakota, are calculated.

6) Sum of North Dakota, Montana, and South Dakota productions gives the total production of undrilled wells in Williston Basin

The total production in Williston Basin is the sum of productions of existing and undrilled wells.

Production Forecast Results

The grand total production forecasts for gas, oil, and water in Williston Basin is the sum of the productions of existing and undrilled wells. Figs. 7, 8, and 9 show the total production forecasts for oil, gas, and water, respectively.

Water and Gas Injection Forecasts

The Secondary recovery is applied in Williston Basin. Water and gas are injected into reservoirs to both maintain reservoir pressure and displace hydrocarbons toward the wellbore. Water and gas injections require the sources, transportation, injection, separation, and disposal of the injected fluids. Therefore, the implementation of water and gas injection projects depends on a mature infrastructure. The capacity of the infrastructure needs to be able to accommodate the injected fluid volume.

The water and gas injection forecasts base on the historical trends. Regulations require all produced water to meet the environmental requirement before it is disposed. Producers opt to reinject the produced oilfield water back to the aquifer or depleted zone. Some waterflood projects also inject the treated oilfield water back to reservoir to improve the oil recovery. Therefore the total injected water volume is slightly higher than the produced water. The gas injection in some enhanced oil recovery projects will continue the injection. The total water and gas injection volumes in Williston Basin are shown in Figs. 10 and 11.

Comparison of Production Forecast with Production Data

The production forecast was done in August 2012. To evaluate the accuracy of model, we compare the calculated from model with the production data from September, 2012 to September, 2013. Fig. 12 shows the comparison. It is noticed that the difference is very small.
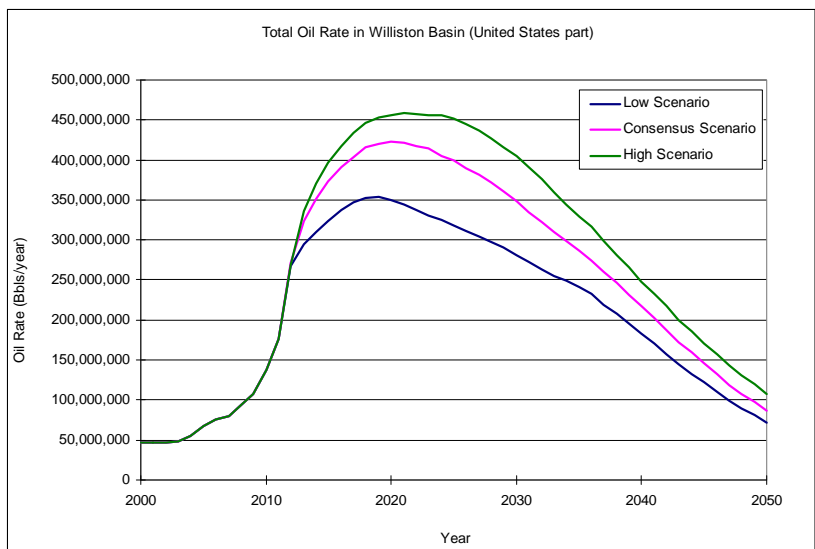
FIG. 7. THE TOTAL OIL PRODUCTION FORECAST IN WILLISTON BASIN (UNITED STATES PART)

FIG. 8. THE TOTAL GAS PRODUCTION FORECAST IN WILLISTON BASIN (UNITED STATES PART)
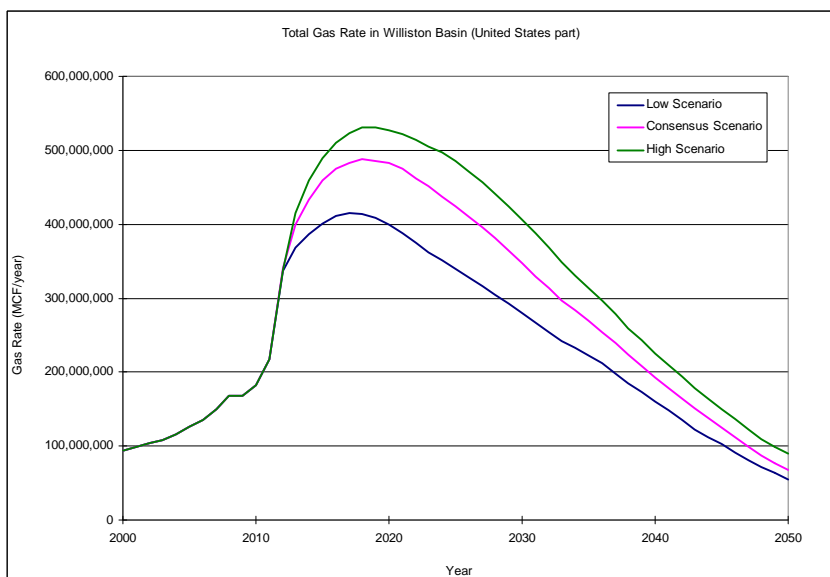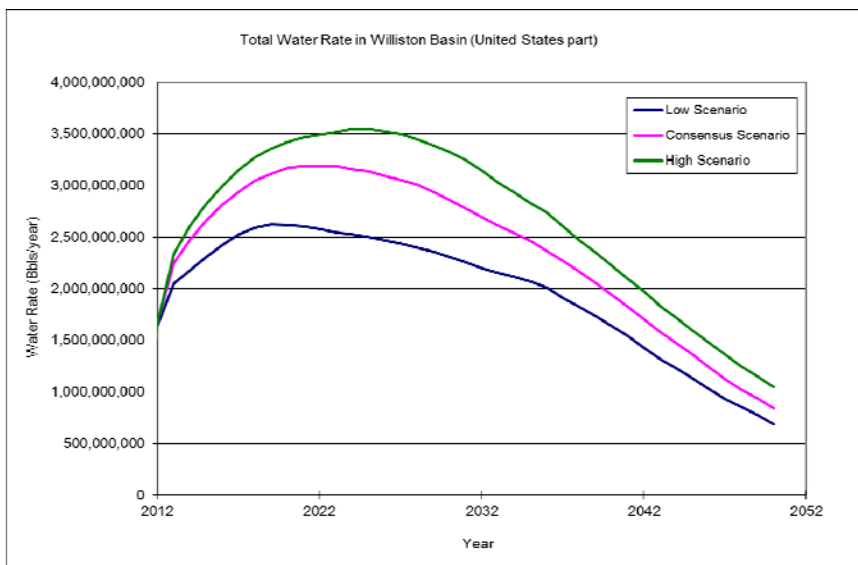

FIG. 9. THE TOTAL WATER PRODUCTION FORECAST IN WILLISTON BASIN (UNITED STATES PART)
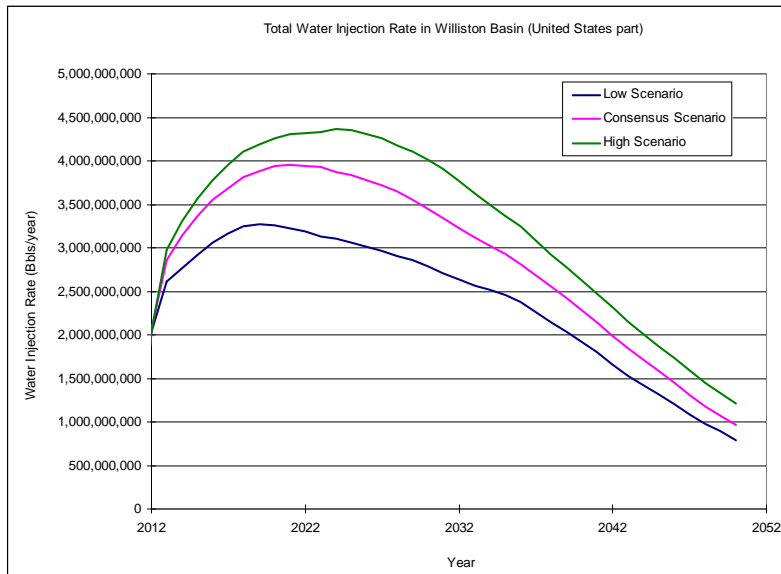
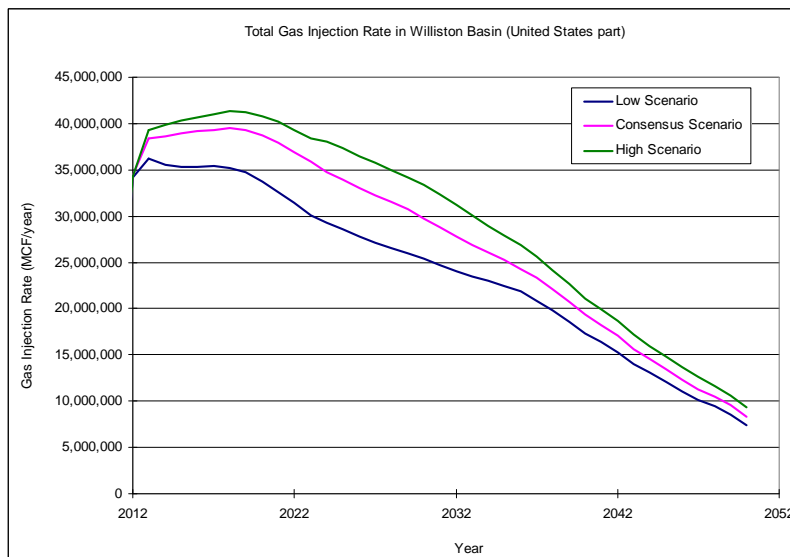FIG. 10. THE TOTAL WATER INJECTION FORECAST IN WILLISTON BASIN (UNITED STATES PART)

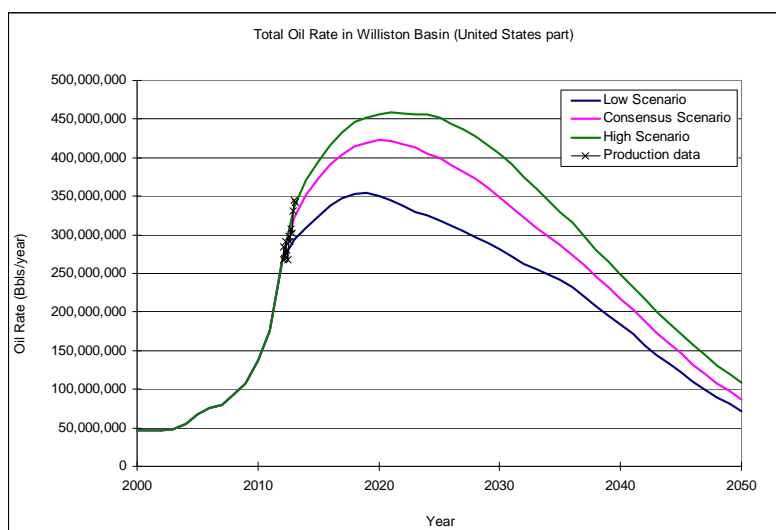FIG. 11. THE TOTAL GAS INJECTION FORECAST IN WILLISTON BASIN (UNITED STATES PART)

FIG. 12. THE COMPARISON OF PRODUCTION FORECAST WITH PRODUCTION DATA IN WILLISTON BASIN (UNITED STATES PART)

Conclusions

We have presented a method to forecast the production of unconventional resource in a basin level.

The production forecast calculated from the model agrees with the production data.

Our study provides a guideline for forecasting production in a basin with similar geological setting.

ACKNOWLEDGMENT

REFERENCES

Agarwal, R.G., Gardner, D.C., Kleinsteiber, S.W., and Fussell, D.D. 1999. Analyzing Well Production Data Using Combined-Type- Curve and Decline-Curve Analysis Concepts, SPEREE, October, 1999, p. 478-486.

Arps, J.J. 1945. Analysis of Decline Curves, Trans. AIME 160, p. 228-247

Arps, J.J. 1956. Estimation of Primary Oil Reserves, Trans., AIME, 207, p. 182-191

Callard, J.G. 1995. Reservoir Performance History Matching Using Rate/Cumulative Type-Curves, paper SPE 30793 presented at the 1995 SPE Annual Technical Conference and Exhibition, Dallas, October 22–25, 1995

Chen, H.Y. and Poston, S.W. 1989. Application of a Pseudotime Function to Permit Better Decline-Curve Analysis, SPE Formation Evaluation, September 1989, p. 421-428.

Da Prat, G., Cinco-Ley, H., and Ramey, H.J. Jr. 1981. Decline Curve Analysis Using Type Curves for Two-Porosity Systems, SPEJ, June 1981, p. 354-362

Doublet, L. E., Pande, P.K., McCollum, T. J., and Blasingame, T. A. 1994. Decline Curve Analysis Using Type Curves-Analysis of Oil Well Production Data Using Material Balance Time: Application to Field Cases, paper SPE 28688 presented at the 1994 Petroleum Conference and Exhibition of Mexico held in Veracruz, Mexico, 10-13 October, 1994

Duong, A.N. 1989. A New Approach for Decline-Curve Analysis, paper SPE 18859 presented at the 1989 SPE Production Operations Symposium, Oklahoma City, Oklahoma, March 13-14, 1989

Ehilg-Economides, C.A. and Ramey, H.J., Jr. 1981. Transient Rate Decline Analysis for Wells Produced at Constant Pressure, SPEJ, February 1981, p. 98-104.

Fetkovich, M.J. 1971. A Simplified Approach to Water Influx Calculations-Finite Aquifer Systems, JPT, July 1971, p. 814-823

Fetkovich, M.J. 1980. Decline Curve Analysis Using Type Curves, JPT, June 1980, p. 1065-1077

Heck, T.J., LeFever, R.D., Fischer, D.W. and LeFever, J. 2002. Overview of the petroleum geology of the North Dakota Williston Basin. North Dakota Geological Survey, Bismarck, ND.

Landes, K. 1970. Petroleum Geology of the United States. John Wiley and Sons, New York.

Lefkovits, H.C. and Matthews, C. S. 1958. Application of Decline Curves to Gravity-Drainage Reservoirs in the Stripper Stage, Trans., AIME, 213, p. 275-280

Ling, K., Han, G., Shen, Z., Zhang, H. 2012. Optimization of Horizontal Well Design to Maximize Recoverable Hydrocarbon, SPE 151531, SPE International Production and Operations Conference and Exhibition held in Doha Qatar, 14–16 May, 2012

Ling, K. and He, J. 2012. Theoretical Bases of Arps Empirical Decline Curves, paper SPE 161767, SPE Abu Dhabi International Petroleum Exhibition and Conference, 11-14 November 2012

Ling, K., Wu, X., Zhang, H., and He, J. 2013. Tactics and Pitfalls in Production Decline Curve Analysis, paper SPE 164503, SPE Production and Operations Symposium held in Oklahoma City, Oklahoma, USA, 23 – 26 March, 2013

Palacio, J.C. and Blasingame, T.A. 1993. Decline Curve Analysis Using Type Curves: Analysis of Gas Well Production Data, paper SPE 25909 presented at the 1993 SPE Rocky Mountain Regional/Low Permeability Reservoirs Symposium, Denver, CO, April 12-14, 1993

Rodriguez, F. and Cinco-Ley, H. 1993. A New Model for Production Decline, paper SPE 25480 presented at the Production Operations Symposium, Oklahoma City, OK, March 21-23, 1993

Kegang Ling is an assistant professor in Petroleum Engineering at University of North Dakota. His research

interests are in the area of production optimization. He holds a BS degree from the China University of Petroleum in geology, an MS degree from University of Louisiana at Lafayette, and a PhD degree from Texas A&M University, both in petroleum engineering.

Jun He is a graduate student at the University of North Dakota. His research interests are in the area of reserve evaluation and reservoir characterization. He holds a BS degree from Southwest Petroleum University in geology, an MS degree from China University of Petroleum in petroleum engineering, and an MS degree from University of North Dakota in Geological Engineering.

Peng Pei is a research engineer at the Institute of Energy Studies, University of North Dakota. He holds a Ph.D. in Geological Engineering from University of North Dakota, and an M.S Mechanical Engineering from University of North Dakota. He also has a B.S. in Mechanical Engineering from North China Electrical Power University. His research area focuses on energy-related rock mechanics.

Microwave Radiation Induced Visbreaking of Heavy Crude Oil

Adango Miadonye[*1], Brittany MacDonald[2],

Department of Chemistry, Cape Breton University, Sydney, NS, Canada

[*1]adango_miadonye@cbu.ca; [2]taffymoe@hotmail.com.

© 2014 Science and Engineering Publishing Company

Abstract

Microwave energy is slowly becoming the most diverse form of energy transfer and has been used in the petroleum industry for inspecting coiled tubing and line pipe, measuring multiphase flow, and the mobilization of asphaltic crude oil. In Canada, efforts have been intensified to develop microwave irradiation technology for in-situ enhanced oil recovery of the country's large deposits of bitumen and heavy oil. The new technology employs specific frequency microwaves targeted into the formation containing heavy hydrocarbons to initiate conversion of the hydrocarbon into synthetic crude. The results of work presented in this report showed strong indications for the microwave technology to be employed not only for hydrocarbon extractions but also for in-situ induced visbreaking of heavy oil and bitumen (to drastically reduce oil viscosity for pipeline transportation without the use of diluents). Overall, the microwave technology presents the best alternative, economically and environmentally, to the existing visbreaking technologies for upgrading of heavy crude oil and bitumen.

Keywords

Heavy Crude Oil; Microwave Energy; Viscosity; Radiation Induced Cracking; Petroleum Visbreaking ;Microwave Sensitizers

Introduction

The application of radiation chemistry in oil industry gained prominence in the early 1960s when only light hydrocarbon substances were used as models in radiation processing experiments (Panchenkov, and Erchenkov, 1980; and Ashton et. al, 1994). Radiation processing was rather expensive then and it was not until the 1990s that the concept of the 'hydrocarbon enhancement electron-beam technology' (HEET) was developed. More recently, microwave irradiation has been used in the petroleum industry for inspecting coiled tubing and line pipe, measuring multiphase flow, and the mobilization of asphaltic crude oil (Gunal, and Islam, 2000; Stanley, 2001; and Zaykina, et. al, 2002). Gunal and Islam (2000) observed permanent alteration of asphaltenes in the colloidal structures of the molecules and an increase in viscosity when exposed to microwave irradiation, due to the re-orientation of molecular structures rather than thermal breakdown. They noted that when exposed to electromagnetic irradiation, the presence of asphaltenes caused permanent changes in crude oil rheology due to the polar nature of asphaltene molecules. Zaykina, et. al (2002) and Zaykin et al. (2004) reported the evidence of much branching and breaking of the paraffin chain during irradiation of paraffinic oil. Thus, microwave heating has been identified to offer numerous advantages such as short start up time, rapid heating, energy efficiency, and precise process control.

Microwave energy can be delivered directly to the reacting or processing species by using their dielectric properties or by adding absorbing material which converts electromagnetic energy into heat. Thus, microwave energy has the ability to crack hydrocarbons and create a method of desulphurization. Through the use of microwave power, along with additives, hydrocarbons high in sulfur content and/or composed of primarily heavy hydrocarbons can be made into useful commercial products which can be burned cleanly and efficiently as a fuel oil, as demonstrated in several patents for the use of microwave irradiation (US Patent 1979, 1988 and 1994).

Materials And Experimental Methods

The visbreaking process was carried out in a 1.1ft[3] domestic microwave oven Dandy model DMW 1048SS

which had been modified to contain a water loop, a reactor (Pyrex glass and Teflon), thermocouples, and a mixer, connected to a products separation and collection system and a computer (for recording temperature and products volume percent during reaction). Also included in the modification was provision for monitoring the temperature and pressure of the process. Table 2 shows the properties of different samples used in the process, which also included refinery residuum and Lloydminster bitumen.

TABLE 2 MATERIALS AND THEIR PROPERTIES

Materials	Properties
Arabian heavy crude oil	°API 27.31, Sulfur content 3.066%
Australian Spirit crude oil	°API 61.2, Sulfur content 0.01%
Bonny light crude oil	°API 33.4, Sulfur content 0.16%
Activated Charcoal	Sensitizer (S2); 12-20 mesh, Laboratory grade; Sigma-Aldrich Canada Co. Oakville, ON.
Palladium Oxide	Catalyst; 99.9 % purity Sigma-Aldrich Inc. St. Loius. MO. USA.
Serpentine	Sensitizer (S1); 98.0% purity Sigma-Aldrich Canada Co. ON.
di-Ethanolamine (DEA)	Polar Additives; purified Fischer Scientific Co., Fair Lawn, New Jersey.

In a typical experiment, heavy crude was mixed with 5 and 10 percent of various proportions of hydrocarbon additives, catalysts and microwave sensitizers (see Table 3).

TABLE 3 TYPICAL FORMULATIONS OF SAMPLES FOR IRRADIATION AND ANALYSES

Oil	Diluent
Arab Heavy Non-Microwaved	-
Arab Heavy Microwaved	10% Diethanolamine
Arab Heavy Microwaved	10% Diethanolamine + Sensitizer 1 or 2 (DEA + S1 or S2)
Australian Spirit Non-Microwaved	-
Australian Spirit Microwaved	10% Diethanolamine
Australian Spirit Microwaved	10% Diethanolamine + Sensitizer 1 or 2 (DEA + S1 or S2)
Bonny Light Non-Microwaved	-
Bonny Light Microwaved	10% Diethanolamine
Bonny Light Microwaved	10% Diethanolamine + Sensitizer 1 or 2 (DEA + S1 or S2)

A 40 gram sample of each formulation was subjected to microwave irradiation for different time periods. The power level and irradiation intensity was at a high level (recorded in this microwave oven as Power Level 10), and the maximum possible irradiation period was

20 minutes. The samples were then examined with GC-MS, to allow for an understanding of compound mass changes along with reduction of compounds upon microwaving. The percent reduction in sulphur contents of the crude oil was also determined. The sample mixtures that were very viscous charred at prolong irradiation periods. Thus, the maximum irradiation period was limited to 20 minutes to avoid excessive loss of volatile components of the samples. The GC instrument is a 5890 Series II Plus Gas Chromatograph coupled with a FID and a 5872 Mass Selective Detector (MS) fitted with a fused silica capillary column.

Results And Discussion

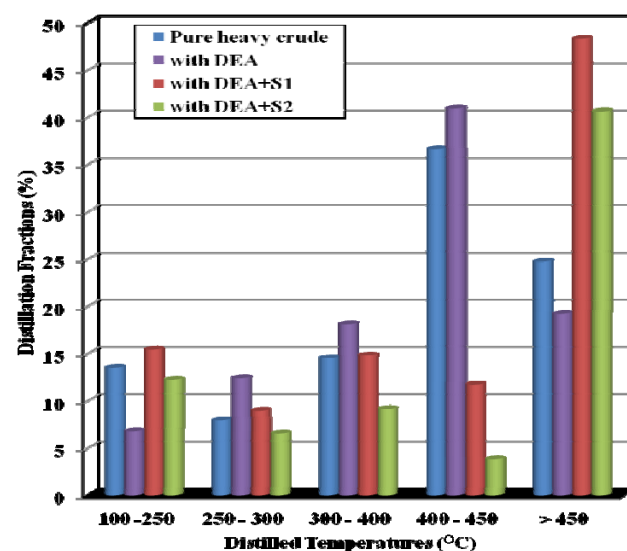### Irradiation Effects on Crude Oil Composition

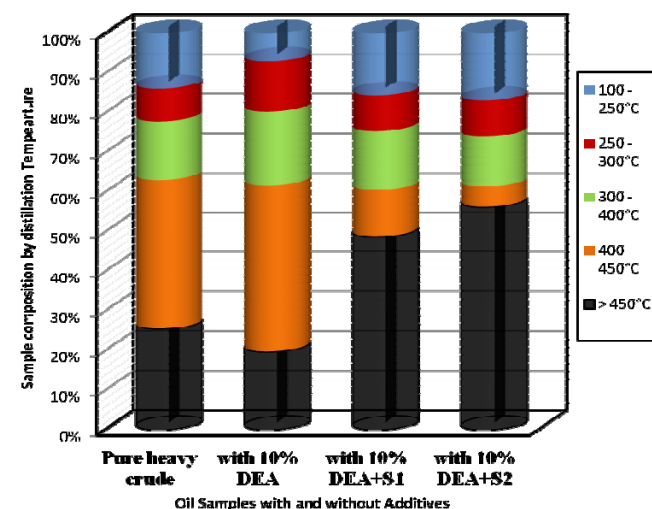FIG.1 COMPARISON OF DISTILLATION FRACTIONS OF IRRADIATED HEAVY OIL

FIG. 2 COMPOSITION OF SAMPLES AFTER 20 MINUTES IRRADIATION

Heavy crude oil was mixed with 5 to 10 percentage of

various hydrocarbon additives, catalysts and microwave sensitizers (S1 and S2). These samples were subjected to microwave irradiation for different time periods. Figures 1 and 2 are the typical distillation fractions of irradiated samples, illustrating the distributions of fractions at different temperature ranges.

As evidenced in the graphs, there were remarkable changes in the composition of each fraction. The irradiated samples containing ethanolamine, sensitizer, and catalyst show reduction in the percentages of lower temperature fractions. In Figure 2, an increase in the heavy fraction (>450°C) is more apparent with samples that contained the sensitizers. As indicated in Figures 1 and 2, the presence of sensitizers and additives improved absorption characteristics of the oil to microwave radiation; identified by the significant shift in molecules distribution to the largest fraction (> 450 each fraction) with sensitizers and an increase in the volume percent of mid-fractions for sample with only polar solvent.

Serpentine (S1) was found to be a poor microwave sensitizer compared to activated charcoal (S2) which gave a better microwave absorption characteristics for the crude oil. The shift to higher molecular weight distribution for crude oil samples is also shown in the GC-MS micrographs (Figures 3-6). The GC-MS micrographs comparing various irradiated and non-irradiated oil samples showed the irradiated samples to shift more towards the high scale, which is an indication an increment in higher molecular weight fractions in the sample. This phenomenon is more noticeable in the chromatograms of heavy crude than those of light crude oil as reported in our previous work (Miadonye et. al, 2008). Figures 3 to 6 compare micrographs of samples irradiated for 20 minutes with non-irradiated ones for Bonny Light oil (Figure 3), Australian spirit crude oil (Figure 4) and Arabian heavy crude (Figures 5 and 6). Figures 3 and 4 showed no significant change in distribution of fractions before and after 20 minutes exposure of the samples to microwave radiation.

The irradiated samples containing ethanolamine, charcoal, and catalyst show reduction in lower hydrocarbon fractions and an increase in higher hydrocarbon fractions (Figure 2) This is in agreement with Figure 5 which showed a shift in the micrograph of irradiated sample to high scale, an indication of an increase in the higher molecular weight fractions in the sample. This effect is well highlighted in Figure 6

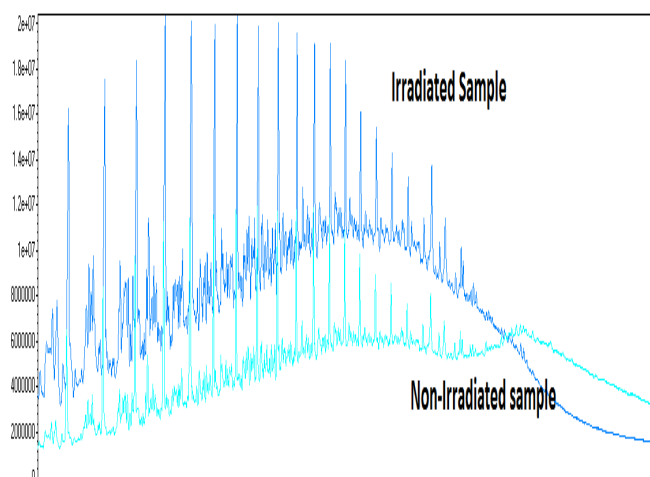for heavy oil with no additives or sensitizers.

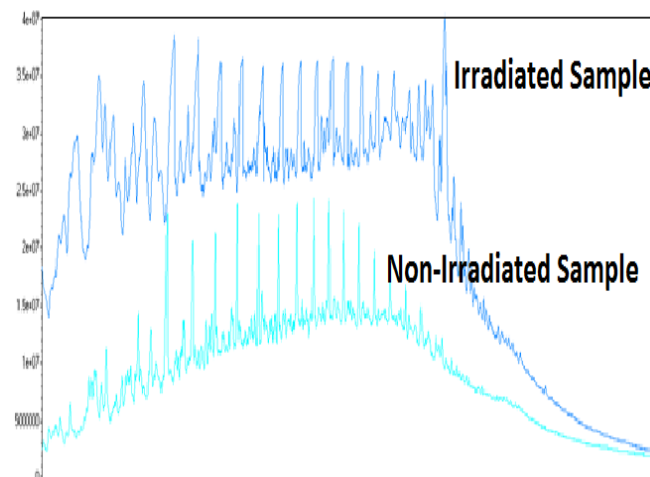FIG. 3 COMPARISON OF MICROGRAPHS OF BONNY LIGHT CRUDE OIL SAMPLES

FIG. 4 COMPARISON OF MICROGRAPHS OF AUSTRALIAN SPIRIT CRUDE OIL SAMPLES

The prevailing conditions in microwave process generally favor non-destructive process due to the low temperature conditions which characterize microwave irradiation. Since crude oil absorbs little microwave radiation, sensitizers and other polar solvents have been used to improve its absorption characteristics. In our previous work (Miadonye et. al, 2008), we indicated that two processes of fragmentation and recombination are present during crude oil irradiation. The irradiated samples containing ethanolamine, sensitizer, and catalyst showed a reduction in the light fractions of the heavy crude oils (Figures 5 and 6). This is an indication of the occurrence of recombination reactions by the lower molecular weight fractions. This is in agreement with Figures 1 and 2 which showed a substantive percent increase in heavier fraction. However, fragmentation reaction appeared to be dominant in the light crude oil samples shown in Figures 3 and 4, and in heavy Arabian crude

containing only 10wt% ethanolamine (Figure 2). It is worthy to mention that at high temperature there was a high rate of evaporation of the light fractions which arguably will significantly affect a recombination reaction in the microwave process.
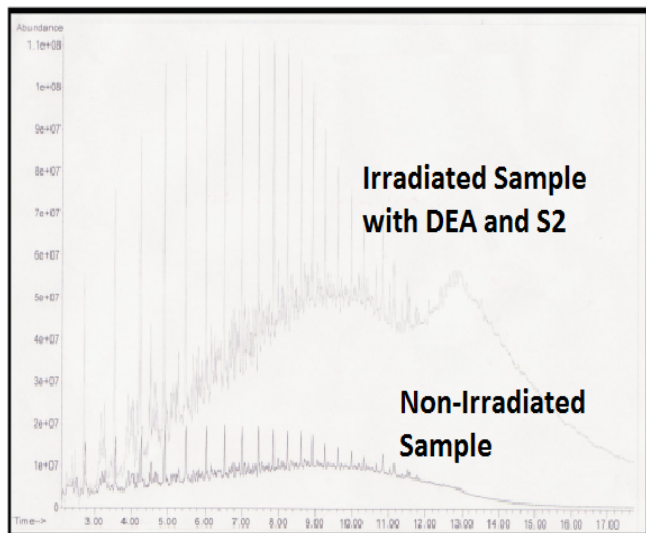

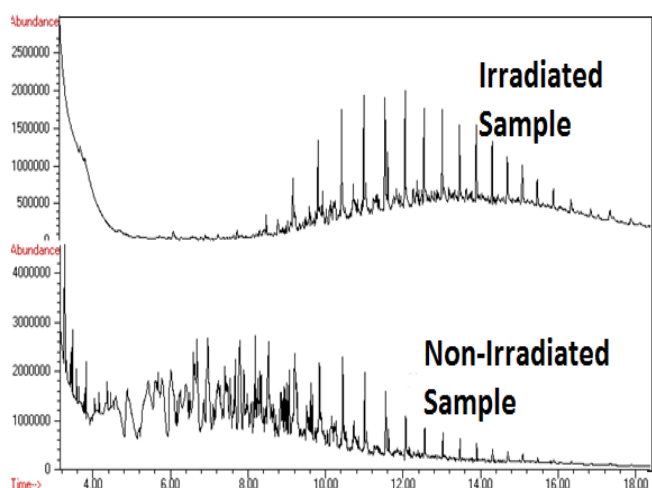FIG. 5 COMPARISON OF MICROGRAPHS OF ARABIAN HEAVY CRUDE OIL SAMPLES

FIG. 6 COMPARISON OF MICROGRAPHS OF HEAVY OIL SAMPLES WITH NO ADDITIVES

Viscosity Characteristics of Irradiated Samples

Viscosity measurements at different temperatures were made for the irradiated samples to examine their flow characteristics. The results are compared in Figure 7 with a pure unmicrowaved sample. Viscosity results illustrate the presence of light fractions at prolonged irradiation time and the strong possibility of the abundance of high molecular weight hydrocarbons at shorter irradiation time. From Figure 7, it is evident that the addition of 10wt% diethanolamine (DEA) lowered the viscosity of the heavy oil to approximately 70cSt at 20°C, but after 10

minute exposure to microwave radiation the viscosity increases to above 95cSt. This is an indication of the domination of recombination reactions over fragmentation reactions at low irradiation time in microwave process. However, when the irradiation time was increased to 25 minutes a lower viscosity of approximately 35cSt was obtained at 20°C. Addition of a microwave sensitizer (charcoal) only made a minimal difference in viscosity reduction. The results from viscosity measurements (Figure 7) and distillation (Figure 1) do not explicitly confirm the degrees of fragmentation and recombination reactions present in a typical irradiated sample, but show a strong dependency of reaction pattern on irradiation time of the sample in the microwave process.
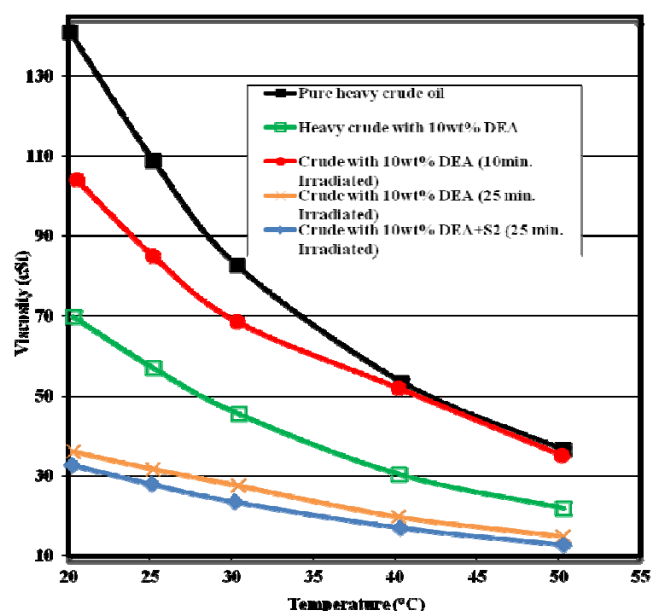
FIG. 7 VISCOSITY OF HEAVY CRUDE OIL SAMPLES AT DIFFERENT TEMPERATURES.

Energy and Cost Efficiency

To determine the amount of power dissipated by the microwave per unit electric field and the energy costs related to this method the equation suggested by Wang and Yang (1994) applies.

$$P = 55.63 * 10^{-12} * F * E^2$$

Where P is the power absorbed per unit volume of mineral (w/m2), F is the frequency of the microwave (Hz), and E is the imaginary part of the complex dielectric constant (dimensionless). Before being able to determine the amount of power dissipated by the microwave, first an experiment to determine the value of E, the imaginary part of the dielectric constant, had to be conducted. Since this experiment can not be carried out in its explicit form the enthalpy data for

each sample was calculated by calorimetric method. Figure 8 shows the energy per kg of different samples irradiated for 25 minutes. For pure crude oil sample, the energy was approximately 50KJ/kg and increased by 7 to 15 fold depending on the types of additives and sensitizers used. The results on enthalpy values (Figure 8) gave an indication on the absorption of sensitizers in inhomogeneous mixtures to determine localized and selective heating in the reaction mixture. It is evident from the results that charcoal has the potential as a good sensitizer in crude oil microwave process. It is worthy to mention here that experiments on samples with both charcoal and catalyst did not yield conclusive results. The energy required to effect reactions in microwave process arguably depend mostly upon property of the sensitizers to improve the microwave absorption characteristics of the crude oil.
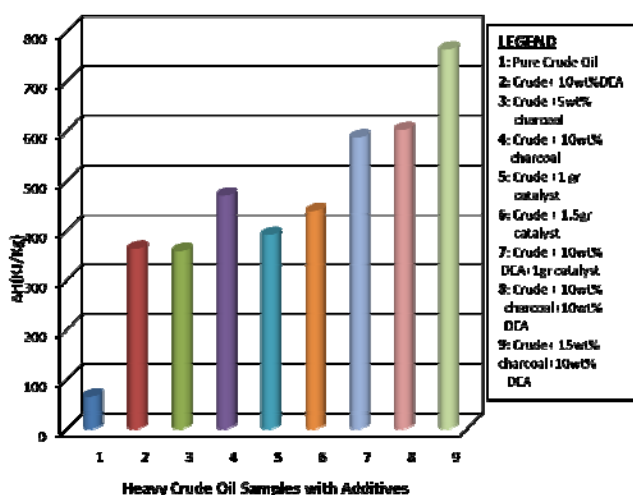

FIG. 8 ENTHALPY OF HEAVY CRUDE OIL WITH VARIOUS ADDITIVES IRRADIATE FOR 25 MINUTES

The results from the analysis using GC-MS showed no significant change in molecular structure for majority of the light crude oil samples after being subjected to microwave irradiation. At temperatures of up to 300°C, corresponding to approximately 590KJ/kg, results obtained from microwave irradiation of these samples showed there was no noticeable change in molecular structure as displayed by the GC-MS analysis (Figures 3 and 4). The desired enthalpy to achieve breaking of the hydrocarbon bonds may not have been obtained at these temperatures. Bond energy or enthalpy is essentially the average enthalpy change for a gas reaction to break all the similar bonds. For the methane molecule for instance, (CH_4), 435kJ is required to break a single C-H bond for a mole of methane. From Figure 8, it is apparent that only a few reaction medium attained the energy necessary to bring about bond cleavage.

Conclusions

The study showed that microwave irradiation in combination with the appropriate catalyst, sensitizer, and /or additives and other process parameters can be used for upgrading of heavy crude oil. It is shown that microwave radiation promotes both fragmentation and recombination reactions simultaneously for upgrading of heavy oil at low temperatures. The crude oil viscosity and irradiation time mostly control the type of reactions that dominate in the microwave process. The results from GC-MS for heavy oil sample suggest that the molecular structure of the sample has changed and higher molecular weight hydrocarbon chains were formed through bonding; an indication of the domination of recombination reactions over fragmentation reactions for high viscosity samples in the microwave process. However, the optimum dose and reaction kinetics for microwave process of crude oil irradiation need to be established.

REFERENCES

Ashton, S.L., Cutmore, N.G, Roach, G.J., Watt, J.S., Zastawny, H.W., McEwan, A.J. "Development and Trial of Microwave Techniques for Measurement of Multiphase Flow of Oil, Water and Gas", *SPE Asia Pacific Oil and Gas Conference*, Melbourne, Australia. 1994, SPE paper No. 28814.

Gunal, O.G., and Islam. M.R. "Alteration of Asphaltic Crude Rheology with Electromagnetic and Ultrasonic Irradiation". Journal of Petroleum Science and Engineering 26 (2000): 263-272.

Miadonye A, Irwin D, and R. M. Khan, "Microwave Desulphurization of Heavy Oil". Paper presented at the 58th Canadian Chemical Engineering Conference, Ottawa, October 19-22, 2008.

Panchenkov, G.M., and Erchenkov, V.V. "Radiation-Chemical Processes". Chemistry and Technology of Fuels and Oils 16(7-8) (1980): 433-436.

Stanley, R.K., "Methods and Results of Inspecting Coiled

Tubing and Line Pipe" presented at SPE/IcoTA Coiled Tubing Roundtable, Houston, Texas, 2001. SPE paper No. 68423.

U.S. Pat. # 4,148,614, April 10, 1979; U.S. Pat. # 4,749,470, June 7, 1988; U.S. Pat. # 4,279,722, Nov. 15, 1994;

Wang, J., and Yang, J.K. "Behavior of Coal Pyrolysis Desulfurization with Microwave Irradiation". *Fuel* (1994): 73: 155-162.

Zaykin, Yu.A., Zaykina, R.F. and Silverman, J. "Radiation Thermal Conversion of Paraffinic Oil". Radiation Physics and Chemistry 69 (2004): 229-238.

Zaykina, R.F., Zaykin, and Yu-A., "Radiation Technologies for Production and Regeneration of Motor Fuel and Lubricants". Radiation Physics and Chemistry 65 (2002): 169-172.

Zaykina, R.F., Zaykin, Yu-A., Mirkin, G., and Nadirov., N.K. "Prospects for Irradiation Processing in the Petroleum Industry". Radiation Physics and Chemistry 63 (2002): 617-620.

Adango Miadonye is a Professor of ChemicalEngineering and the Chair of Department of Chemistry at Cape Breton University. He joined Cape Breton University in 1998 after many years of university teaching and research experience in Chemistry, Chemical Engineering and Petroleum Engineering in several countries. He is a member of editorial boards of several journals for chemical engineering , and petroleum science and engineering, and served as Chair in several Research Award Selection Committees for Government and Private sectors. Dr. Miadonye is an adjunct Professor at the Department of Process Engineering and Applied Science, Dalhousie University.

Brittany MacDonald is currently a Chemical Engineering student at Dalhousie University, Halifax. She holds a BSc (Chemistry) degree from Cape Breton University (CBU). She worked as a research assistant in the chemical engineering research lab and also as a summer term Lab Instructor in Chemistry at CBU. She has been involved as a presenter in several programs including RACE (Research Awareness in Chemistry Education) and SURF (Student Undergraduate Research Forum). Brittany has also been involved in the Women in Science program, CBU Mall of Science exhibition, CBU Chemistry Society and CBU Engineering Society.

Charaterization of the Harmon Lignite for Underground Coal Gasification

Peng Pei[*1], Zhengwen Zeng[2], Jun He[3]

[1]Institute for Energy Studies, University of North Dakota, USA

243 Centennial Drive, Grand Forks, ND, USA, 58202

[2]Department of Geology and Geological Engineering, University of North Dakota, USA

81 Cornell St., Grand Forks, ND USA, 58202 (Current address: 501 Westlake Park Blvd, Houston, TX, USA, 77079)

[3]Department of Petroleum Engineering, University of North Dakota, USA

243 Centennial Drive, Grand Forks, ND, USA, 58202

[*1]peng.pei@und.edu; [2]zhengwen.zeng@bp.com; [3]jun.he@my.und.edu

Abstract

The Harmon lignite bed of the Fort Union Formation (Tertiary Age) beneath western North Dakota presents opportunities for applying underground coal gasification (UCG) technology to recover the unmineable coal resources. However, some characteristics of the formation also present barriers. First, the local aquifers coincide with the lignite bed; second, the lithology of surrounding rocks changes greatly within a short distance. These factors set challenges in site screening, feasibility study and assessment of environmental risks. Although extensive investigation work about the Harmon lignite has been conducted, no work has been done for UCG application. In this paper, we review the site selection criteria of UCG, and apply the experience and tools of reservoir characterization in petroleum exploration to investigate the structure and properties of a target site in western North Dakota. Information and data from state and federal geological surveys, water resource commission and oil companies are collected. A 3-dimensional model is built to simulate the Harmon lignite bed, surrounding rocks and aquifers. This "coal reservoir characterization" work provides a clear view of the structure and composition of the lignite-bearing formation, as well as a better understanding of its *in situ* geology and hydrogeology. Results of this work greatly facilitate the UCG site selection process. Suitability of the potential site for UCG projects is discussed.

UCG Site Characterization

Underground coal gasification (UCG) is a clean coal technology that *in situ* converts coal into syngas through the same chemical reactions that occur in surface gasifiers (Burton et al., 2006). Coupling UCG and the Integrated Gasification Combined Cycle (IGCC) is expected to significantly reduce the cost of a conventional IGCC process, especially if the carbon capture and storage (CCS) system is incorporated. The separated CO_2 can be injected into suitable geological formations for storage, or used for enhanced oil recovery (EOR) to increase the productivity of oil fields and offset part of the cost associated with CO_2 separation. Figure 1 shows the proposed concept of the integrated UCG-EOR process.

However, associated environmental issues and improperly designed gasification processes could limit the applicability of UCG. Major environmental risks include subsidence and groundwater pollution (Sury et al., 2004). Fractures may be generated due to high temperatures during gasification, reducing the integrated and strength of the rock mass, and providing transport paths for UCG-introduced contaminants. Some properties of the formation, including porosity, permeability and elastic properties, will be changed due to the thermal effect during gasification process (He et al., 2013). The UCG design procedure is highly site specific. A successful UCG project will depend on good understanding of the natural properties and *in situ* geological/hydrogeological conditions of the target coal seam and its surrounding rocks. Since these parameters determine the gasification operation strategies and the composition of the product gas, they, in turn, govern the economic and environmental

performances of the UCG plant. Therefore, appropriate site screening criteria and procedures, and optimized operation processes are required to minimize the environmental risks and maintain a satisfactory quality of product gas. The site characterization work will provide detailed knowledge of the geology, hydrogeology, geomechanics and thermophysics of the target sites.

There is extensive literature discussing UCG site selection (Sury et al., 2004; Burton et al., 2006; Shafirovich et al., 2008; Shafirovich and Varma, 2009). Selection criteria are based on considerations of resource abundance, mitigation of environmental risks and security of good product gas quality. Many characteristics of the coal-containing strata need to be investigated during the site selection process. Table 1 lists part of, if not all, the parameters of the target formation that should be investigated during the site screening, and their functions in the process design and operation control.

Hydrogeological issues are very important in UCG site selection and operation. If the coal seam coincides with an aquifer, special attention should be paid to the potential of groundwater pollution. Two methods can be applied to protect groundwater from pollution in a UCG project. The first method is to keep the gasification pressure below the hydrostatic pressure in the formation. In such cases, water from the aquifer enters the gasification zone due to the pressure difference and is involved in the reactions, particularly the water-gas-shift reaction, to increase hydrogen content in the product gas (Linc Energy, 2006). However, water influx is also controlled by the permeability of the surrounding rocks, and could be higher than the desired quantity for chemical reactions. Excessive water influx will decrease the calorific value of the product gas. The second method is to select a site with shale-prone surrounding rocks. Shale rocks have lower permeability than sandy rocks, and as a result, they can function as a seal to prevent propagation of contaminants from the gasification zone (Sury et al., 2004; Zhao et al., 2013). Therefore, we propose that the clay content of the surrounding rocks should be considered as an import factor in UCG site selection. Since the physical variation of the strata is mainly controlled by depositional environment, sedimentology reports about the target site can provide a rough, but fast, image of the isolation capability of the surrounding rocks. If coals were deposited in deltaic or fluvial successions, they would be likely to be overlain by permeable layers. If coals were formed in a lacustrine system, they would be likely to be buried by shales or high-clay content rocks, therefore with good isolation. In addition to the primary permeability system, natural fractures and thermal-induced fractures during UCG operation should be well understood as they could be the major channels for fluid transport.
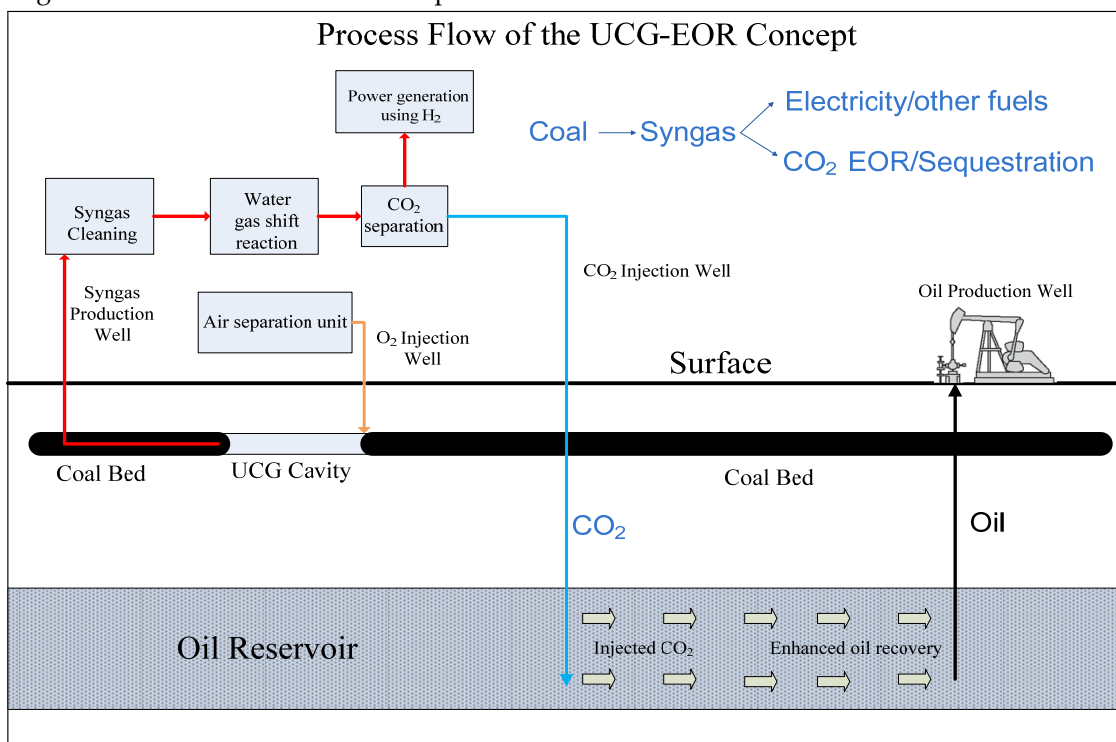

FIG. 1 CONCEPT OF UCG-EOR PROCESS

TABLE 1. KEY FORMATION PROPERTIES AND THEIR MAJOR FUNCTIONS IN UCG SITE CHARACTERIZATION

| Property	Function
Coal seam thickness and depth	Assessment of resource, well design and gasification module design
Coal seam structure and inclination	Gasification zone design, well design and assessment of contaminants migration
Coal permeability	Well linkage, transport of injected gases and gaseous products
Hydrostatic pressure and capillary pressure	Water influx control, gasification pressure and gas leakage
Rock permeability	Water influx control and propagation of contaminants
Rock porosity, water saturation	Water available for chemical reaction
Rock thermal conductivity, thermal expansion coefficient	Temperature distribution, thermal stress and its effects
Rock strength, thermal expansion coefficient	Heat induced fractures, rock response and failure risks
Rock-quality designation (RQD)	Gas leakage, transport of contaminants and rock failure risks
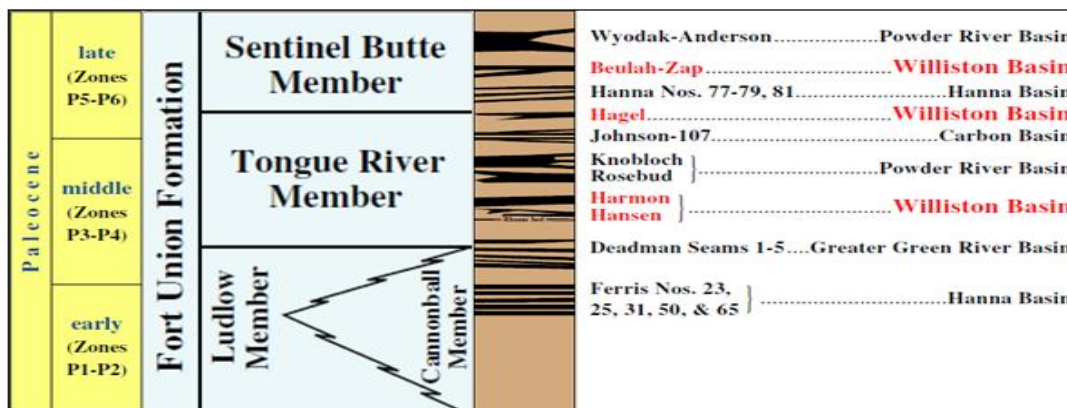
FIG. 2 STRATIGRAPHIC COLUMN OF THE FORT UNION FORMATION (AFTER FLORES ET AL. 1999)

On the other hand, the target coal seam should have a sufficient permeability in order to transport injected oxidants and gaseous products. Other factors that need to be considered in site selection include impact on nearby mines or sites of other underground activities and infrastructures for construction and product transportation.

Based on the above introduction about UCG site screening, this paper presents our work in selection and characterization of a potential UCG site in the Fort Union Formation, western North Dakota. The structure of the target coal seam and its overburden is presented. The amount of resource is calculated. Aquifers in the vicinity of the coal seam are recognized and modeled. A 3-dimensinal model containing the clay content and facies distribution is constructed for selecting appropriate locations for the gasification reactor.

The Fort Union Lignite in North Dakota, USA

The North Dakota portion of the Williston Basin hosts significant coal resources of lignite rank in the Paleocene Fort Union Formation. Most of these lignite resources are contained in the coal zones named Harmon and Hansen in the southwestern part of the basin, and in the Hagel and Beulah-Zap coal zones in the east-central part. As Figure 2 shows, the Harmon

and Hansen coal zones lay in the lowermost part of the so-called Tongue River Member. The Hagel coal zone is in the lower part of the Sentinel Butte Member. The Beulah-Zap coal zone is in the upper part of the Sentinel Butte Member (Flores et al., 1999).

Lignite resources in North Dakota have been investigated by the North Dakota Geological Survey (NDGS) and the U.S. Geological Survey (USGS) in detail. Reports and maps provide the depth, thickness, lateral structure of the lignite beds and locations of economically mineable reserves. The literature can be conveniently used in primary UCG site selection with regard to depth and thickness. Studies have indicated that there is huge lignite resource in North Dakota, about 1.27 trillion tons. However, the economically recoverable reserve by surface mining is about 25 billion tons, or only 2% of the entire resource (Murphy et al., 2006).

For the upper part of the Fort Union Formation (Tongue River and Sentinel Butte Members) where the Harmon coal is located, the strata are interpreted as mainly fluvial and deltaic deposits. Thick seams like Harmon coal and associated sediments probably accumulated in swamps on abandoned deposits of fluvial-channel belts that migrated into nearby interfluvial areas. The Harmon coal zone will be an ideal candidate for UCG utilization due to its

abundant resource, sufficient thickness and good continuity in structure. However, because the depositional system is probably a mixture of inter-channel fluvial system and lacustrine swamp, the lignite may be overlain by impermeable sediments, and sandy sediments commonly encountered in channels. The Harmon coal zone is interbedded with floodplain mudstone and siltstone, and overlain by fluvial channel sandstone and interfluvial silty sandstone, siltstone, and mudstone (Flores et al., 1999). Lithological face variation of the surrounding rocks can be great within a short distance. The fact that the overlying lithology is highly variable makes the site selection process challenging. Detailed investigation and modeling to the surrounding rock with advanced simulation tools are necessary.

Characterization of the Potential Site

Data Processing and Model Construction

The Harmon lignite zone in the Fort Union Formation, western North Dakota is considered to be the candidate coal seam because of its abundant resources. Our goal is to select a site suitable for UCG project and to obtain detailed data in geology, hydrogeology and rock properties of the site. Available information used in this study include reports, dissertations, conference and journal papers, lithological interpretation logs and unprocessed well logs. Most of the literature and data are published by researchers in NDGS, USGS, North Dakota Industry Commission (NDIC), and the University of North Dakota (UND). Reviewed literature covers topics in depositional history of the Fort Union Formation, geological structure of the Fort Union strata, stratigraphy description, strippable coal map, coal resource estimation, water resource and aquifer investigation, petroleum resource report, petroleum production data, geological structure of the Williston Basin, and etc.

Based on the reviewed literature and the primary selection criteria, a site with an area of 4 townships (373 km², or 144 mi²) in Dunn County, North Dakota (Figure 3) is screened out. A 3-dimensional model of this site is built to simulate the Harmon lignite bed, surrounding rocks and aquifers using the numerical modeling package Petrel. This model provides a visualized structural demonstration to the coal seam and surrounding rocks; describes the lithology facies, clay content, presence of aquifers; and will serve as an input for further dynamic modeling of the gasification process.

FIG. 3 LOCATION OF THE MODELING SITE IN NORTH DAKOTA, USA

Two sets of logs are used in constructing the model: the lithological interpretation logs, and oil and gas electrical logs. The lithological interpretation logs are obtained from USGS, and are generated based on information from oil and gas wells, coal drill holes, and outcrops. Twenty-six logs are found within the selected area. After necessary processing, the logs are input into the simulator Petrel. As the selected site is located in an area intensively drilled with oil wells, a significant amount of the electrical logs is obtainable. However, the Fort Union Formation is not the interest to the oil companies, so most of the electrical logs are not run through it. We screen out 40 wells with Gamma Ray (GR) logs from the selected site. As suggested by Murphy et al. (2006), the lignites generally have readings of around 5 to 10 gamma counts per second, and the mudstone has counts around 20. The well logs are first digitized using Petra, a petroleum software package, and then the clay contents are interpreted by Petrophysics, another software package. The results are input into Petrel where the two sets of log data are compared with each other, and with lithology descriptions in other literature. Based on the comparisons, well correlation is carried out; and finally a 3-demensional model of the Harmon coal seam and surrounding rocks is generated. It should be noticed that although the Harmon bed may be split into several beds, the thickest single bed is considered as the continuous part in our model. To check the clay contents in detail, layers which are 9.1 m (30 ft), 18.3 m (60 ft) and 30.5 m (100 ft) above and below the coal seam are sliced out respectively.

Structure of the Coal Seam and Surrounding Rocks

The measured depth and thickness of the coal seam is indicated in Figures 4 and 5 respectively. As shown in

the figures, most part of the coal seam has a depth greater than 244 m (800 ft) below the surface, and a thickness greater than 6 m (20 ft). Based on the thickness and depth, the Harmon coal seam is an ideal candidate for UCG utilization. The coal seam is almost flat, with a slight northeastward dip. The topography of the selected site and the coal seam is shown in Figure 6. The north and northwest portion of the topography is hilly. The rest of the site is flat and easy to access. The calculated bulk volume of the Harmon lignite of a single bed contained in this area is 2.67×10^9 m^3 (9.44×10^{10} ft^3), which is about 3,793 million metric tons (4,181 million short tons) of lignite resource.
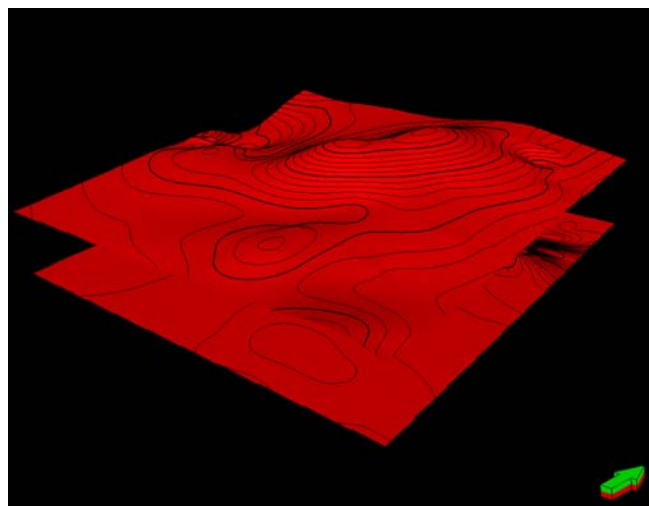
FIG 6. TOPOGRAPHY AND THE HARMON COAL SEAM OF CANDIDATE UCG SITE (10 TIMES VERTICAL EXAGGERATION, THE GREEN ARROW TO THE NORTH).

Geological Properties of the Coal Seam and Surrounding Rocks

The clay contents of the surrounding formation above the coal seam are shown in Figure 7. It can be seen that for the layer 9 m (30 ft) above the coal seam, the clay content is higher than 60% in most part of it. Figure 8 shows the clay contents of layers below the coal seam. It is clear that for the layer which is 9 m (30 ft) below the coal seam, the clay content is higher than 80% in most part of it. According to the simulation result, about 88% of the overburden by volume is claystone. The locations of the gasification zone should be carefully selected to avoid the low-clay content rocks for the purpose of preventing contaminants leakage.

Hydrogeological Conditions

The selected lignite-bearing formation in the candidate site coincides with the Lower Tertiary Aquifer. This confined aquifer consists of sandstone beds, interbedded with shale, mudstone, siltstone, lignite and limestone. It is one of the five major aquifers in the Northern Great Plains Aquifer System. The Lower Tertiary Aquifer is not highly permeable, but is an important source for water supply due to its large quantity (USGS, 2010). According to the description in the USGS report, water recharges into the aquifers at outcrops high altitude and discharges from the aquifer into major streams, such as the Missouri River. From the local ground-water resources report of Dunn County (Klausing, 1979), aquifers in the Tongue River Member are also recharged by leakage from aquifers in the overlying Sentinel Butte Formation. Aquifers in the Tongue River Member include very fine- to fine-grained sandstone beds which range in thickness from
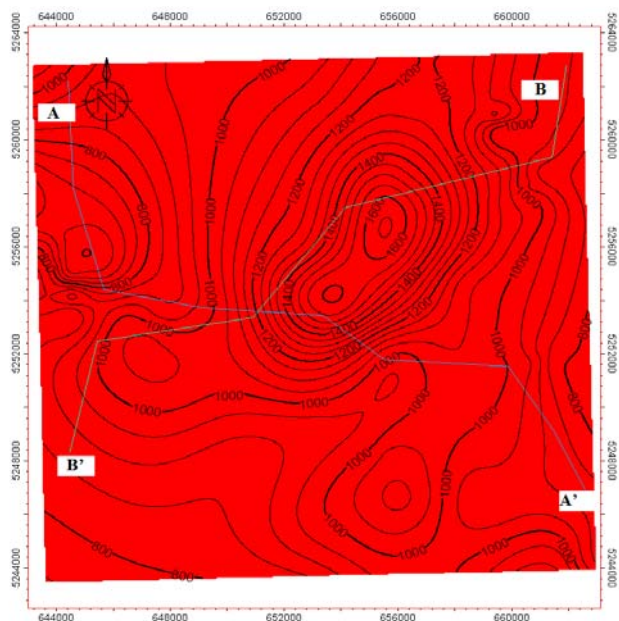
FIG 4. CONTOUR MAP OF THE MEASURED DEPTH OF THE HARMON LIGNITE BED, FT.
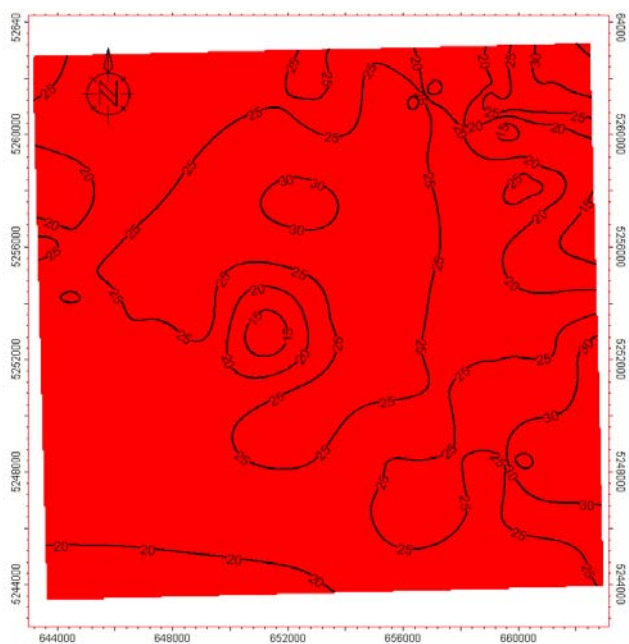
FIG 5: ISOPACH MAP OF THE HARMON LIGNITE BED, FT.

about 3 m to 30 m (10 to 100 ft), and frequently pinch out into siltstone or sandy clay. The water head in the selected area is about 607 m (2000 ft) above sea level, and the water flow direction is generally northeastward (Klausing, 1979). Available data are insufficient to determine if there is a hydraulic connection between the sandstone beds; consequently each bed is considered as an isolated aquifer.

Through interpretation and comparison of well logs and lithology logs, five aquifers of relatively large size are recognized. One aquifer (AQ1) is located under the Harmon lignite bed, and some part of it is almost attached to the coal seam. The other four aquifers (AQ2, AQ3, AQ4 and AQ5) are above the coal bed. AQ2 is very close to the Harmon coal bed while others are separated by claystone layers. Figure 9 shows the locations of the above four aquifers related to the lignite bed. Figure 10 shows the cross-section view of A-A' in Figure 4, and Figure 11 shows the cross-section view of B-B'. There are some other aquifers within the overburden, but are of small size and not close to the coal bed. So they are not considered as being threatened by the UCG operation. The North Dakota State Water Resource Commission has conducted laboratory tests and slug tests to measure the hydraulic conductivity of the sandbed aquifers in the Tongue River Formation, and values are shown in

Table 2. Although none of the locations of these tests is in the selected site, these values do provide a good reference. Preferred UCG reactor sites are suggested to avoid these aquifers, especially AQ1 and AQ2 which are very close to the lignite seam.

TABLE 2: HYDRAULIC CONDUCTIVITY OF THE TONGUE RIVER AQUIFER IN DUNN COUNTY (AFTER KLAUSING, 1979)

Sidewall-core analyses		
Location	Sampling depth (ft)	Hydraulic conductivity (ft/d)
141-096-29CCC	675	0.950
141-096-29CCC	892	0.088
142-092-09DAB	421	0.173
142-092-09DAB	605	0.010
148-097-33ABB	345	0.176
Slug tests		
Location	Screened interval (ft)	Hydraulic conductivity (ft/d)
143-091-19AAA1	652-670	0.4
144-097-26CBD1	700-718	0.9

However, it is possible that the claystone is fractured, providing channels for the water movement and hence the Lower Tertiary is a complex dual system.
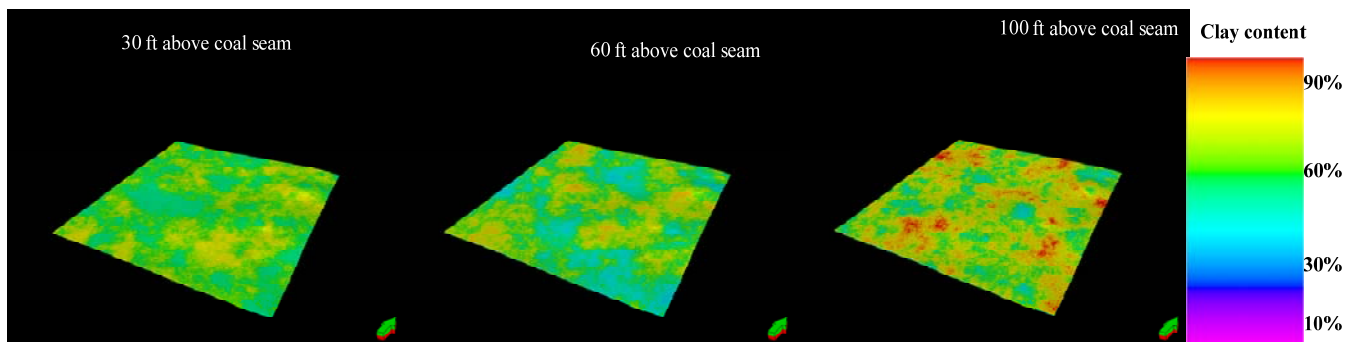
FIG. 7 CLAY CONTENTS OF THE SURROUNDING ROCKS 9.1 M (30 FT), 18.3 M (60 FT) AND 30.5 M (100 FT) ABOVE THE HARMON COAL SEAM RESPECTIVELY (10 TIMES VERTICAL EXAGGERATION, THE GREEN ARROW TO THE NORTH).
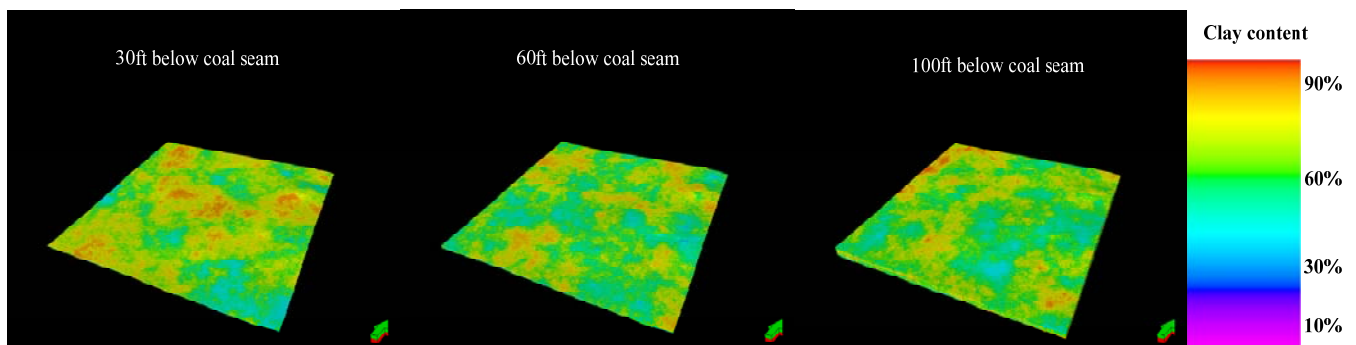
FIG. 8 CLAY CONTENTS OF THE SURROUNDING ROCKS 9.1 M (30 FT), 18.3 M (60 FT) AND 30.5 M (100 FT) BELOW THE HARMON COAL SEAM RESPECTIVELY (10 TIMES VERTICAL EXAGGERATION, THE GREEN ARROW TO THE NORTH).
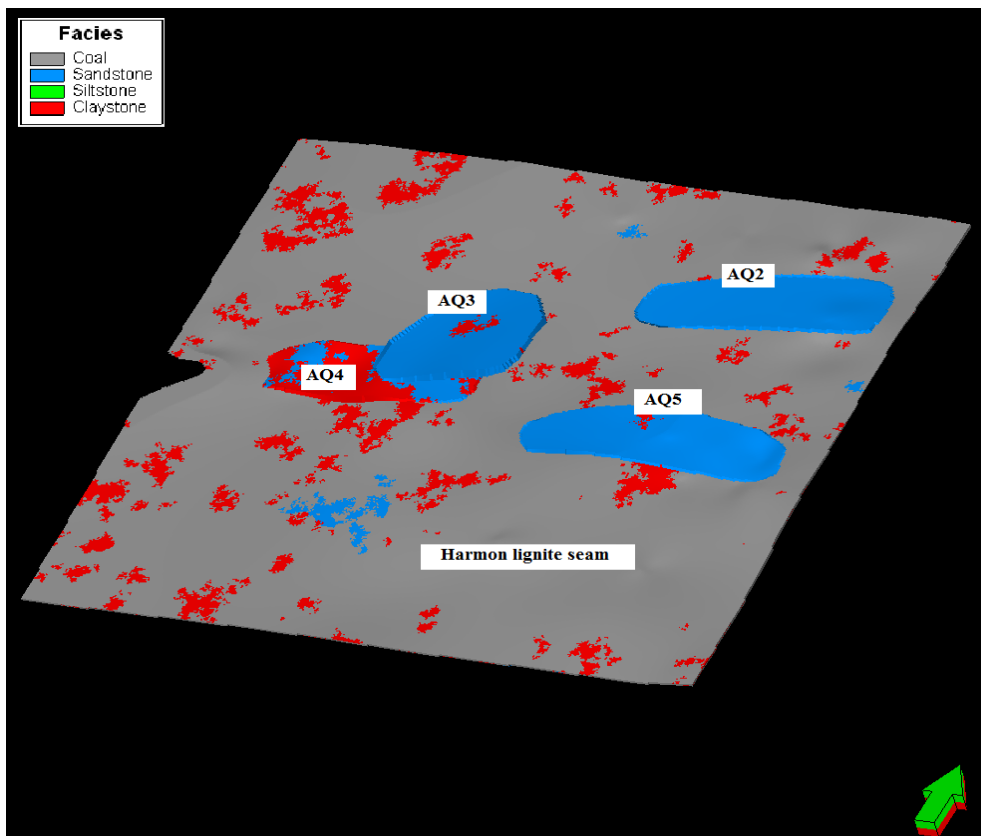
FIG. 9 AQUIFERS ABOVE THE HARMON LIGNITE SEAM (10 TIMES VERTICAL EXAGGERATION, THE GREEN ARROW TO THE NORTH).
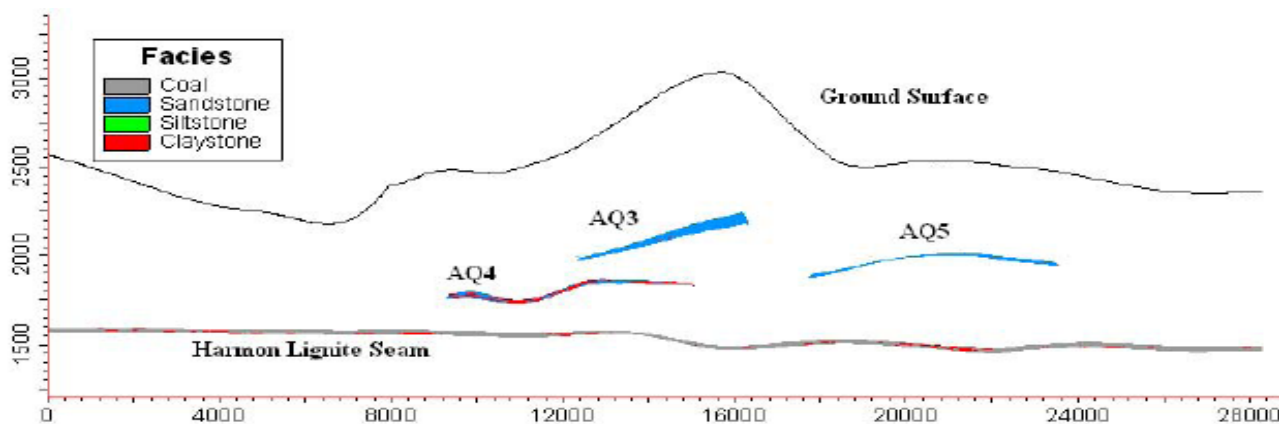

FIG. 10 A-A' CROSS-SECTION VIEW OF FIGURE 4 (10 TIMES VERTICAL EXAGGERATION).
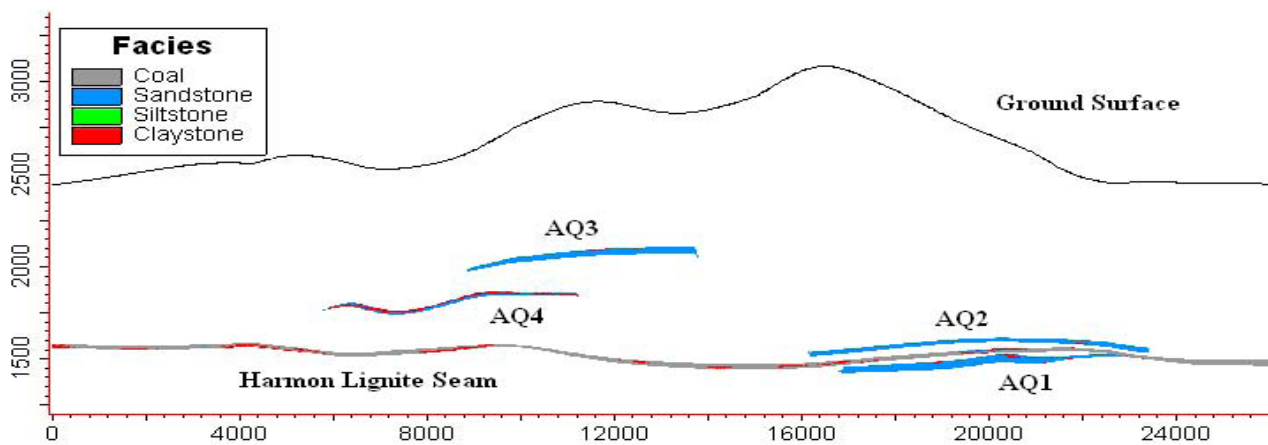

FIG. 11 B-B' CROSS-SECTION VIEW OF FIGURE 4 (10 TIMES VERTICAL EXAGGERATION).

Discussion and Future Plan

The underground coal gasification technology offers a clean and economically efficient approach to recover the huge lignite resources in North Dakota. As described in this paper, a candidate site in Dunn County, North Dakota, which is suitable for UCG-IGCC project has been selected out, and a 3-dimensional model has been constructed to visualize the structure, lithological composition, clay content and hydrological condition of the lignite-bearing formation. Some aquifers exist in close distance to the lignite seam, and should be avoided during the gasification operation. Most parts of the surrounding strata, except some areas where the aquifers locate, have high clay content which will function as a seal for the gasification zone. At the southern part of the candidate site, the topography is flat with good infrastructure such as roads and electricity ready for plant engineering works. The proposed area overlies with the Little Knife Anticline, which is an major oil producing zone in North Dakota. Main producing pools include Bakken, Duperow, Madison, and Red River. Some oil fields in this area are now at the secondary or tertiary production phase, meaning a potentially big demand for CO_2 EOR process in the future. The area is also tectonically stable, and no major fault exits in the selected site (Fischer et al., 2005).

In the next stage of our work, rock samples will be collected and the properties listed in Table 1 will be measured through a series of laboratory tests, and plugged into the 3-D model. The dynamic gasification process will be simulated, and behaviors of the surrounding rocks in the high temperature environment will be analyzed. Based on the simulation results, risks associated with the UCG process will be evaluated, and operation strategies to mitigate the risks and improve the plant performance will be developed.

REFERENCES

Burton, Elizabeth, Julio Friedmann, and Ravi Upadhye. "Best practices in underground coal gasification". US DOE Report Contract W- 7405-Eng-48, Lawrence Livermore National Laboratory: Livermore, CA, 2006.

Fischer, David, Julie LeFever, Richard LeFever, Sideny Anderson, Lynn Helms, Steve Whittacker, James Sorensen, Steven Smith, Wesley Peck, Edward Steadman, and John Harju. "Overview of Williston Basin geology as it relates to CO_2 sequestration". Report of the Plains CO_2 Reduction (PCOR) Partnership, Grand Forks, ND, 2005.

Flores, R.M., C.W. Keighin, A.M. Ochs, P.D. Warwick, L.R. Bader, and E.C. Murphy. "1999 Resource assessment of selected tertiary coal beds and zones in the Northern Rocky Mountains and Great Plains Region, Part II: Williston Basin, Chapter WF, Framework of Coal Geology of the Fort Union Coals in the Williston Basin". In U.S. Geological Survey Professional Paper 1625-A, 1999.

He, Jun, Peng Pei, Kegang Ling, Zhenwen Zeng, and Hong Liu. "Quantificiaton of rock porosity changes before and after freezing". Journal of Petroleum Science Research 2 (3): 128-137, 2013.

Klausing, Robert L. "Ground-water resources of Dunn County, North Dakota". Prepared by the U.S. Geological Survey in cooperation with the North Dakota Geological Survey, North Dakota State Water Commission, and Dunn County Water Management District, 1979.

Linc Energy. "Groundwater use in UCG", LINC-ENV-06.2, Linc Energy Ltd: Brisbane, Australia, 2006.

Murphy, Edward C., Ned W. Kruger, Gerard E. Goven, Quentin L. Vandal, Kimberly C. Jacobs, and Michele L. Gutenkunst. "The lignite resources of North Dakota, North Dakota Geological Survey", Report of Investigation No. 105. Bismarck, ND, 2006.

Shafirovich, Evegny, and Arvind Varma. "Underground Coal Gasification: A brief review of current status". Industrial and Engineering Chemistry Research 48

(2009): 7865-7875.

Shafirovich, Evgeny, Maria Mastalerz, John Rupp, and Arvind Varma. "The potential for underground coal gasification in Indiana", Phase I report to the Indiana Center for Coal Technology Research (CCTR), 2006.

Sury, Martin, Matthew White, Jenny Kirton, Peter Carr, Roland Woodbridge, Marc Mostade, Robert Chappell, David Hartwell, Douglas Hunt, and Nigel Rendell. "Review of Environmental Issues of Underground Coal Gasification". Report COAL R272; DTI/Pub URN 04/1880; Department of Trade and Industry Technology (DTI): London, United Kingdom, 2004.

USGS. "Lower Tertiary Aquifers, Northern Great Plains aquifer system, USGS H730-I Ground Water Atlas of the United States". U.S. Geological Survey, 2010.

Zhao, Lin, Aifen Li, Xiongjun Wu, Haojun Xie, Jinjie Wang, and Sixun Zhang. "Oil-water interfacial tension effects on relative permeability curves in low-permeability reservoirs". Journal of Petroleum Science Research 2 (2): 75-81, 2013.

Peng Pei is currently a research engineer in the Institute for Energy Studies, University of North Dakota. He holds a Ph.D. degree from University of North Dakota and an M.S. Mechanical Engineering from University of North Dakota. He also has a B.S. in Mechanical Engineering from North China Electrical Power University. His research area focuses on energy-related rock mechanics.

Zhengwen Zeng is currently a senior engineer at BP America. The work reported in this paper was completed when he was an associate professor at The University of North Dakota. His research interest is geomechanics. He holds a B.S. and M.S. degree in Engineering Geology from Southwest Jiaotong University, China, a D.Sc. degree in Tectonophysics from Institute of Geology, State Seismological Bureau, China, and a Ph.D. degree in Petroleum & Geolgoical Engineering from The University of Oklahoma, USA.

Jun He is a Ph.D. student at the University of North Dakota. His research interests are in reserve evaluation and reservoir characterization. He holds a B.S. degree Southwest Petroleum University in Geology, M.S. degree from University of North Dakota in Geology, and M.S. degree from China University of Petroleum in Petroleum Engineering.

Investigation and Comparison of Production in Vertical, Horizontal, Slanted and Hydraulically Fractured Wells in a Gas Condensate Field

Babak Moradi[1], [2]Amin Tahami[3], Hosein Dehghani[4] , Mosayeb Alishir[5`], Amir Dehghan[6]  `

[1,4] Department of Petroleum Engineering, Science and Research Branch, Islamic Azad University, Fars, Iran

[2] Iranian Central Oil Fields Co.

[3] Mad Daneshgostar Tabnak Co.(MDT),Tehran, Iran

[4] Petro Pajohesh Ahoura Co. (PPA), Shiraz, Iran

[5]Academic Center for Education, Culture & Research (ACECR) on TMU, Tehran, Iran

[6] Global Petro Tech Co. (GPT), Tehran, Iran

[1] b.moradi@ut.ac.ir

Abstract

Different well types (Vertical, Slanted, Horizontal and Hydraulically Fractured Wells) have different effect on production profile. Each well type would have had effects on final recovery. Besides, finding the best production scenario in gas condensate reservoirs were so challenging and utilizing the best scenario need to be done smartly. So to get higher recovery from these kinds of reservoirs and due to sensitivity of them -especially fluids to pressure gradient-exploiting the best well type in each reservoir is more important.

This paper focuses on investigation and comparison of production in vertical, slanted, horizontal and hydraulically fractured wells in a semi-real model of a gas condensate reservoir. Here different well type scenarios were investigated in a gas condensate model that has been customized for this goal. Comparison of the results shows practical facts that would be so helpful in selecting well type in Gas condensate reservoirs.

Keywords

Gas Condensate Reservoirs; Horizontal Well; Slanted Well; Hydraulically Fractured Well

Introduction

Near Wellbore Effects in Gas Condensate Reservoirs

Well deliverability is an important issue in the development of many gas condensate reservoirs. When the well bottom hole flowing pressure falls below the dew point, condensate liquid builds up around the well bore, causing a reduction in gas permeability and well productivity. The liquid saturation may reach values as high as 50 or 60 per cent, and the well deliverability may be reduced by up to an order of magnitude [Mott et al., 2000].

The loss in productivity due to this 'condensate banking' effect may be significant, even in very lean gas condensate reservoirs [Mott et al., 1997]. In the Arun reservoir [Afidik et al., 1994], the productivity reduced by a factor of about two as the pressure fell below the dew point, even though the reservoir fluid was very lean with a maximum liquid drop out of only 1%.

Most of the pressure drop from condensate blockage occurs within a few feet of the well bore, where flow rates are very high. The condensate bank around the wellbore contains two phases, reservoir gas and liquid condensate. This bank grows as the reservoir pressure declines and progressively impedes the flow of gas to the well, causing a loss of well productivity [Fussel, 1973]. Laboratory studies [Danesh et al., 1994;Hendersen et al., 1995; Mott et al.,1999], however, have shown that the oil saturation actually decreases

at high production rate in the immediate vicinity of the well, due to capillary number effects (representing the ratio of viscous to capillary forces). Consequently, the relative permeability to gas increases, resulting in a recovery of much of the gas mobility lost from condensate blockage. Ignoring this phenomenon leads to pessimistic recovery predictions. Gringarten [2000] confirmed the existence of this increased mobility zone near the wellbore from well test data by showing that it often creates a three-zone radial composite well test behavior, yielding three stabilizations on the pressure derivative.

The most important parameter for determining the impact of condensate blockage is the effective gas permeability in the near-well region. In the flow of gas condensate fluids through porous media at high velocities, there appear to be two competing phenomena which may cause the effective gas permeability to be rate dependent, First is an increase in relative permeability with velocity that is sometimes termed 'velocity stripping' or 'positive coupling' and second is Inertial (non-Darcy) flow effects, which reduce the effective gas permeability at high velocity [Mott et al., 2000].

Horizontal Wells in Gas Condensate Reservoirs

In last few years, many horizontal wells have been drilled around the world. The major purpose of horizontal well is to enhance reservoir contact and thereby enhance well productivity [Joshi, 1991]. Numerous studies have been done to investigate the performance of horizontal well in oil and gas reservoir but there are a few studies on the application of horizontal well in gas condensate reservoir. For gas condensate reservoir when the pressure falls below the dew point, a region of condensation is formed around the well, which impairs the well deliverability. The condensate bank may be minimized using a horizontal well due to less pressure draw down of a horizontal well compared to that for a vertical well. The application of horizontal wells instead of vertical wells was reported in Dejel Bissa [Dehane et al., 2000] and Hassi R Mel [Muladi et al., 1999].

Hashemi and Gringranten [2005] have compared the well productivity between vertical, horizontal and hydraulically fractured wells in a gas condensate reservoir using a single well compositional model. They examined the impact of the length of the horizontal well on the pressure draw down and condensate blockage around the well. Their results showed that the pressure draw-down and condensate

blockage is smaller for a horizontal well compared to that of a vertical well. They accounted for the coupling and inertial effect by choosing a fine grid near the well bore and calculating the core specific constant that simulator needs for expressing these two effects from well test data.

The performance of a horizontal (Highly slanted) well or a slanted well (SW), is mostly believed to be better than that of a vertical well (VW) due to its greater contact to the reservoir. However, the budgets of drilling and completion are extra and the choices for monitoring, control and interference often restricted. Gas-Condensate reservoirs are increasingly considered as proper candidates for drilling SWs or HWs. These reservoirs attitude special challenges selecting one type or the other due to the complex nature of fluid flow in porous media. These challenges are exhibited by these low interfacial tension systems, which are different from those of conventional gas-oil systems.

In another side of view, condensate banking near well bore due to pressure reduction cause condensates production loss that are so valuable. In order to prevent or decrease condensate banking near wellbore many methods such as using Horizontal or Slanted wells and Hydraulic fracturing have been proposed.

In this study we are trying to investigate the performances of SW, HW and VW as well as Hydraulic Fracturing in a layered gas-condensate reservoir.

Model and Scenarios Description

Model Description:

The model that has been selected for this study is extracted from one of Iranian Gas condensate reservoirs and been customized for this goal. This reservoir has 4 main layers and the model has been divided into 16 sub layers. The sector that been selected for this study have 43 blocks in length and 14
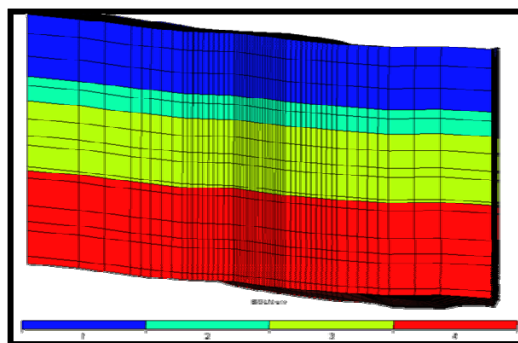

FIG. 1 CROSS SECTION OF RESERVOIR SECTOR MODEL

blocks in width. Each block has 1600*1600 feet dimension. And the height of the reservoir is around 1445 feet. Figure 1 shows the cross section of the reservoir sector model.

As the sector blocks are so large (1600*1600 feet), due to investigate the change in dynamic properties of reservoir around the well, near well bore blocks (a 9*9 block dimension square around the well's top block) refined (Figure 2)
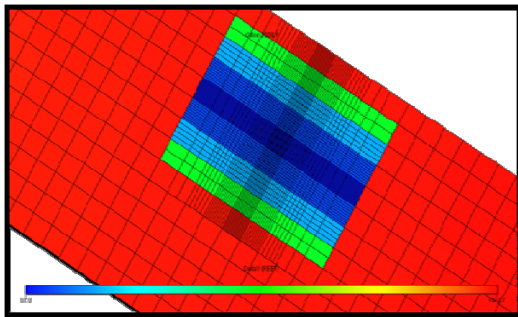

FIG. 2 REFINED BLOCKS AROUND THE WELL

Reservoir properties distribution in this sector model - especially in vertical direction- is so vast. Figure 3 to 5 show porosity, permeability in X direction and water saturation distribution in this section of the reservoir. Table 1 also shows the average reservoir's static properties.
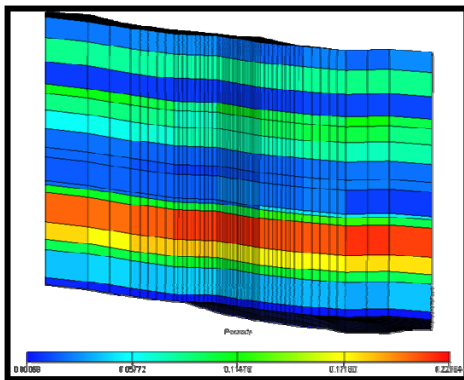
FIG. 3 POROSITY DISTRIBUTION IN SECTOR MODEL
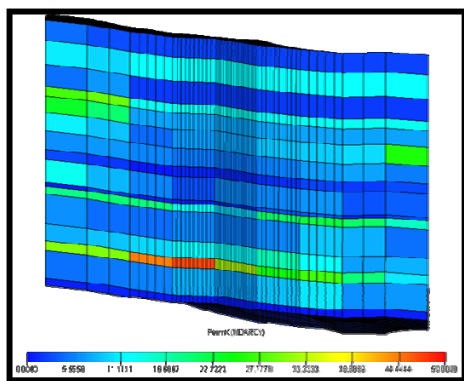
FIG. 4 PREMEABILITY DISTRIBUTION IN SECTOR MODEL
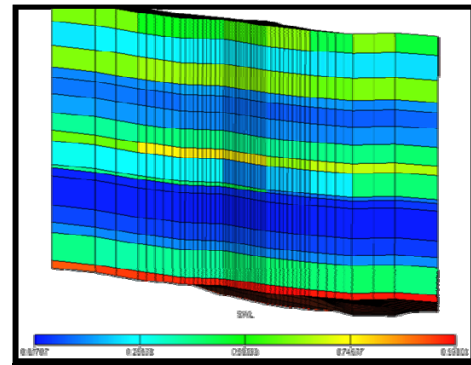
FIG. 5 INITIAL WATER SATURATION DISTRIBUTION IN SECTOR MODEL

TABLE 1 AVERAGE RESERVOIR STATIC PROPERTIES

Parameter	Min	Max
Porosity (%)	0.068	22.884
Permeability-X (md)	0	137.68
SWL (%)	1.707	99

Initial pressure and representative dew point of each also summarizes in Table 2. The PVT model that been used in this model is composed of 8 pseudo components that are following Peng-Robinson EOS. All four layers have the same pseudo components but the mole fractions are different. For example dew point increases when we go deeper in the reservoir and layer 1 has the leanest reservoir fluid. Some information about the reservoir properties are summarizes in Table 3. Figure 6 also shows the 4 layers rank from condensate richness point of view.

TABLE 2 INITIAL PRESSURE AND RESPECTIVE DEW POINT OF EACH LAYER

Layer No.	Initial Pressure (Psia)	Dew point (Psia)
1	5207	5129
2	5234	5162
3	5266	5162
4	5317	5209
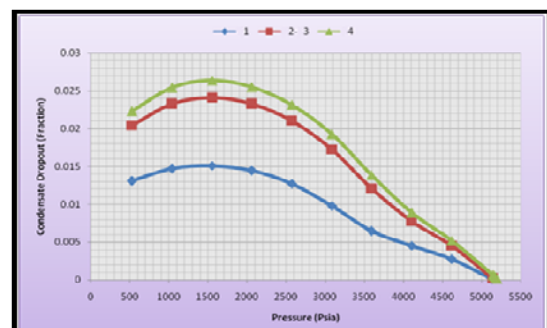
FIG. 6 CONDENSATE DROPOUT OF EACH LAYER

Defining Different Well Types in the Sector Model

Here we try to define vast groups of well type

scenarios in this sector model, due to do sensitivity and get the best technical scenarios.

Vertical Well:

Cases Definitions:

- Vertical wells are defined in the center of refined blocks.
- Production scenarios are defined in 5 years period with the maximum rate of 120 MMscf/Day
- Three scenarios has been defined as below:
  a. One well that is completed in layers 1 to 3
  b. One well that is completed in layers 3 and 4
  c. One well that is completed in all 4 layers.

Result Comparison:

- Low reservoir quality (Low porosity and high initial water in layers 1 and 3) caused high bottom-hole pressure drop.
- Due to different fluid properties in all layers, the maximum condensate production has been resulted from the well that is completed in layers 3 and 4.

Figure 7 and 8 show the Field total condensate production and bottom-hole pressure in different scenarios and cases.
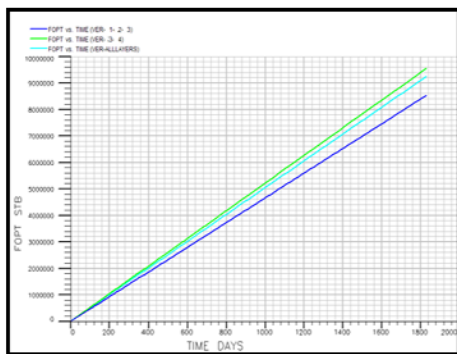
FIG. 7 FIELD TOTAL CONDENSATE PRODUCTION VERSUS TIME (VERTICAL WELLS)
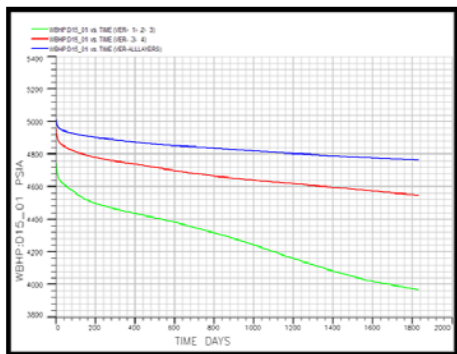
FIG. 8 WELLS BOTTOM-HOLE PRESSURE IN DIFFERENT SCENARIOS (VERTICAL WELLS)

- Upper layers with 39 STB/MMsscf CGR, have the lowest CGR and layers 3 and 4 with 43.5 STB/MMscf CGR, have the higher one in comparison to the above layers (Figure 9).
- With gas production and initiating condensate dropout around the well, production index decreases but with increasing liquid saturation and establishing 2-phase flow, production index approximately fixed (Figure 10).
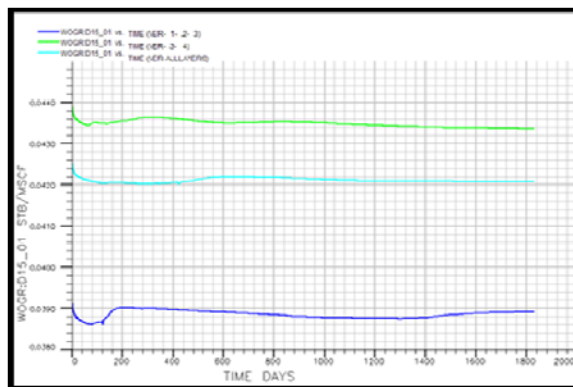
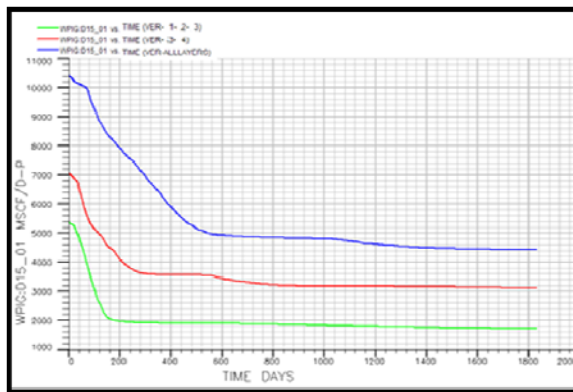FIG. 9 CONDENSATE GAS RATIO OF DIFFERENT SCENARIOS (VERTICAL WELLS)

FIG.10 PRODUCTION INDEX OF DIFFERENT SCENARIOS (VERTICAL WELLS)

Horizontal Well:

Cases Definitions:

- Top of horizontal wells are defined in the center of refined blocks.
- Dew to non-permeable layers in the reservoir, defining horizontal wells in majority of layers is impossible.
- At last 5 different well scenarios with 963, 1442 and 3332 feet long -in horizontal section- have been defined.

Results Comparison:

Pressure drop in layer 4, in the case that been defined in layer 4 is too low (Figure 11). This phenomenon

raises from properties of forth layer as below:

- High thickness of the layer
- High average porosity of the layer (around 23%)
- Low initial water saturation
- High pore volume and pressure and flow support that builds a restriction on pressure drop

A break can be seen in down-hole pressure profile in the case that a horizontal well is producing from forth layer (Figure 11). This is due to:

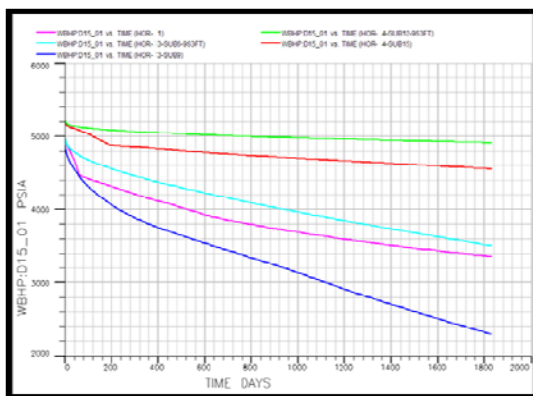- Reaching pressure drop front, to the end of the reservoir.
- Changing the flow pattern from radial to linear.

FIG.11 WELLS BOTTOM-HOLE PRESSURE OF DIFFERENT SCENARIOS (HORIZONTAL WELLS)

Total condensate that is produced from sub layers 12 and 15 (layer 4) are extremely higher than the other layers condensate production (Figure 12).
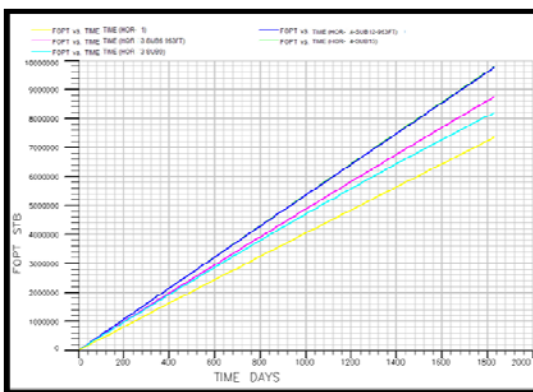
FIG.12: FIELD TOTAL CONDENSATE PRODUCTION VERSUS TIME (HORIZONTAL WELLS)

Effect of horizontal length of the well:

- Horizontal wells increases the contact between well and the reservoir and as the result causes the decreases in pressure drop.
- Due to complex behavior of gas condensate

fluids and non-homogenous distribution of reservoir properties, with increasing the horizontal section from 963 feet to 3332 feet, pressure drop in 5 years of production decreases around 200 Pisa (Figure 13).

- Cumulative condensate that been produced in different cases with dissimilar horizontal lengths, were almost the same (Figure 14).
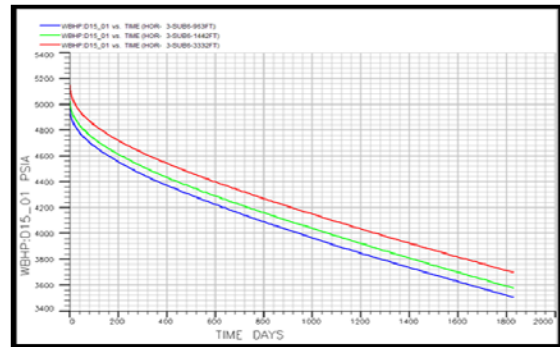

FIG. 13 WELLS BOTTOM-HOLE PRESSURE OF DIFFERENT HORIZONTAL SCENARIOS IN LAYER 3
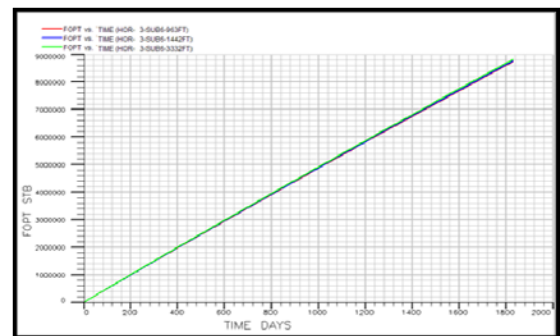

FIG.14: FIELD TOTAL CONDENSATE PRODUCTION VERSUS TIME IN DIFFERENT HORIZONTAL SCENARIOS IN LAYER 3

Slanted Wells

Cases Definition:

In order to investigate the effect of slanted wells on production profile, two slanted wells defined in the sector model:

- The first well extended 671 feet in vertical section and after that the well deviated with 36.57 degrees and completed in layers 1 to 3. The length of completed section in layers 1 to 3 is 1126 feet.
- The second well extended 881 feet in vertical section. After that the well deviated with 38.1 degrees and completed in layers 3 to 4. The length of completed section in layers 3 to 4 is 1427 feet.

Results Comparison:

As been predicted the well that entered to layer 4, had more production potential (Figure 15). This phenomenon also happened to the well that been completed in layers 3 and 4.

Due to low pressure drop in layers 3 and 4 and as these layers pressure has been dropped just a little bit below the dew point pressure, condensate that been produced from these layers were higher (Figure 16).
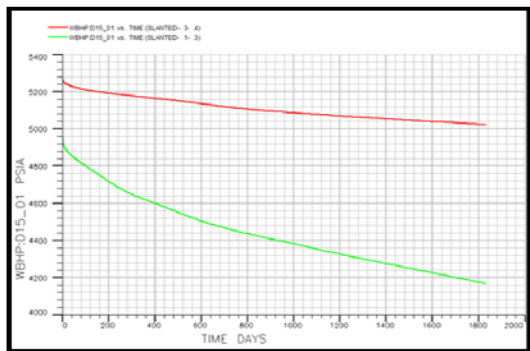

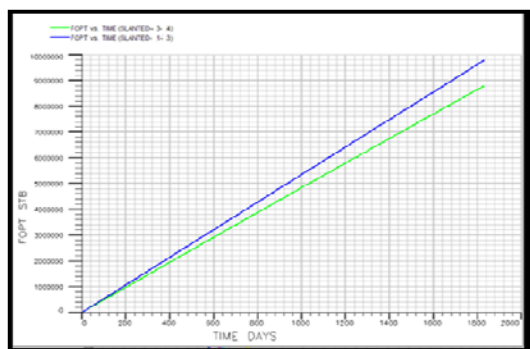FIG.15: WELLS BOTTOM-HOLE PRESSURE OF DIFFERENT SCENARIOS (SLANTED WELLS)

FIG.16: FIELD TOTAL CONDENSATE PRODUCTION VERSUS TIME (SLANTED WELLS)

Hydraulic Fracturing

Cases Definition:

- A fracture with 800 feet half-length, 0.05 foot opening and the height exactly the same as the layer that it was defined in, has been demarcated.
- Fracture permeability has been set to 225 Darcy and the capillary pressure in fractures has been selected as zero.

Results Comparison:

- Comparison of different cases results show that hydraulic fracturing causes decrease in pressure-drop in all the scenarios (Figure 17).
- The fracture that been defined in layer 4, has the most positive effect on decreasing pressure drop (Figure 17).

- Somehow, hydraulic fracturing does not have a bold effect on cumulative condensate production (Figure 18).
- Hydraulic fracturing causes water production increase in all the scenarios (Figure 19).
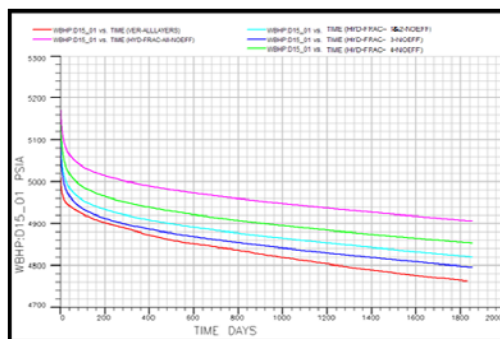

FIG.17 WELLS BOTTOM-HOLE PRESSURE OF DIFFERENT SCENARIOS (H-FRACTURED WELLS)
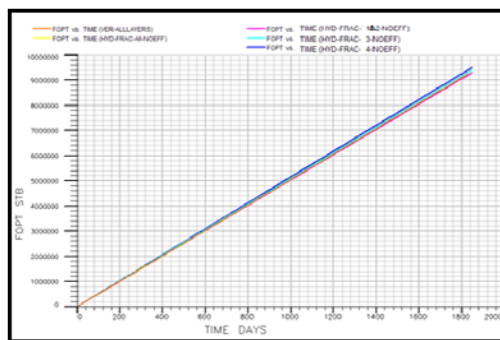

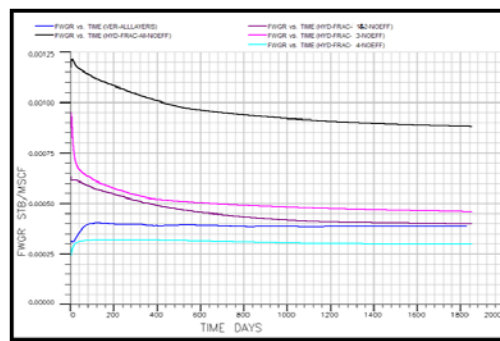FIG.18 FIELD TOTAL CONDENSATE PRODUCTION VERSUS TIME (H-FRACTURED WELLS)

FIG.19: FIELD WATER GAS RATIO VERSUS TIME (H-FRACTURED WELLS)

Different Scenarios Comparison

In order to compare all the scenarios here three categories have been defined:

Wells with the Almost 950 Feet Length:

Figure 20 shows bottom-hole pressure versus time in different scenarios. As been clear in this figure the lowest pressure drop has occurred in the horizontal well that been drilling in 12 sub layer (layer 4).
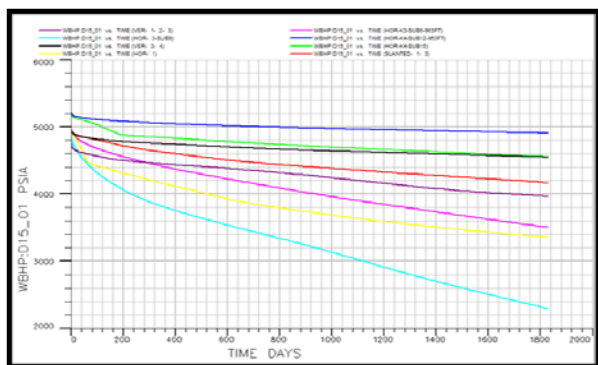
FIG.20 BOTTOM-HOLE PRESSURE VERSUS TIME (WELLS WITH 950 FEET LENGTH)

Wells with the Almost 1450 Feet Length:

As figure – shows the best scenarios for this case are the horizontal wells that are completed in layers 6 and 12 and the slanted well that is completed in layers 3 and 4.
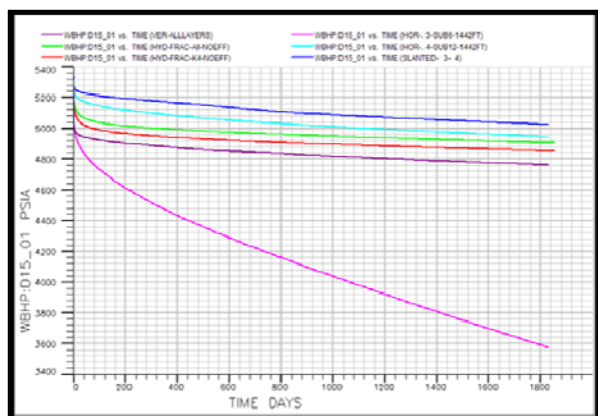

FIG.21: BOTTOM-HOLE PRESSURE VERSUS TIME (WELLS WITH 1450 FEET LENGTH)

By comparison of different scenarios from technical point of view the best four scenarios selected as listed below:

- Vertical Well that is completed in all layers
- Horizontal well that is completed in sublayer-12 with the length of 1442 feet
- Slanted well that is completed in layers 3 and 4
- Hydraulic fractured wells that are fractured layers 1 and 2.

Economic Analysis

After categorizing the best technical scenarios, it was time to compare the best scenarios from economic point of view. As it was told, in this study the raw data has been taken from a real condensate field. So Table 3 shows the real estimated costs of drilling each type of well.

TABLE 3 ESTIMATED DRILLING COSTS OF BEST TECHNICAL SCENARIOS

Well Type	Estimated Drilling Cost (MMUS$)
Vertical Well (in all layers)	43
Horizontal in Sublayer-12 with 1442 ft	37.5
Slanted in Layers 3&4	33.5
Hydraulic Fractured(in layers 1& 2)	47

Here in this study in order to compare the best technical scenarios economically, NPV and NPVR for all four scenarios had been calculated. As it is seen in Tables 4and 5 the highest NPVR is for slanted wells that are completed in layers 3 and 4.

TABLE.4 NPV FOR BEST TECHNICAL SCENARIOS

Well Type	NPV (Based on US$)
Vertical Well (in all layers)	508,523,303
Horizontal in Sublayer-12 with 1442 ft	535,645,321
Slanted in Layers 3&4	541,270,639
Hydraulic Fractured(in layers 1& 2)	494,837,095

TABLE 5 NPVR FOR BEST TECHNICAL SCENARIOS

Well Type	NPVR
Vertical Well (in all layers)	11.83
Horizontal in Sublayer-12 with 1442 ft	14.28
Slanted in Layers 3&4	16.16
Hydraulic Fractured(in layers 1& 2)	10.53

Conclusion

In this study, diverse scenarios has been defined to compare different well type's effect on production in a semi real reservoir model. Results show that, heterogeneity and the connectivity of layers and sub layers plays a big role on efficiency of each well type. For this case study after economic analysis, slated wells that are completed in layers 3 and 4 showed the best results in comparison to other cases.

REFERENCES

Afidick, D.; Kaczorowski, N. J. and Bette, S., "Production Performance of a Retrograde Gas Reservoirs: A Case Study of Arun Field", paper SPE 28749, November 1994.

Danesh, A.; Henderson, G.D.; Tehrani, D.H. and Peden, J.M, "Gas condensate recovery studies," DTI Improved Oil Recovery and Research Dissemination Seminar, London,

June 1994.

Dehane, Sonatrach PED, Tiab, D. and Osisanya, S.O. "Performance of Horizontal Wells in Gas condensate Reservoirs, Djebel Bissa Field", SPE 65504, Nov 2000.

Fussell, D. D., "Single-Well Performance Predictions for Gas Condensate Reservoirs" JPT (July 1973), pp. 860-870.

Gringarten, A.C.; Al-Lamki, A., and Daungkaew, S., "Well test Analysis in Gas Condensate Reservoirs", paper SPE 62920 presented at the SPE Annual Technical Conference and Exhibition, Dallas, Texas, October 2000.

Hashemi, A. and Gringarten, A.C. "Comparison of Well Productivity between Vertical, Horizontal and Hydraulically Fractured Wells in Gas Condensate Reservoirs", paper SPE 94178, 13-16 June 2005.

Henderson, G. D.; Danesh, A.; Tehrani, D. H.; Al-Shaidi, S. and Peden, J. M., "Measurement and Correlation of Gas Condensate Relative Permeability by Steady-State Method", SPE paper 30770 presented at the SPE Annual Technical Conference and Exhibition, Dallas, Texas, October 1995.

Joshi, S.D. "Horizontal Well Technology", 1991.

Mott, R., "Calculating Well Productivity in Gas Condensate Reservoirs", Presented at the IBC Technical Services Conference on Optimization of Gas Condensate Fields, Aberdeen, UK, June 1997.

Mott, R; Cable, A., Spearing, M., "Measurements and Simulation of Inertial and High Capillary Number Flow Phenomena in Gas-Condensate Relative Permeability", paper SPE 62932 presented at the SPE Annual Technical Conference and Exhibition, Dallas, Texas, October 2000.

Muladi, A. and Pinczewski, W.V. "Application of Horizontal Well in Heterogeneity Gas Condensate Reservoir", SPE 54351, April 1999.